



MASTER THESIS TECHNICAL MEDICINE

# OPTICAL INNOVATIONS IN ENDOBRONCHIAL DIAGNOSTICS

Renée Geraats

20<sup>th</sup> December 2019

Technical Medicine - Faculty of Science and Technology - University of Twente Enschede  
Department of Pulmonary Diseases – Radboudumc Nijmegen

EXAMINATION COMMITTEE:

Chairman University of Twente:

Medical supervisor Radboud UMC:

Daily supervisor Radboud UMC:

Technical supervisor University of Twente:

Additional member University of Twente:

Process supervisor University of Twente:

Dr. Ir. Ferdi van der Heijden

Erik van der Heijden MD PhD

Roel Verhoeven MSc

Dr. Ir. Ferdi van der Heijden

Dr. Ir. Frank Simonis

Elyse Walter MSc

## Summary

Bronchoscopy is a pulmonary intervention in which a flexible endoscope is inserted in the central airways to perform diagnosis or execute interventions. Optical enhancement is the emittance of specific wavelengths of light to illuminate the tissue. This illumination method causes certain tissue properties to stand out in endoscopic images. Optical enhancement was initially designed for gastrointestinal purposes. Two modes of optical enhancement settings are currently available on clinical bronchoscopy systems; optical enhancement mode 1 and optical enhancement mode 2. The aim of this research is to assess the value of optical enhancement techniques in endobronchial diagnostics and interventions. This research consists of three parts.

First, a technique validation of optical enhancement for bronchoscopy was done. An optical setup using lowpass and highpass filters was built to mimic commercially available optical enhancement spectra and to alternate the optical settings. Resulting images were analysed for surface texture, capillary and vessel contrast. A broad range of wavelengths resulted in the best surface texture visualisation. This was proven by the significant relationship between histogram peak width and surface visualisation ( $p \ll 0.01$ ). As expected, blue light seemed to be favourable for capillary visualisation, but this observation could not be significantly proven ( $p = 0.636$ ). As expected, red light was significantly proven to be essential for deep vein visualisation ( $p = 0.020$ ). Based on this technique assessment, commercially available optical enhancement spectra seem suitable for clinical application in bronchoscopy.

Secondly, the possibilities of direct improvement of bronchoscopy interpretation by the application of optical enhancement was investigated. 176 patient bronchoscopy reports were studied to register complications and assess imaging pitfalls. This analysis resulted in a list of complication causes in the Radboudumc hospital (Nijmegen, the Netherlands) and a list of challenging aspects in bronchial wall visualisation for which optical enhancement can improve the visualisation. Furthermore, a prospective case series of endobronchial images of fourteen patients either with or without central airway lesions were analysed. When visually inspecting the collected images, optical enhancement mode 1 contained more additional information about the bronchial wall than optical enhancement mode 2. This observation supports the quantification results in which optical enhancement images contain additional information about bronchial arches, vascular beds and bronchial abnormalities.

Lastly, the starting steps for automatic detection of systemic disease were taken. A literature research was carried out to determine the tissue properties of tissue affected by lung cancer, nontuberculous mycobacteria and sarcoidosis. A research proposal for a prospective database registry for bronchoscopy images was submitted and approved (CMO 2019-5583). The applications of the bronchoscopy database and the required future research that is needed to accomplish these applications were described.

Optical enhancement is an innovation that has potential for endobronchial application in routine practice. Improved vessel, arch and bronchial abnormality visualisation can prevent bronchial bleeding and perforation, and detect pathological lesions in an early stage. The first step for future research in optical enhancement is filling the prospective database of endobronchial images to allow for automatic distinction between healthy and affected airways.

# Contents

Summary .....	1
List of abbreviations .....	4
1. General introduction .....	5
1.1 Endobronchial diagnostics.....	5
1.2 Bronchoscopy innovations .....	5
1.2.1 History of bronchoscopy .....	5
1.2.2 Virtual chromoendoscopy .....	6
1.2.3 Optical enhancement .....	7
1.3 Aims and research questions .....	8
2. Technique validation of optical enhancement for bronchoscopy .....	10
2.1 Introduction.....	10
2.1.1 Bronchoscopy setup .....	10
2.1.2 The optical enhancement spectra .....	11
2.1.3 RGB colour scale .....	11
2.1.4 Quantification of contrast and texture .....	12
2.2 Methods .....	15
2.2.1 Building variable spectra .....	15
2.2.2 Spectra for optical testing .....	17
2.2.3 Phantoms for optical testing .....	19
2.2.4 Measuring spectrum intensity.....	19
2.2.5 Hypotheses .....	20
2.2.6 Experiment protocol.....	21
2.3 Results .....	21
2.3.1 Surface texture .....	21
2.3.2 Capillary vessels.....	24
2.3.3 Deep veins .....	28
2.4 Discussion and conclusion .....	31
2.4.1 Optical setup .....	31
2.4.2 Visualisation of surface texture.....	31
2.4.3 Visualisation of capillary vessels.....	32
2.4.4 Visualisation of deep veins .....	32
2.4.5 General conclusions .....	34

3	Improvement of bronchoscopy interpretation .....	35
3.1	Introduction.....	35
3.2	Complication registration .....	36
3.2.1	Methods complication registration .....	36
3.2.2	Results complication registration.....	36
3.3	Case series .....	39
3.3.1	Methods case series .....	39
3.3.2	Results case series .....	40
3.4	Discussion and conclusion .....	44
3.4.1	Complication registration.....	44
3.4.2	Case series .....	45
3.4.3	General conclusion .....	47
4	Automatic detection of systemic disease.....	48
4.1	Introduction.....	48
4.1.1	Systemic pulmonary diseases and their tissue properties .....	48
4.1.2	Tissue properties caused by comorbidities and individual patient factors.....	51
4.1.3	Bronchial wall in systemic disease .....	52
4.1.4	Need for automatic interpretation.....	53
4.1.5	Optical enhancement as input for automatic detection .....	53
4.2	Prospective database registry for bronchoscopy .....	54
4.3	Applications of bronchoscopy database registry .....	54
4.4	General conclusion .....	55
5	General discussion and conclusion.....	56
6	References.....	58
7	Appendices .....	61
7.1	Camera response model.....	61
7.2	Interaction of tissue and light of various wavelengths .....	62
7.3	Names and descriptions of MATLAB scripts.....	63
7.4	Tables results technique validation of optical enhancement for bronchoscopy .....	65
7.5	Research protocol prospective database registry .....	69
7.6	Patient information letter prospective database registry (Dutch).....	78

## List of abbreviations

3D	Three-Dimensional
AIDS	Auto Immune Deficiency Syndrome
CCD	Charged-Coupled Device
CM	Co-occurrence Matrix
CMOS	Complementary Metal Oxide Semiconductor
COPD	Chronic Obstruction Pulmonary Disease
ECG	Electrocardiography
HD	High Definition
HP	High Pass optical filter
ISO	International Standards Organisation
LED	Light Emitting Diode
LP	Low Pass optical filter
$\mu\text{m}$	micrometre, $10^{-6}$ meter
OE	Optical Enhancement
OE1	Optical Enhancement filter mode 1
OE2	Optical Enhancement filter mode 2
NBI	Narrow Band Imaging
nm	nanometre, $10^{-9}$ meter
NSCLC	Non-Small Cell Lung Cancer
NTM	Nontuberculous Mycobacteria
ROI	Region of Interest
RGB	Red Green Blue
SCLC	Small Cell Lung Cancer
WLB	White Light Bronchoscopy

# 1. General introduction

## 1.1 Endobronchial diagnostics

Bronchoscopy is a pulmonary intervention in which a flexible endoscope is inserted in the central airways (figure 1). A bronchoscopy procedure is aimed at obtaining and visually interpreting images of the endobronchial condition of the patient. At the Radboudumc hospital in Nijmegen, the Netherlands, bronchoscopies are performed by pulmonologists. Besides collecting visual information, bronchoscopy allows for the collection of cytological and histological material for further diagnostic analysis. Different techniques are available to collect endobronchial material during bronchoscopy. Lastly, pulmonary interventions such as tumour debulking, bronchial stenting, abscess drainage or foreign body removal can be executed during a bronchoscopy procedure.

Diffuse or localized lung infiltrates, recurrent or unresolved pneumonia, bronchiectasis, haemoptysis, persistent cough, aspirated objects and symptoms of endobronchial obstructions are indications for a bronchoscopy procedure. [1]

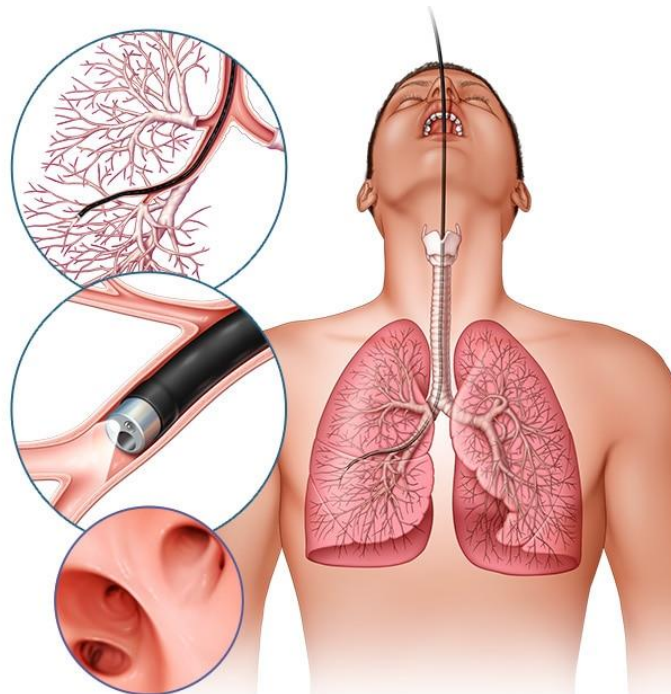


**Figure 1:** Schematic representation of a bronchoscopy procedure. [2]

## 1.2 Bronchoscopy innovations

### 1.2.1 History of bronchoscopy

The physician most commonly identified as the founding father of modern bronchoscopy is Gustav Killian. In 1876, this German otolaryngologist examined the trachea and main bronchi of a volunteer using a rigid laryngoscope. Afterwards he proceeded to remove an aspirated pork bone from the right main bronchus of a farmer. [3]

Flexible fibre optic bronchoscopy was invented by Shigeto Ikeda, a Japanese thoracic surgeon. The first prototype of a flexible fibre optic bronchoscope became commercially available in 1968, also known as the *year of the second revolution* in bronchoscopy. [3] Two years later, Olympus Corporation (Tokyo, Japan) brought the first bronchoscope with improved imaging and handling capacities to the market. [4]

Asahi Pentax Corporation, now known as Pentax Medical (Tokyo, Japan), developed the first video bronchoscope in 1987. In its first design, a fibre optic bronchoscope transferred the endobronchial image to the eye of the bronchoscopist using optical fibres. Later designs now commonly include video camera imaging chips such as a charged-coupled device (CCD) chip or a complementary metal oxide semiconductor (CMOS) chip in the tip of the bronchoscope for capturing endobronchial images. The digital signal is transferred to a video screen where multiple spectators can inspect the image. The invention of the video bronchoscope has created the possibilities of saving and digitally analysing bronchoscopic images.

While a standardized measure for high definition (HD) is lacking, video bronchoscopes with continually improving image qualities have been manufactured since 1987. These HD image quality bronchoscopes provide higher image resolution, creating possibilities for more advanced diagnostics. Video bronchoscopes are still an integral part of the practice of chest medicine these days. [3] But also rigid bronchoscopes have never left clinical practice. Rigid bronchoscopes have a wider working channel that allows more instruments to pass while maintaining an adequate airway during the procedure. Rigid bronchoscopes are most commonly used to perform endobronchial interventions such as bronchial stenting and tumour debulking. [5]

### 1.2.2 Virtual chromoendoscopy

Recognising visual cues is the main method to detect central lung pathologies during bronchoscopy. Recognising deviations in vascular characteristics is essential for the diagnosis of endobronchial processes such as malignant growths. [6] While regular white light bronchoscopy (WLB) is the most broadly used imaging method, it does not always offer the best surface visualisation and vessel contour. To enhance these visual cues in endobronchial images, digital processing can be applied. This technique, such as commercially available in the Pentax i-scan settings, is called virtual chromoendoscopy. This technology was introduced by Pentax Medical in 2010. [7] The i-scan imaging technique can be used to distinguish pathological tissue from healthy tissue more effectively.

In the analysis of bronchoscopic images, a relationship between vessel diameter, capillary pattern and malignancy grade has been proven. [6] Manipulation of the colour space without spectral filtering of the reflected light causes the representation of certain colours on the screen to be suppressed or enhanced. This digital manipulation causes vascular characteristics of vessel diameter, capillary pattern and malignancy grade to be easier to distinguish. [8][9] Since the virtual chromoendoscopy technology is purely an imaging processing technology, white light bronchoscopy and virtual chromoendoscopy can be derived from the same input image. In current clinical practice in the Radboudumc hospital in Nijmegen, the Netherlands, i-scan settings are used when the interpretation of mucosal abnormalities in the central airways is unclear.

Two clinical studies on the Pentax i-scan settings have been performed in the Radboudumc hospital. It has been shown that i-scan settings detect additional lesions in one third of patients compared to white light bronchoscopy. In 8.4% of cases, these additional findings were clinically relevant. [10] The other study has shown that virtual chromoendoscopy results in better detection of subtle vascular abnormalities compared to white light bronchoscopy and autofluorescence bronchoscopy (AFB). [11] Autofluorescence bronchoscopy is based on the interaction between a specific wavelength of light and tissue fluorophores. Healthy, inflamed and neoplastic tissue have different autofluorescence characteristics and emit fluorescent light with different characteristics. [12] In optical enhancement multiple ranges of wavelengths are being applied, contrary to AFB in which only one wavelength is applied.

### 1.2.3 Optical enhancement

To further enhance visual cues in bronchoscopic images, one can also alter the light that is emitted by the bronchoscope. An image-enhanced endoscopic technology that emits selective wavelengths of light has been brought to the market in 2005 by Olympus Corporation (Tokyo, Japan) under the name Narrow Band Imaging (NBI). [13] Recently, Pentax Medical (Tokyo, Japan), also incorporated this optical technique in their endoscopes and bronchoscopes, naming it optical enhancement imaging (OE). Since this research was conducted using Pentax bronchoscopes, this optical technique will be referred to as optical enhancement imaging throughout this report. The OE technology combines digital processing and optical filters that define the spectral characteristics of the emitted light. [14] The emitted light is filtered, resulting in a selective spectrum of light that is being absorbed and reflected. A camera response model describing how different signals are perceived by the endoscope camera is given in appendix 7.1. Optical enhancement is not the same as virtual chromoendoscopy such as described in section 1.2.2 “Virtual chromoendoscopy”, since OE alters the emitted light while virtual chromoendoscopy is purely a post-processing technology based on the white light bronchoscopic image.

OE typically uses multiple bandwidths of light. An example is an optical enhancement setting (called OE mode 1) with blue light emittance at 390 to 450 nm which is absorbed by superficial capillaries, combined with green light emittance at 530 to 555 nm which is absorbed by deeper blood vessels below the mucosal capillaries (figure 2a). This particular OE setting ensures distinction of superficial and deep capillaries, because the peaks of the emitted light correspond with the peaks in the haemoglobin absorption spectrum. Blood vessels absorb the blue and green light while surrounding tissue reflects light of these wavelengths. This maximizes the contrast between blood vessels and surrounding tissue (figure 2b). Different combinations of emitted bandwidths are fine-tuned for different tissue types. Depending on the desired tissue visualisation, the spectrum can be altered. [15] A more detailed description of the interaction of tissue and light, which forms the technological principle of optical enhancement, is given in appendix 7.2.

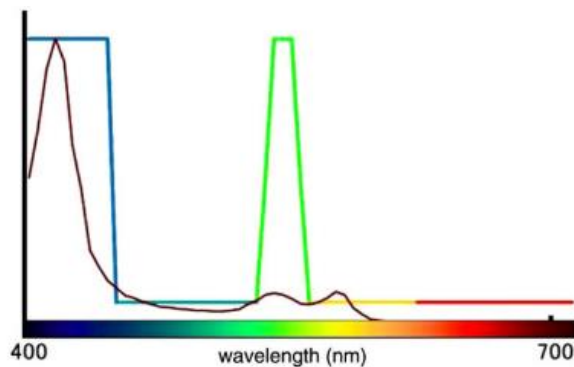


**Figure 2a:**  
Example of an OE emittance spectrum with two bandwidths of light. The absorption spectrum of haemoglobin is shown in dark purple. [16]

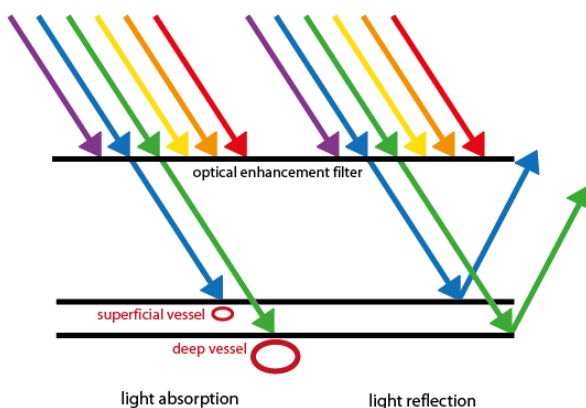


**Figure 2b:**  
Schematic representation of OE working mechanism. Light penetration depth is related to wavelength. Vessels absorb light (situation on the left) while surrounding tissue reflects light (situation on the right), maximizing the contrast between them. [17]



The principle of optical enhancement is illustrated in figure 3. In white light bronchoscopy, superficial and deep vascularisation are difficult to distinguish (figure 3a). When using optical enhancement imaging, the deep vessels absorb a large portion of the light with longer wavelengths (figure 3b) while the superficial vessels absorb a large portion of the light with shorter wavelengths (figure 3c). Post processing ensures the visualisation as seen in figure 3d.

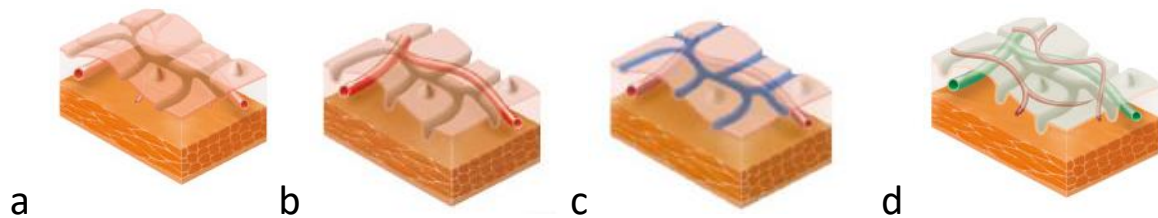


**Figure 3:** (a) Tissue illuminated with white light. (b) In OE, deep vessels absorb red light. (c) In OE, superficial vessels absorb blue light. (d) Resulting OE image after image post-processing. [18]

The use of optical enhancement during endoscopy was initially focused on gastrointestinal applications. In gastrointestinal endoscopy, there is a need to enhance tissue properties for better recognition and classification of polyp lesions and gastric abnormalities. [9][14][19] OE has also been used in the diagnosis of oesophageal squamous cell carcinoma. [16]

For the application of OE and NBI in bronchoscopy, little research has been published. However, capillary bed aspects such as capillary loops, dotted vessels, complex vascular networks of tortuous vessels and abrupt ending vessels have been proven to be indications for pathology. [15] It might be possible to improve the visualisation of these vascular abnormalities using optical enhancement. Also premalignant airway lesions might be detected more accurately using optical enhancement. [19]

### 1.3 Aims and research questions

Lung pathologies can be diagnosed during bronchoscopy by recognising visual cues. While regular white light bronchoscopy is the most broadly used imaging method, it does not always offer the best surface and vessel visualisation. Changes in surface texture and vascular patterns can indicate lung pathologies that need further diagnosis and treatment. When these endobronchial aspects are not clearly visualised, there is a risk of missing pathological lesions or underestimating the extend of pathological lesions. Since the indications for further diagnostics or treatment are based on the diagnostic outcome of the bronchoscopy, it is of essential importance to visualise the bronchial wall as thoroughly as possible.

Optical enhancement, initially designed for gastrointestinal endoscopy, is a promising innovation for application in bronchoscopy. In optical enhancement, blood vessels and surrounding tissue absorb wavelengths in different manners, making vascular patterns easier to distinguish. This improved vascular visualisation is thought to be of added clinical value in the diagnostics of lung diseases during bronchoscopy. A more thorough examination of the bronchial tissue ensures more accurate diagnosis, aiding in the early diagnosis of lung disease. When added clinical value is proven, optical enhancement should be implemented in the standard of care for bronchoscopy.

When implementing an existing technology for an innovative application, as is the case for optical enhancement imaging, multiple steps need to be taken. The suitability and safety of the existing technology for the new application needs to be determined. If required, the technology needs to be fine-tuned for the intended new application. Substantiated hypotheses need to be formulated to determine the clinical focus for the application of the technology. Lastly, patient data needs to be collected to test the hypotheses and find out whether the innovative application of the existing technology is contributing to better patient care.

This internship was aimed at the first steps of optical enhancement implementation in bronchoscopy with the main research question:

*“What is the value of optical enhancement in endobronchial diagnostics and interventions?”*

The sub question that this report aims to answer are:

- Which *ex vivo* optical setup can mimic the commercially available optical enhancement settings and alter the spectrum of the emitted light?
- Which wavelengths of light are the most suitable to visualise surface texture, capillary vessels and deep veins of the bronchi?
- Are the commercially available optical enhancement settings suitable for application in bronchoscopy?
  
- What are the incidences and causes of complications in bronchoscopy in the Radboudumc hospital in Nijmegen?
- Which challenging aspects of bronchoscopic visualisation can potentially be improved by the application of optical enhancement?
- For which aspects of bronchoscopic visualisation do optical enhancement images carry additional information compared to white light bronchoscopic images?
  
- Which diagnosis of systemic pulmonary diseases can potentially be improved by the application of optical enhancement?
- How should data acquisition for future clinical research on optical enhancement be executed?
- How can automatic detection of systemic disease in bronchoscopy images be realized in clinical practice?

This internship report focuses on three subjects and is therefore divided into three chapters. In chapter 2, a technique validation is done to find out whether the available optical enhancement settings are optimal for the application in bronchoscopy. In chapter 3, the immediate clinical benefits of the application of optical enhancement in the interpretation of bronchoscopy are studied. In chapter 4, the possibilities and requirements of automatic detection of central systemic disease using OE in bronchoscopy images are covered.

## 2 Technique validation of optical enhancement for bronchoscopy

In this chapter, the optical enhancement technique as commercially available is validated for endobronchial application by various *ex vivo* optical experiments. These experiments aim to assess the following questions:

- Which *ex vivo* optical setup can mimic the commercially available optical enhancement settings and alter the spectrum of the emitted light?
- Which wavelengths of light are the most suitable to visualise surface texture, capillary vessels and deep veins of the bronchi?
- Are the commercially available optical enhancement settings suitable for application in bronchoscopy?

### 2.1 Introduction

#### 2.1.1 Bronchoscopy setup

A bronchoscopy setup consists of two main components, the bronchoscope and a compatible processor. The bronchoscope consists of a flexible distal end that is inserted into the airways of the patient. Attached to the distal end is a handle with a steering lever and several buttons. [20] The handle is operated by the bronchoscopist to manoeuvre the tip of the distal end and to initiate air suction, alterations between settings and image recordings. The bronchoscope handle is connected to the bronchoscope processor in which a xenon light source is embedded. Various filters can be mechanically laid upon the light source to create different optical enhancement spectra. The desired light spectrum is transmitted to the tip of the bronchoscope through optical fibres. The light reflected by the bronchial tissue is registered on a chip in the tip of the bronchoscope, from which the digital signal is then transmitted back to the bronchoscopy processor. Various image processing settings can be applied to these raw images. The resulting video output is displayed to a screen for immediate evaluation while the video output is also stored on a server for future reference and scientific research. The schematic setup in figure 4 shows where the spectrum alterations and image acquisition steps take place.

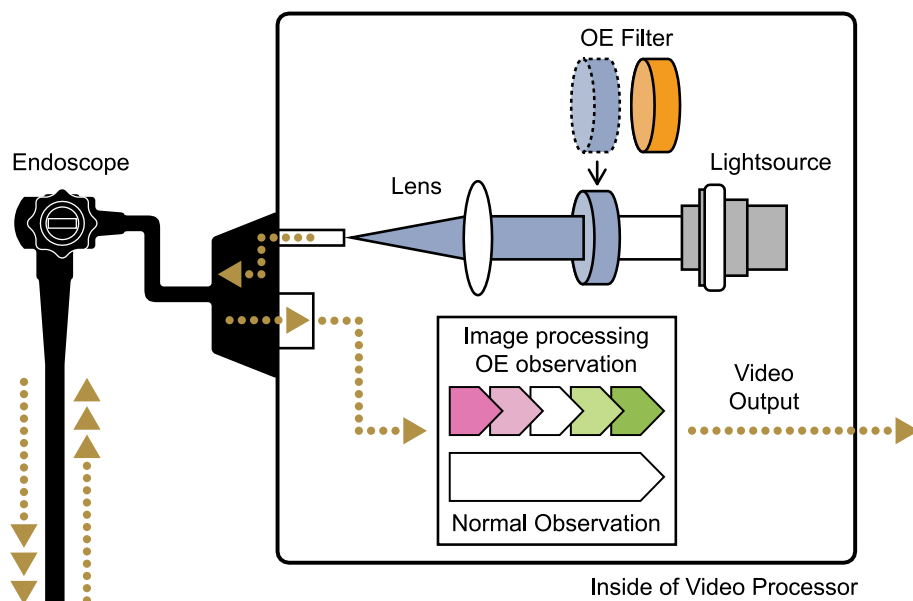
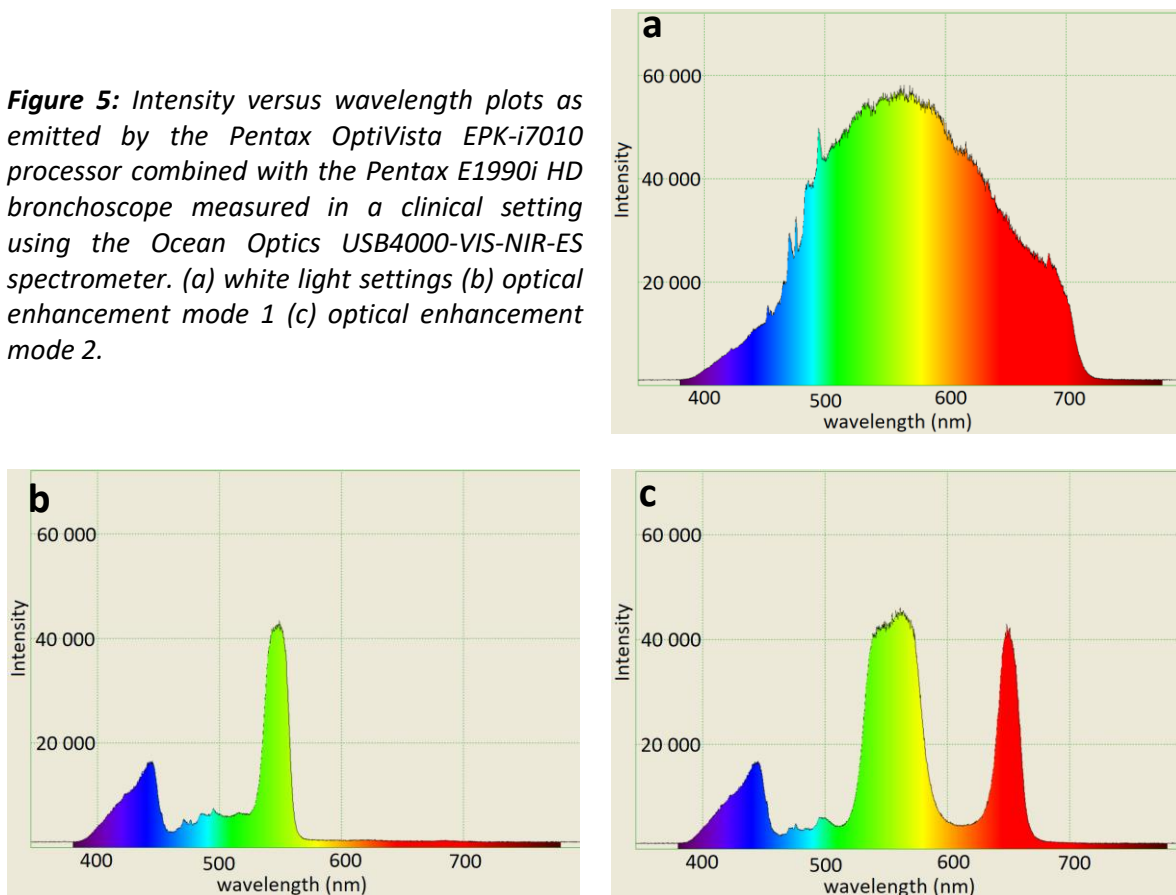


**Figure 4:** Schematic representation of a bronchoscopy setup. [18]

### 2.1.2 The optical enhancement spectra

The optical enhancement spectra as provided on the OptiVista EPK-i7010 processor (Pentax Medical, Tokyo, Japan) are available in two modes. [18] OE mode 1 emits a band of blue light at 390-450 nm and a band of green light at 530-555 nm. The green peak is 2.6 times as intense as the blue peak (figure 5b). OE mode 2 emits a band of blue light at 390-450 nm, a band of green light at 530-580 nm and a band of red light at 640-660 nm. The ratio of the intensities of the blue, green and red peaks respectively is 1, 2.7 and 2.5 (figure 5c). [8] The ratios between the height of the peaks in the intensity diagrams are relevant for an accurate replication of the optical enhancement spectra. The spectra as shown in figure 5 were produced using the Pentax OptiVista EPK-i7010 processor combined with the Pentax E1990i HD bronchoscope. [18][21] As expected, the optical enhancement spectra produced by a EG29-i10N gastroscope (Pentax Medical, Tokyo, Japan) are exactly the same as the bronchoscope spectra since the optical filters are applied inside the processor which is identical for both scopes. [22]

**Figure 5:** Intensity versus wavelength plots as emitted by the Pentax OptiVista EPK-i7010 processor combined with the Pentax E1990i HD bronchoscope measured in a clinical setting using the Ocean Optics USB4000-VIS-NIR-ES spectrometer. (a) white light settings (b) optical enhancement mode 1 (c) optical enhancement mode 2.



### 2.1.3 RGB colour scale

When describing and analysing endoscopic images, the depiction method of the reflected light on the video screen is of major importance. Different ways of assigning pixel values can result in different quantifications of contrast. For the application of this research, the RGB (Red Green Blue) colour model is described but it should be noted that numerous other colour depiction scales are available.

RGB is a three-dimensional colour model that describes what kind of light needs to be emitted to produce a certain colour. The individual intensity values for red, green and blue light can be depicted as a location in a three-dimensional cubical space (figure 6). A common application of the RGB colour model is the display of colours on a cathode ray tube, liquid-crystal display, plasma display or organic light emitting diode. Also charged-coupled device sensors operate using the RGB model. [23][24]

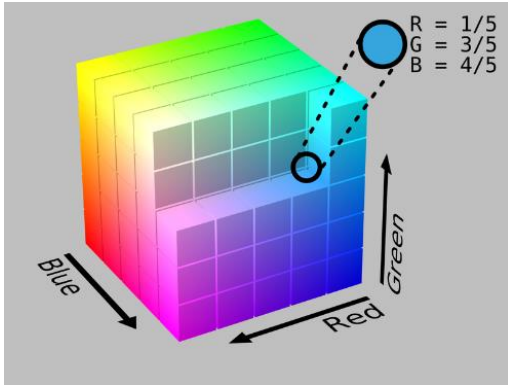


**Figure 6:** 3D representation of the RGB colour space. When using this representation, any colour can be described by a combination of three coordinates along the red, green and blue axis. [23]

#### 2.1.4 Quantification of contrast and texture

The development and presence of various endobronchial pathologies is related to changes in surface texture and vascular patterns. [6] Therefore the optical enhancement modes (Pentax Medical, Tokyo, Japan) are fine-tuned for the absorption spectrum of haemoglobin as shown in figure 2a. To compare different light spectra in their suitability to detect the contrast between vascular patterns and mucosal surface texture, objective methods for contrast and texture quantification are needed.

##### 2.1.4.1 Quantifying RGB contrast

To quantify the RGB contrast between two regions of interest (ROI) in an image, a group of pixels can be quantified in a colour histogram. A histogram plots pixel counts versus RGB values for all of the pixels within the ROI. [25] For all three colour channels, the histogram can be described with a mean pixel value and a standard deviation. The mean RGB values of two regions can be compared by computing the three-dimensional Euclidean distance between these values in the cubic RGB colour space using equation 1. This method is effective in capturing contrast in one descriptive value, but carries no information regarding the relative position of pixels in respect to each other. [26] Colour contrast defined by this method does not correspond fully to the way the human eye perceives colour contrast. Various other methods that attempt to quantify contrast in accordance to human perception are available. [27]

**Equation 1:** Computation of 3D colour distance in RGB colour space.

$$RGBdist_{1,2} = \sqrt{(R_2 - R_1)^2 + (G_2 - G_1)^2 + (B_2 - B_1)^2} \quad (1)$$

$RGBdist_{1,2}$  = colour distance in RGB colour space for the quantification of RGB contrast between region of interest 1 and region of interest 2.

$(R_1, G_1, B_1)$  = mean RGB colour values for region of interest 1

$(R_2, G_2, B_2)$  = mean RGB colour values for region of interest 2

### 2.1.4.2 Quantifying texture

To quantify texture, a co-occurrence matrix (CM) can be computed. Co-occurrence matrices can be defined for greyscale images. In order to analyse coloured images using co-occurrence matrices, the colours need to be indexed into greyscale categories. A co-occurrence matrix  $\mathbf{G}$  of image  $f$  is a matrix of which an element  $g_{ij}$  is the number of times that pixel pairs with intensities  $z_i$  and  $z_j$  occur in  $f$  as specified by operator  $Q$  that defines the position of two pixels relative to each other. [28][29] The value of  $Q$  can be chosen in any direction and any magnitude smaller than the greyscale image. Co-occurrence matrices are often computed only for the eight values of  $Q$  that indicate the adjacent pixels in all directions relative to the pixel of interest. In that case, eight co-occurrence result from a single picture. These eight possible values of operator  $Q$  are shown in figure 7a. For example, a  $0^\circ$  co-occurrence matrix describes the relationship of pixels with their adjacent pixel on the right. An illustration of the creation of a  $0^\circ$  co-occurrence matrix is depicted in figure 7b.

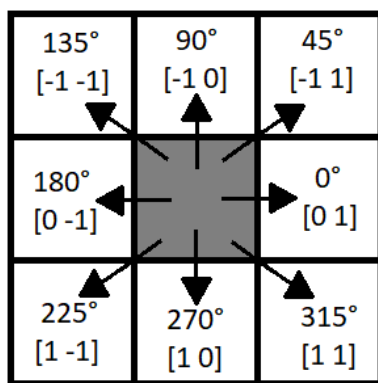


**Figure 7a:** Eight possible values of operator  $Q$  that describes the direction in which two pixels are being compared. [30]

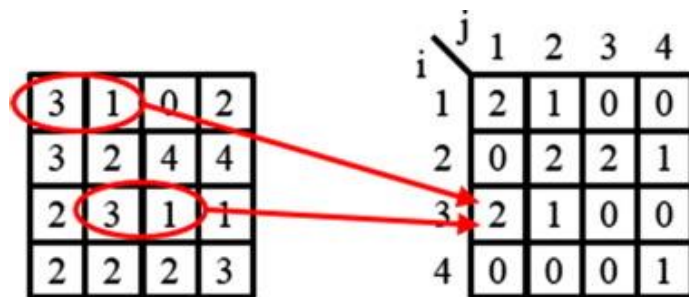


**Figure 7b:** The creation of a  $0^\circ$  co-occurrence matrix. [31]

To quantify and compare the content of co-occurrence matrices, co-occurrence matrix descriptors are needed. In table 1, four descriptors of co-occurrence matrices and their equations are given.

**Table 1:** Descriptors and equations of co-occurrence matrices [28][32]

$p(i, j)$  = normalized co-occurrence matrix, describing the chance of values being situated at positions  $(i, j)$ .  $p(i, j)$  is derived by dividing the co-occurrence matrix by the sum of the samples in the co-occurrence matrix. Therefore, the sum of all values in  $p(i, j)$  equals 1.

$\sigma_i$  = the standard deviation of values of  $p$  over the  $i$  axis of the co-occurrence matrix.

$\sigma_j$  = the standard deviation of values of  $p$  over the  $j$  axis of the co-occurrence matrix.

$\mu_i$  = expected value of  $i$

$\mu_j$  = expected value of  $j$

Property	Description	Equation
Co-occurrence matrix (CM) Contrast	Returns a measure of the intensity contrast between a pixel and its neighbour over the whole image. Range = [ 0 (size(CM,1) - 1) <sup>2</sup> ] CM contrast is 0 for a constant image.  High CM contrast is a requirement for successful surface visualisation	$\sum_{i,j} (i - j)^2 p(i, j) \quad (2)$
Correlation	Returns a measure of how correlated a pixel is to its neighbour over the entire image. Range = [ -1 1 ] Correlation is 1 or -1 for a perfectly positively or negatively correlated image. Correlation is NaN (not a number) for a constant image.  High correlation is a requirement for successful surface visualisation	$\sum_{i,j} \frac{(i - \mu_i)(j - \mu_j)p(i, j)}{\sigma_i \sigma_j} \quad (3)$
Energy (also called Uniformity)	Returns the sum of squared elements in the CM. Range = [ 0 1 ] Energy is 1 for a constant image.  Low energy is a requirement for successful surface visualisation	$\sum_{i,j} p(i, j)^2 \quad (4)$
Homogeneity	Returns a value that measures the spatial closeness of the distribution of elements in the CM to the CM diagonal. Range = [ 0 1 ] Homogeneity is 1 for a diagonal CM.  Low homogeneity is a requirement for successful surface visualisation	$\sum_{i,j} \frac{p(i, j)}{1 +  i - j } \quad (5)$

## 2.2 Methods

To investigate whether the commercially available spectra are optimal for the visualisation of bronchial tissue texture and vascular RGB contrast, different illumination spectra need to be assessed. This section covers the different aspects of an *ex vivo* optical setup that allows for this assessment. Analysis of the results has been executed in MATLAB 2018a (MathWorks, Natick, United states of America). A list of programmed scripts is provided in appendix 7.3. These scripts are available on the digital research server of the Pulmonary department of the Radboudumc in Nijmegen, the Netherlands.

### 2.2.1 Building variable spectra

In order to assess the effect of different combinations of wavelengths of light, an optical setup needs to be designed. This optical setup should be able to create a variable spectrum in which various combinations of bands of wavelengths can be created. The variable spectrum can be used to assess the effect of different spectra on surface texture and vascular contrast visualisation. Four possible methods to achieve this goal are described.

#### 2.2.1.1 Specific optical filters

The first and most straightforward method to create variable spectra is to purchase specifically fabricated filters. However, this option is very costly and would consequently require concessions on the number of spectra that can be tested. It is believed that making this concession would diminish the value of the analysis and therefore other methods of variable spectrum creation were tried.

#### 2.2.1.2 Variable LED lamps

The second method for the building of variable spectra is the use of a combination of variable coloured light emitting diodes (LED). This method is widely applied in electronic applications and is able to create all possible colours perceivable to the human eye. However, an LED spectrum is constructed from distinct peaks in red, green and blue wavelengths and is thus not representative for the continuous spectrum created by a xenon lamp. To illustrate this discrepancy, figure 8 shows two spectra that both appear white to the human eye but consist of different combinations of wavelength intensities.

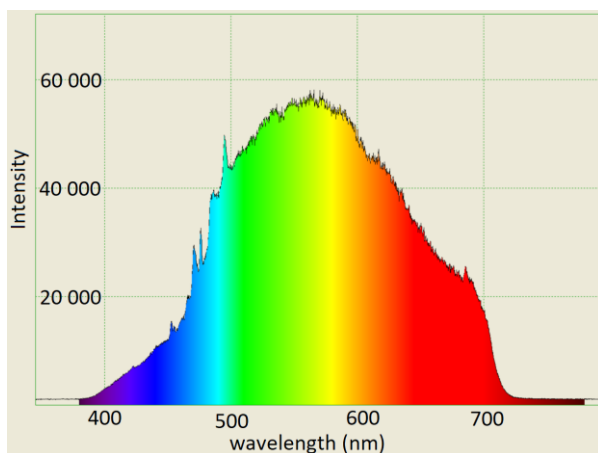


**Figure 8a:** Intensity versus wavelength plot of white light spectrum as emitted by xenon lamp.

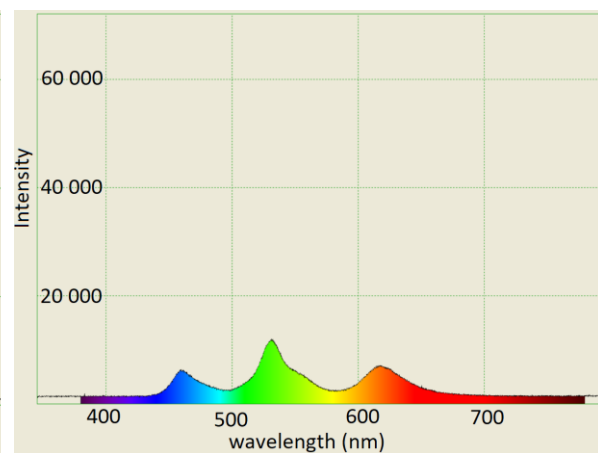


**Figure 8b:** Intensity versus wavelength plot of white light spectrum as emitted by LED lamp.



### 2.2.1.3 Diffraction gratings

The optical setup of the third method for the creation of a variable spectrum is visualised in figure 9. The wavelengths of an incandescence lamp were spatially separated using a diffraction grating. After blocking selective wavelengths of light with narrow objects, the spectrum was directed into another diffraction grating to create a parallel beam of light again. Theoretically, this method provides the possibilities to create any desired spectrum.

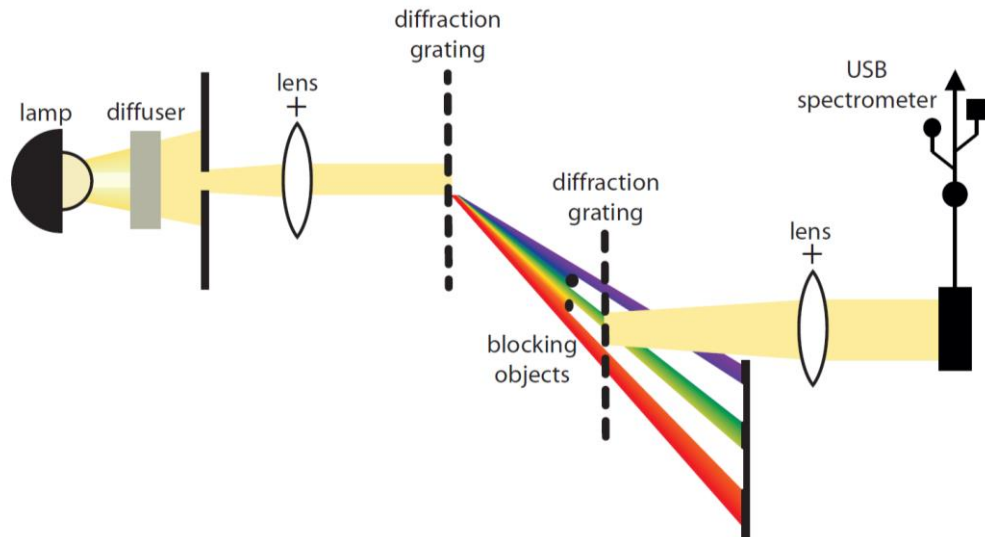


**Figure 9:** Setup of optical diffraction gating experiment that blocks undesired bands of wavelengths.

However, after experimenting it needs to be concluded that the spectra created by this method were certainly not resembling the characteristics of optical enhancement spectra. The intensity of undesired wavelengths was only halved instead of diminished completely, and the ranges of wavelengths that were affected by the blocking objects were over 200 nm wide. Narrowing the blocking objects did not improve these flaws. This method is not specific enough to reproduce the optical enhancement spectrum. These results can be explained by the fact that an incandescence light source has a diameter and is not a point light source. This causes blending of the wavelengths at the diffraction grating instead of a clean separation.

### 2.2.1.4 Highpass and lowpass filters

Since the methods described above were not viable for the selective creation of variable spectra, a setup using optical highpass and lowpass filters was used (figure 10). These filters were available in intermediate steps of 50 nm, meaning that the possibility to vary the spectra with smaller steps than 50 nm was lost. Furthermore, this setup was limited to only two identical incandescence light sources. This allows for the creation of spectra with a maximum of two continuous peaks. By connecting the light sources to variable power supplies, differences in peak ratio were realised. Since the bronchial tree is tube-shaped, the distal end of the bronchoscope illuminates the bronchial wall from an acute angle of 30 to 45 degrees. [20] To replicate the clinical situation as closely as possible, the illumination direction was set accordingly.

The spectra were measured using an Ocean Optics (Largo, United States of America) USB4000-VIS-NIR-ES spectrometer. The spectra were always corrected for the background spectrum as measured in the dark experiment room. The elimination of unwanted wavelengths was nearly faultless with cut-off values shaped like a step function. Images were obtained with a CASIO (Tokyo, Japan) EX-FH20 camera. The focal point, white balance and ISO (International Standard Organisation) value were manually set and remained constant during the experiment.

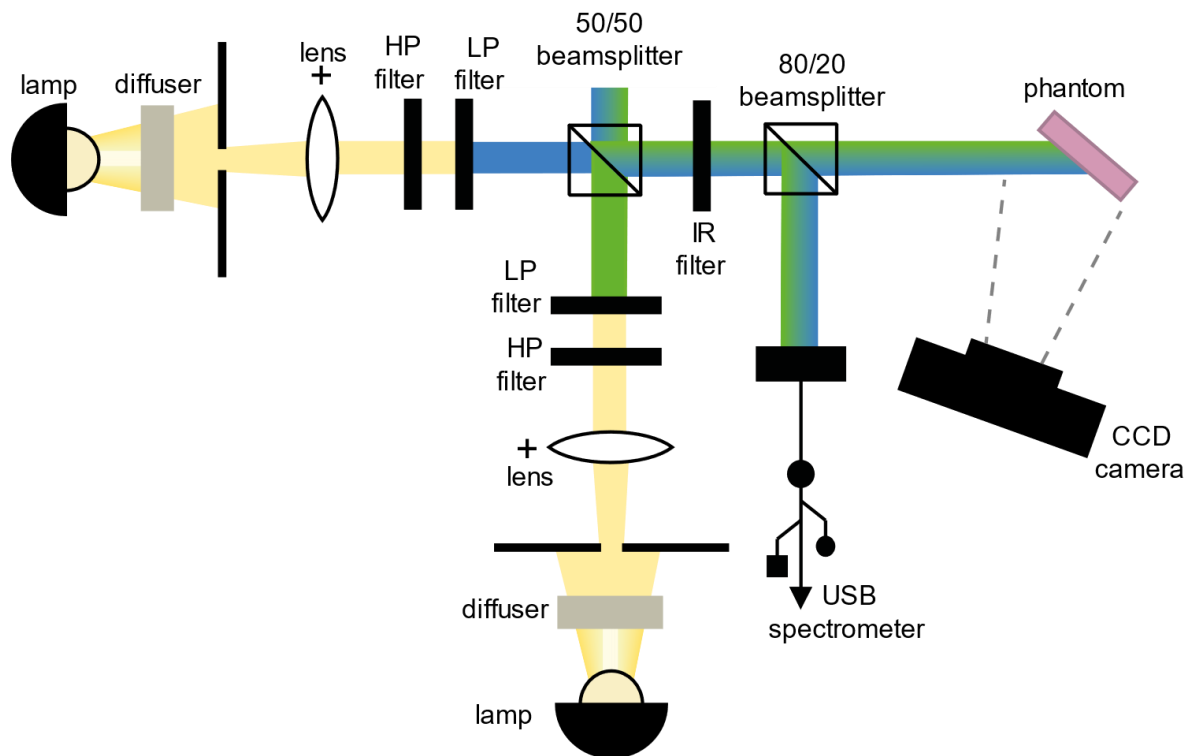


**Figure 10:** Setup of optical experiment using highpass (HP) and lowpass (LP) filters.

### 2.2.2 Spectra for optical testing

To assess the effect of different illumination spectra on the visualisation of surface texture and vessel RGB contrast, 28 different optical filter combinations were assessed. The optical setup as shown in figure 10 can create spectra with a maximum of two continuous peaks and intermediate steps of 50 nm. In table 2, the 28 different spectra as assessed in this experiment are visualised. The optical enhancement spectra as provided by Pentax are provided as well.

To mimic the optical enhancement modes, combinations of blue, green and red wavelength bands were assessed. All possible variations of wavelength bandwidth and position were tried out. These combinations of wavelength bands can be seen in spectrum 1 – 16 and spectrum M1 – M3. To identify the visualisation properties of separate bands of wavelengths spectrum B1 – B3 and spectrum A1 – A5 were assessed. Lastly, spectrum 17 functions as a reference spectrum without the application of any optical filters.

**Table 2:** The 28 spectra used for optical testing.

Spectrum number	Transmitted wavelengths	
	[nm]	$\lambda$
The Pentax optical enhancement spectra		
OE1		
OE2		
Group 1: recreating the optical enhancement spectrum with one blue peak and one green peak.		
1		
2		
3		
Group 2: recreating the optical enhancement spectrum with one blue peak and one red peak.		
4		
5		
6		
7		
Group 3: recreating the optical enhancement spectrum with one green peak and one red peak.		
8		
9		
10		
11		
12		
13		
14		
15		
16		
Group 4: the full incandescence light spectrum without optical filters.		
17		
Group 5: individual band components of the optical enhancement spectra.		
B1		
B2		
B3		
Group 6: combinations of individual band components of the optical enhancement spectra		
M1		
M2		
M3		
Group 7: narrow bands of increasing wavelengths.		
A1		
A2		
A3		
A4		
A5		

### 2.2.3 Phantoms for optical testing

To compare the different spectra, three phantoms were used. The different phantoms were chosen for their ability to quantify the visualisation of tissue surface, capillary vessels and deep vessels. A further explanation why these three tissue properties are important in bronchoscopy is provided in section 4.1.3 “Bronchial wall in systemic disease”.

For the model of irregular tissue surface, flesh coloured polymer clay was moulded into a tubular shape and irregularities were applied to the surface (figure 11a). A varnish was applied to replicate the moist bronchial wall tissue. It needs to be noted that polymer clay does not absorb and reflect in the same manner as tissue, but using a polymer clay model ensured a reproducible irregular surface to compare the effect of illumination by different spectra. [33]

To study the visualisation of capillaries, a piece of porcine trachea was used (figure 11b). To eliminate a shift in phantom position, this *ex vivo* tissue specimen was used. The porcine airway is an appropriate animal model for translational respiratory research, both *in vivo* as well as *ex vivo*. [34] The lungs were donated by an abattoir and were derived from a 22 weeks old pig weighing approximately 90 kilograms. Due hygiene regulations, the porcine trachea could not be examined using the clinical bronchoscopy setup. For this reason, the underside of a living human tongue has been used as a phantom to study capillary perfusion with a clinical bronchoscope. The underside of the human tongue is an easy accessible capillary bed which is representative for endobronchial capillaries. [35][36]

The phantom to study deep veins was the back of a living human hand, since the presence of haemoglobin in blood is the working mechanism of the optical enhancement technique to distinguish vessel from background. Reference points were indicated on the skin to transform the obtained images during analysis (figure 11c).

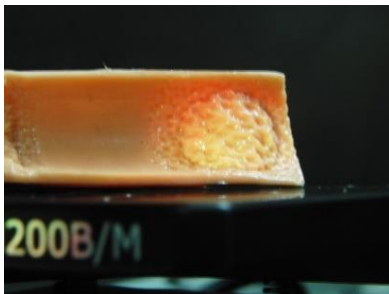


**Figure 11a:** Polymer clay phantom to study tissue surface.

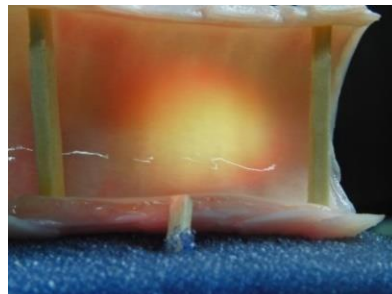


**Figure 11b:** Porcine trachea phantom to study endobronchial capillaries.



**Figure 11c:** Back of living human hand to study deep veins.

### 2.2.4 Measuring spectrum intensity

The properties of light spectra can be measured using a spectrometer. As visible in figure 10, a USB-spectrometer is part of the optical setup. This spectrometer generates a graph of light intensity over wavelengths. In this research, spectra were measured using the Ocean Optics (Largo, United States of America) USB 4000-VIS-NIR-ES spectrometer. The acquired data was processed using OceanView (Largo, United States of America) version 1.6.7 and Overture software (Largo, United States of America). [37]

To make the spectroscopy measurements of spectra mutually comparable, the spectra obtained by the spectrometer need to be corrected for the integration time settings. Integration time corresponds with the number of photons that get the chance to reach the spectrometer. A lower integration time results in lower measured light intensity. The integration time is variable to prevent saturation of the spectrometer. [37]

The total intensity of the spectrum corresponds with the area under curve of the intensity versus wavelength plot. Spectrum intensity can be calculated using equation 6.

**Equation 6:** Calculation of spectrum intensity.

$$I_{spectrum} = \sum_{\lambda_{min}}^{\lambda_{max}} I_{\lambda} \Delta_{\lambda} \quad (6)$$

$I_{spectrum}$	= the intensity of the total spectrum	[number of photons]
$\lambda_{min}$	= shortest wavelength that was measured by the spectrometer	[nanometre]
$\lambda_{max}$	= longest wavelength that was measured by the spectrometer	[nanometre]
$I_{\lambda}$	= light intensity for wavelength $\lambda$	[number of photons]
$\Delta_{\lambda}$	= bandwidth of each spectrometer measurement	[nanometre]

## 2.2.5 Hypotheses

### 2.2.5.1 Light intensity

It is hypothesized that spectrum light intensity is positively and linearly correlated with successful texture visualisation. This relationship is assumed linear because the amount of signal collected by the camera is linearly influenced by the intensity of the light under which an object is illuminated. When using higher intensities of light, all crevices of the rough surface visualisation phantom will be illuminated. The signal-to-noise ratio of the resulting picture will become higher and therefore will result in a more favourable surface visualisation. This linear relationship is not applicable when suffering from overexposure since information regarding surface structure will get lost when specular reflections due to overexposure occur.

It is hypothesized that capillary and deep vein visualisation is positively and linearly correlated with the intensity of the light. Capillary and deep vein visualisation is quantified by selecting regions of interest in the image and comparing the areas of the blood vessels to areas of adjacent mucosa. The contrast is defined as the absolute difference in colour between the regions of interest. The contrast will increase when applying a higher light intensity, since the difference between light reflection will increase when applying a higher intensity of light.

### 2.2.5.2 Histogram peak width

The histogram peak width indicates the ranges of the colour channels that are being used by an image. The width of the red, green and blue peaks above a relative intensity threshold can be summed to compute one value for histogram peak width per image. The relative threshold was determined at 10% of the maximum intensity of the highest of the three RGB channel peaks. It is hypothesized that the histogram peak width is positively and linearly correlated with successful texture visualisation. This relationship is assumed because a wide histogram peak width indicates the utilisation of many different shades of colour, creating the most detailed visualisation of surface structure.

### 2.2.5.3 Spectrum wavelengths

It is hypothesized that spectra containing short wavelengths (blue light) are best for capillary vessel visualisation because short wavelengths have a shallow penetration depth in tissue. [17][16] It is hypothesized that spectra containing long wavelengths (red light) are best for deep vein visualisation because long wavelengths have a deeper penetration depth in tissue. [17] A more detailed description of the interaction of tissue and light on which these hypotheses were based is given in appendix 7.2.

### 2.2.6 Experiment protocol

Six experiments have been done to assess the effect of the 28 light spectra on the visualisation of surface texture, capillary vessels and deep veins. Three experiments have been done in an optical laboratory using the setup as described in section 2.2.1.4 “Highpass and lowpass filters”. The other three experiments have been done in an endoscopy room using a clinical bronchoscopy setup. In both settings, the visualisation of surface texture, capillary vessels and deep veins was assessed.

The polymer clay phantom was used for the surface structure experiments and the back of a living human hand has been used for the deep vein experiments in both the optical laboratory and the clinical setting. In the optical laboratory, a piece of porcine trachea was used for the capillary vessels experiment. Because of hygiene regulations, the porcine trachea could not be examined using the clinical bronchoscopy setup. For this reason, the underside of a living human tongue has been used as a phantom to study capillary perfusion with the clinical bronchoscopy setup.

## 2.3 Results

The measured intensities for all 28 tested spectra are provided in table II in appendix 7.4. Since spectrum intensities were measured during the surface texture measurements and the capillary vessel measurements, two intensity values are given for each spectrum.

### 2.3.1 Surface texture

#### 2.3.1.1 Quantifying surface texture in a polymer clay phantom

This experiment was done using the polymer clay phantom as depicted in figure 11a. The phantom was illuminated consecutively by the 28 different light spectra as shown in section 2.2.2 “Spectra for optical testing”. The collected data consists of 28 images of the phantom and 28 spectrometer measurements.

In one of the images, a region of interest was manually selected (figure 12a). The region of interest was used as a mask to delete the surrounding image (figure 12b). The coloured image was indexed into 1000 grey levels so that the dimension of the co-occurrence matrix becomes 1000 by 1000 (figure 12c).



**Figure 12a:** Selected region of interest.

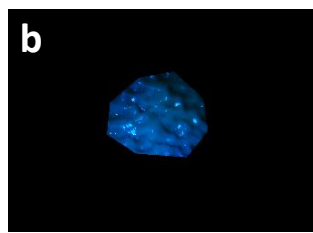


**Figure 12b:** Region of interest mask. Surrounding pixels are deleted.

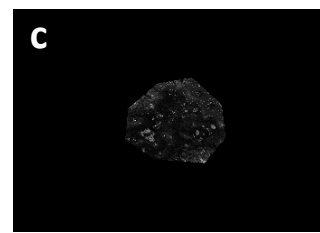


**Figure 12c:** Indexed region of interest in 1000 grey level categories.

The region of interest as shown in figure 12a was transformed to the other 27 images using Procrustes translation, scaling and rotation which principle is shown in figure 13. This transformation ensures similar positioning of the region of interest in all 28 pictures, enabling comparison of the images. Procrustes transformation was necessary because optical filter exchange in between experiments caused the phantom and camera position to move slightly. The transformation was executed using the manually indicated points of specular reflection in each image. These specular reflections occur at the same position on the phantom in every picture.

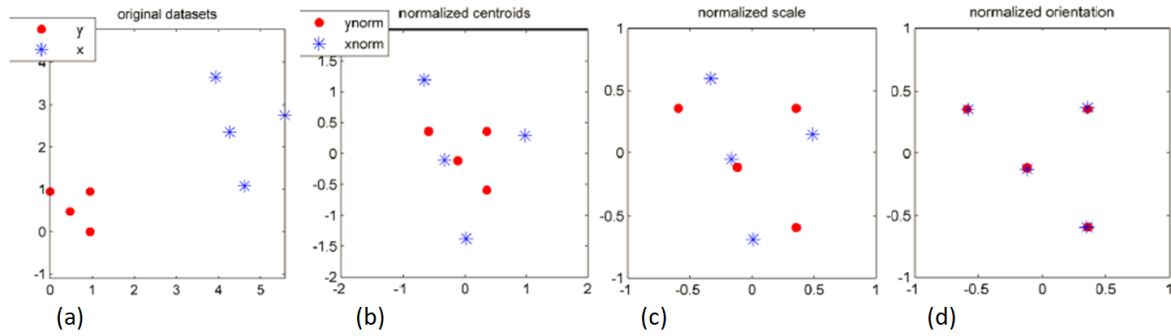


**Figure 13:** Principle of Procrustes transformation (a) original datasets, (b) normalized centroids by translation, (c) normalized size by scaling, (d) normalized orientation by rotation. [38]

For each of the 28 images of the polymer clay model, co-occurrence matrices have been calculated in eight directions relative to the pixel of interest as described in section 2.1.4 “Quantification of contrast and texture”. Mean values for co-occurrence matrix (CM) contrast, correlation, energy and homogeneity over the eight directions were calculated for each spectrum. The results are shown in table III in appendix 7.4. The top 3 of best performing spectra as classified by the four co-occurrence descriptors have been provided in table 3. High values for CM contrast and correlation indicate successful texture quantification. Energy and homogeneity are inversely correlated with texture visualisation, therefore the top 3 in these categories consist of the five lowest values.

**Table 3:** Top 3 best performing spectra for surface texture visualisation, according to the four co-occurrence matrix descriptors. Values of the co-occurrence matrix descriptors and corresponding spectrum numbers (#) are given.

Top 3	CM contrast	#	Correlation	#	Energy	#	Homogeneity	#
1	0.1456	9	0.7901	3	0.9383	8	0.9877	8
2	0.1427	8	0.7870	9	0.9400	7	0.9878	9
3	0.1277	7	0.7846	7	0.9403	9	0.9882	7
<b>Worst spectrum</b>	0.0010		0.1999		0.9996		0.9999	

Using spectrum 9, 7 and 8 results in the best surface texture visualisation. A representation of the wavelengths of these spectra is given in figure 14. All these spectra contain a broad range of wavelengths.

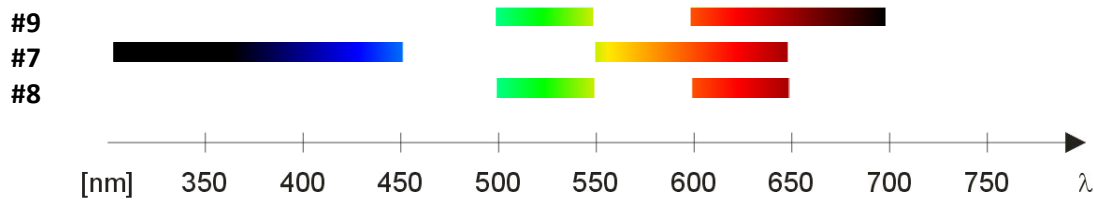


**Figure 14:** Spectra that perform the best surface texture visualisation.

The values for CM contrast, correlation, energy and homogeneity were correlated to the measured values for spectrum intensity and tested to see whether a significant correlation between the intensity of the illuminating spectrum and the descriptors of the co-occurrence matrices exists. Correlation was quantified by calculating the Pearson linear correlation coefficient  $\rho$ . The ranges of  $\rho$  are -1 to 1. Values close to -1 indicate perfect negative correlation, values close to 1 indicate perfect positive correlation. A value of zero means that there is no linear correlation between two values. The corresponding p-value tests the hypothesis of no correlation against the alternative hypothesis of a nonzero correlation. If the p-value is smaller than 0.05, then the linear correlation coefficient  $\rho$  is significantly different from zero. [39]

As indicated in table 4, the co-occurrence matrix descriptors, which are values for surface texture visualisation, are poorly correlated to the spectrum intensity. [40] With p-values larger than 0.05, the zero hypothesis of no correlation between the variables could not be rejected.

**Table 4:** Linear correlation coefficient  $\rho$  and corresponding p-value for the correlation between the co-occurrence matrix descriptors and spectrum intensity.

Co-occurrence matrix descriptor	Linear correlation coefficient $\rho$	p-value
CM Contrast	0.073	0.717
Correlation	0.247	0.213
Energy	-0.095	0.638
Homogeneity	-0.135	0.503

The values for CM contrast, correlation, energy and homogeneity were also correlated to the measured values of the peak width in the colour histogram. Histograms were created for the RGB colour channels. The width of the peaks of the histogram indicate the ranges of the colour channels that are being used. The width of the red, green and blue peaks above a threshold were summed to analyse the width of the total of channels. The resulting sum of the peak widths is provided in table IV in appendix 7.4.

As indicated in table 5, the co-occurrence matrix descriptors, which are values for surface texture visualisation, are moderately to strongly correlated to the sum of the width of the R, B and peaks. [40] As expected, CM contrast and correlation are positively correlated with the histogram peak width, while energy and homogeneity are negatively correlated with the histogram peak width. With p-values smaller than 0.05, the zero hypothesis of no correlation needs to be rejected, meaning that the correlation coefficients are significantly different from zero.



**Table 5:** Linear correlation coefficient  $\rho$  and corresponding  $p$ -value for the correlation between the co-occurrence matrix descriptors and width of the R+G+B histogram peak.

Co-occurrence matrix descriptor	Linear correlation coefficient $\rho$	$p$ -value
CM Contrast	0.788	$\ll 0.01$
Correlation	0.625	$\ll 0.01$
Energy	-0.804	$\ll 0.01$
Homogeneity	-0.836	$\ll 0.01$

### 2.3.1.2 Quantifying surface texture in bronchoscope images

This experiment was done using the polymer clay phantom as depicted in figure 11a. The images shown in figure 15 were obtained using a clinical setup with the E1990i HD bronchoscope and the EPK-i7010 processor from Pentax Medical (Tokyo, Japan). [20][18] The images were obtained in twin-mode, meaning that the optical enhancement filter is applied every other image frame. This alteration is done with a frequency of 30 Hz. Since the displacement of the distal tip of the bronchoscope is minimal between these timeframes, the images are directly comparable without Procrustes transformation.

A region of interest was manually selected in one of the images and copied to the other images. For each of the four settings (WLB, OE1, WLB and OE2), eight co-occurrence matrices have been calculated as described by the equations in section 2.1.4 “Quantification of contrast and texture”. Mean values for CM contrast, correlation, energy and homogeneity over the eight directions were calculated for each of the four measurements. The resulting mean values of co-occurrence descriptors are given in table 6 and do not indicate an evident superior spectrum for texture visualisation. Only little variations in surface quantifications were observed.

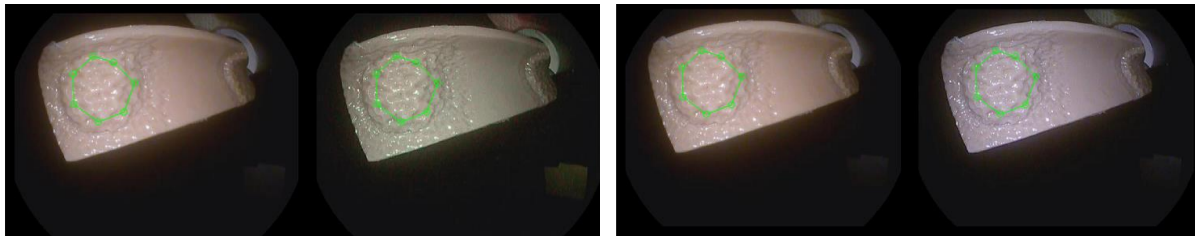


**Figure 15a:** Twin mode image of polymer clay model. WLB1 on the left, OE1 on the right.

**Figure 15b:** Twin mode image of polymer clay model. WLB2 on the left, OE2 on the right.

**Table 6:** Co-occurrence matrix descriptors for white light, OE1 and OE2 spectra.

Light setting	CM Contrast	Correlation	Energy	Homogeneity
WLB1	0.0296	0.7300	0.9817	0.9964
OE1	0.0215	0.7504	0.9830	0.9967
WLB2	0.0313	0.7184	0.9825	0.9963
OE2	0.0312	0.7225	0.9811	0.9964

### 2.3.2 Capillary vessels

#### 2.3.2.1 Quantifying capillary vessel RGB contrast in a porcine trachea

This experiment was done using the porcine trachea phantom as depicted in figure 11b. The phantom was illuminated consecutively by the 28 different light spectra as shown in section 2.2.2 “Spectra for optical testing”. The collected data consists of 28 images of the phantom and 28 spectrometer measurements.

A region of interest and a region of reference were manually selected in one image as shown in figure 16. The regions of interest were transposed to the other 27 images using Procrustes transformation on manually selected reference points. This enables similar positioning and comparison of the images.

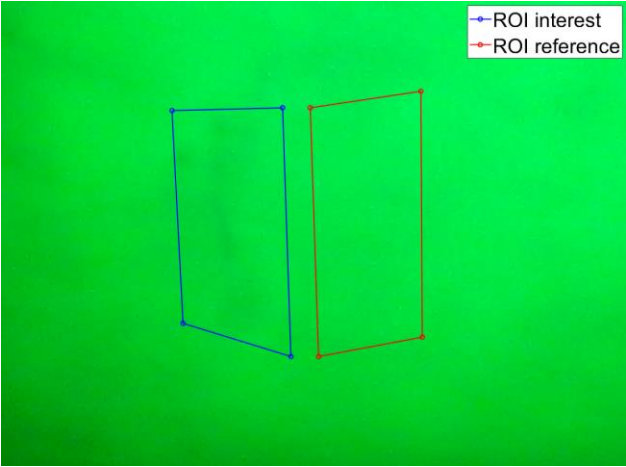


**Figure 16:** Region of interest around a capillary vessel and a region of reference on the background mucosa indicated in an image of porcine trachea. Image obtained during illumination by spectrum 10 with wavelength bands between 500 – 550 nm and 650 – 700 nm.

For the pixels within these regions of interest, the colour values were determined in the RGB colour space. A mean colour of the capillary ROI and a mean colour of the background ROI was calculated. The 3D distance between the mean colour in the ROI of interest and the mean colour in the ROI of reference was computed and is a quantification for the colour difference. The 3D colour distances and the contrast in three RGB colour channels for all 28 pictures can be found in table V in appendix 7.4. The top 3 of best performing spectra as classified by the 3D colour distance in RGB colour space have been provided in table 7. A large 3D distance between the mean colour of the capillary and the mean colour of the background represents a big colour contrast indicating favourable capillary visualisation.

**Table 7:** Top 3 best performing spectra for capillary visualisation, according to the 3D distance in RGB colour space. Values for 3D distance and corresponding spectrum numbers are given.

Top 3	3D RGB distance	Spectrum #
1	33.1114	7
2	31.7750	1
3	30.5616	A3
<b>Worst spectrum</b>	1.0665	

Using spectrum 7, 1 and A3 results in the best capillary vessel visualisation. A representation of the wavelengths of these spectra is given in figure 17. Spectrum 7 and spectrum 1 contain blue wavelengths. It is remarkable that spectrum 1 and spectrum A3 perform nearly similar, but do not have any overlap in wavelengths.

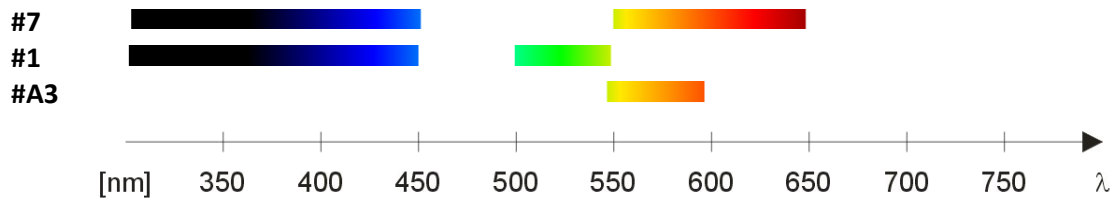


**Figure 17:** Spectra that perform the best capillary vessel visualisation.

Since it was hypothesized that spectra containing blue light perform better in capillary visualisation, a two sample t-test was performed. [39] Spectra 1 – 7, 17, B1, M1, M3 and A1 contain blue light. Spectra 8 – 16, B2, B3, M2 and A2 – A5 do not contain blue light. The spectra containing blue light resulted in a mean 3D distance of  $21.0954 \pm 9.8454$  while the spectra not containing blue light resulted in a mean 3D distance of  $19.4211 \pm 8.5947$ . The zero hypothesis of no variance between the groups could not be rejected because the difference in means between the two groups was not significant.

The values for three-dimensional RGB distance and the three individual colour channels were correlated to measured values of spectrum intensity to assess a significant correlation between the intensity of the illumination and the measures of contrast.

As indicated in table 8, the three-dimensional distance in colour space and the contrast in the individual colour channels are poorly correlated with the intensity of the illumination. With p-values larger than 0.05, the zero hypothesis of no correlation between the variables could not be rejected.

**Table 8:** Linear correlation coefficient  $\rho$  and corresponding p-value for the correlation between the RGB contrast quantifications and spectrum intensity.

3D distance or channel colour quantification	Linear correlation coefficient $\rho$	p-value
3D RGB distance	0.130	0.509
Red channel	-0.050	0.801
Green channel	0.249	0.201
Blue channel	0.138	0.486

### 2.3.2.2 Quantifying capillary vessel RGB contrast in bronchoscope images

This experiment was done using the underside of a living human tongue as a phantom. The images were obtained using a clinical setup with the E1990i HD bronchoscope in combination with the EPK-i7010 processor from Pentax Medical (Tokyo, Japan). [20][18] The images were obtained in twin mode and can be seen in figure 18.

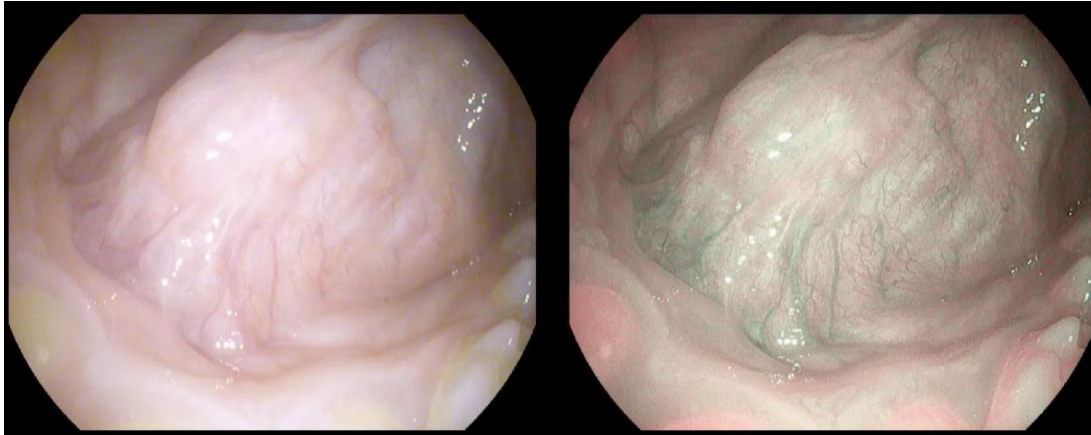


**Figure 18a:** Twin mode image of the underside of a living human tongue. WLB left, OE1 right.

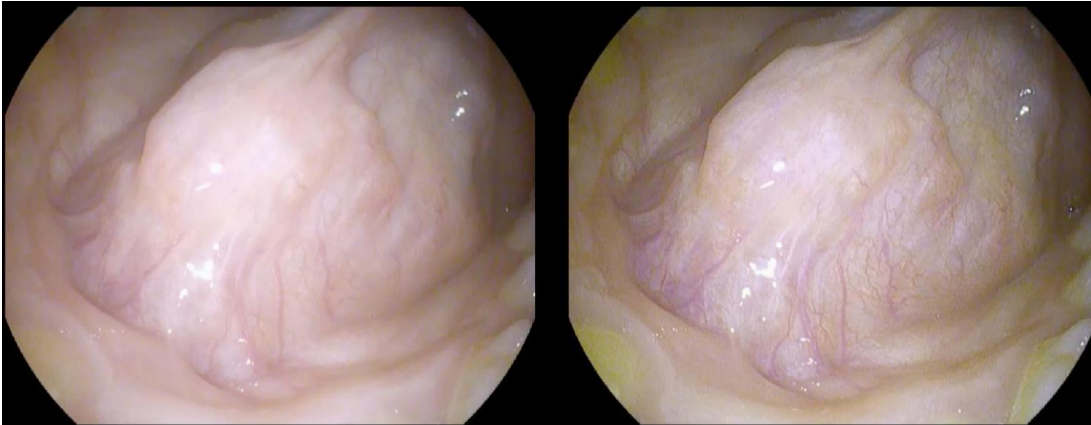


**Figure 18b:** Twin mode image of the underside of a living human tongue. WLB left, OE2 right.

A region of interest around a capillary vessel and a region of reference in an adjacent mucosal area were manually selected in one of the images. Since the tongue moves in between measurements, these selections were transposed using Procrustes transformation based on manually indicated reference points. For each of the four settings (WLB, OE1, WLB and OE2), the mean RGB colour has been calculated for the region of interest and the region of reference. The 3D distance in colour space between the region of interest and region of reference was calculated to classify the contrast between capillaries and surrounding mucosa. The resulting values are given in table 9. Both optical enhancement settings lead to an increase in 3D distance in the RGB colour scale.

**Table 9:** Capillary contrast as classified by the 3D distance in the RGB colour space for different bronchoscope settings.

Light setting	3D distance between colour of interest and colour of reference in RGB
WLB1	13.2959
OE1	22.9776
WLB2	7.6709
OE2	13.6446

### 2.3.3 Deep veins

These experiments were done using the back of a living human hand as a phantom (figure 11c). The phantom was illuminated consecutively by the 28 different light spectra as shown in section 2.2.2 “Spectra for optical testing”. The collected data consisted of 28 images of the phantom.

#### 2.3.3.1 Quantifying vein RGB contrast on the back of a human hand

In one image, a region of interest for a deep vein and a region of reference for the surrounding tissue were indicated as shown in figure 19. Three reference dots were placed on the phantom to allow for position alignment using Procrustes transformation.

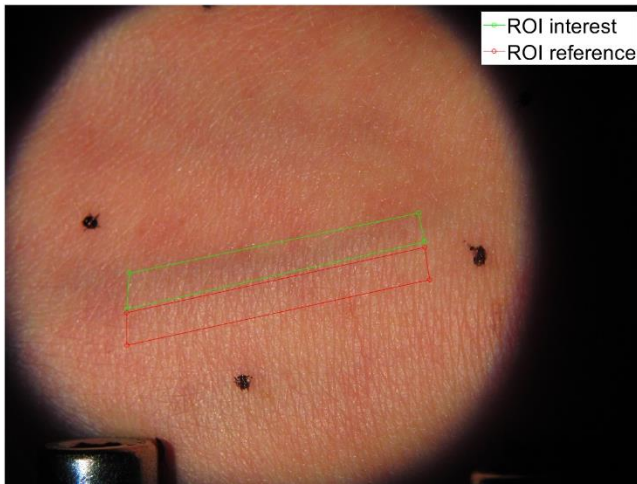


**Figure 19:** Black reference dots, region of interest in green around a deep vein and region of reference in red on the background.

For the pixels within these regions of interest, the colour values were determined in RGB colour space. A mean colour of the deep vein ROI and a mean colour of the background ROI were calculated. The 3D distance between the mean colour in the ROI of interest and the mean colour in the ROI of reference was computed and is a quantification for the colour difference. The 3D colour distances and the contrast in three RGB colour channels for all 28 pictures can be found in table VI in appendix 7.4. The top 3 of best performing spectra as classified by the 3D colour distance in RGB colour space have been provided in table 10. A large 3D distance between the mean colour of the vein and the mean colour of the background represents a big colour contrast indicating favourable deep vein visualisation.

**Table 10:** Top 3 best performing spectra for deep vein visualisation, according to the 3D distance in RGB colour space. Values for 3D distance and corresponding spectrum numbers are given.

Top 3	3D RGB distance	Spectrum #
1	26.6567	4
2	25.0291	7
3	24.7438	9
<b>Worst spectrum</b>	0.8353	

Using spectrum 4, 7, and 9 results in the best deep vein visualisation. A representation of the wavelengths of these spectra is given in figure 20.

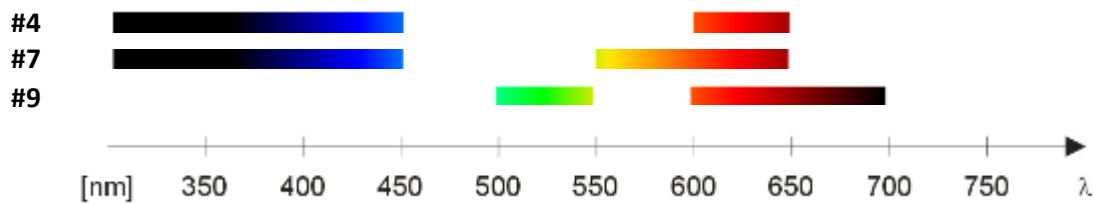


**Figure 20:** Spectra that perform the best deep vein visualisation.

Since it was hypothesized that spectra containing red light perform better in deep vein visualisation, a two sample t-test was performed. [39] Spectra 4 – 17, B3, M3, A4 and A5 contain red light. Spectra 1 – 3, B1, B2, M1, M2 and A1 – A3 do not contain red light. The spectra containing red light resulted in a mean 3D distance of  $17.9328 \pm 5.4377$  while the spectra not containing red light resulted in a mean 3D distance of  $11.4472 \pm 8.4080$ . The zero hypothesis of no variance between the groups could be rejected with a p-value of 0.020 and the difference in means between the two groups was therefore proven to be significant.

The values for three-dimensional RGB distance and the three individual colour channels were correlated to measured values of spectrum intensity to assess a significant correlation between the intensity of the illumination and the measures of contrast. As indicated in table 11, the three-dimensional distance in colour space and the contrast in the individual colour channels are poorly correlated with the intensity of the illumination. With p-values larger than 0.05, the zero hypothesis of no correlation between the variables could not be rejected.

**Table 11:** Linear correlation coefficient  $\rho$  and corresponding p-value for the correlation between the contrast quantifications and spectrum intensity.

3D distance or channel colour quantification	Linear correlation coefficient $\rho$	p-value
3D RGB distance	0.184	0.350
Red channel	0.277	0.154
Green channel	0.242	0.214
Blue channel	-0.054	0.784

### 2.3.3.2 Quantifying vein RGB contrast using bronchoscope images

The images were obtained using a clinical setup with the E1990i HD bronchoscope in combination with the EPK-i7010 processor from Pentax Medical (Tokyo, Japan). [20][18] The images were obtained in twin mode and can be seen in figure 21. Regions of interest around a deep vein were selected and are indicated in green. Regions of interest around the background skin were selected and indicated in red. Five reference dots were placed to allow for Procrustes position transformations of the regions of interest.

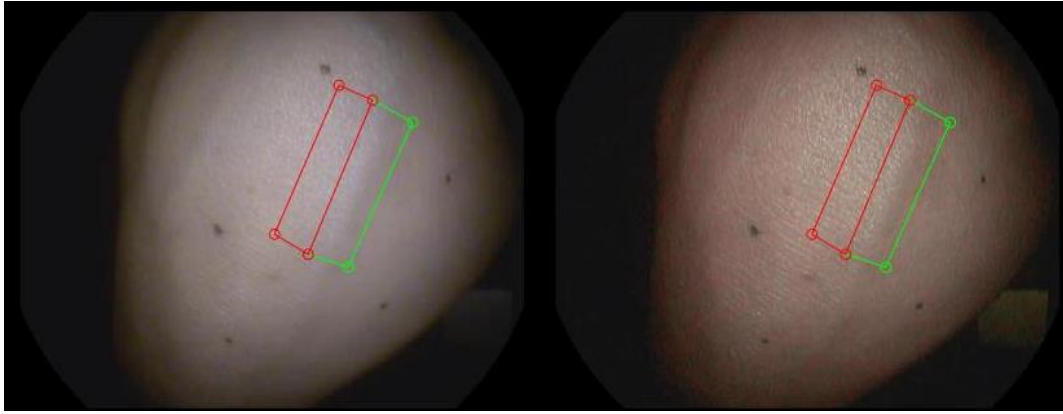


**Figure 21a:** Twin mode image of the back of a human hand. WLB left, OE1 right. Vein indicated with green, background indicated with red.

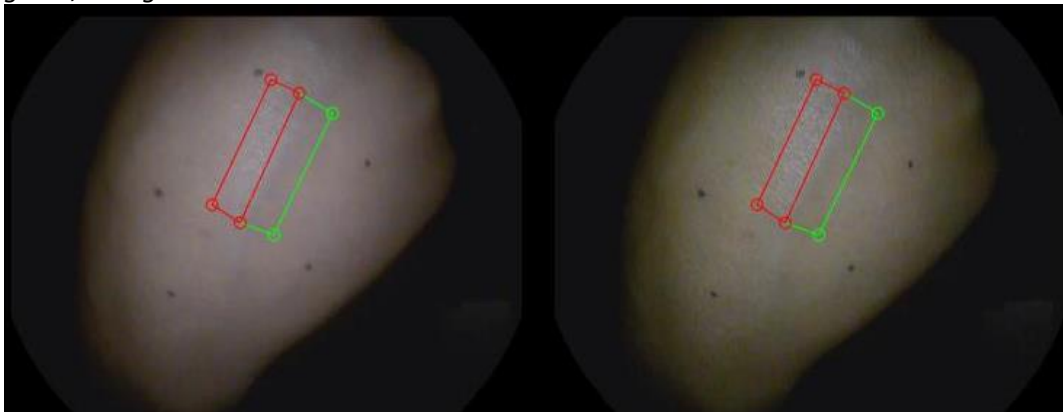


**Figure 21b:** Twin mode image of the back of a human hand. WLB left, OE2 right. Vein indicated with green, background indicated with red.

For each of the four settings (WLB, OE1, WLB and OE2), the mean RGB colour has been calculated for the region of interest and the region of reference. The 3D distance in colour space between the region of interest and the region of reference was calculated to classify the contrast between deep veins and surrounding tissue. The resulting values are given in table 12. Only optical enhancement mode 2 leads to an increase in 3D distance compared to white light bronchoscopy. It is remarkable that OE mode 1 and OE mode 2 show high differences between 3D distance in RGB colour space.

**Table 12:** Deep vein contrast as classified by the 3D distance in the RGB colour space for different bronchoscope settings.

	3D distance between colour of interest and colour of reference in RGB
WLB1	29.9157
OE1	30.6774
WLB2	16.3897
OE2	20.8863

## 2.4 Discussion and conclusion

### 2.4.1 Optical setup

The first aim of this chapter was to investigate which *ex vivo* optical setup can mimic the optical enhancement settings and alter the spectrum of the emitted light. The setup with two incandescence lights, highpass and lowpass optical filters as shown in figure 10, has been the most effective and feasible in achieving this goal. The spectrum of the incandescence lamps closely resembles the spectrum of the xenon lamp as used in a clinical bronchoscope processor.

Since the optical filters were available with intermediate steps of 50 nm, the concession was made to lose the possibility to vary the spectrum with steps smaller than 50 nm. It can be concluded that it is possible to design an optical setup that can produce an alterable spectrum. But since the variability of the wavelengths is limited, a perfect resemblance of the optical enhancement spectrum was not achieved.

### 2.4.2 Visualisation of surface texture

Spectrum 9, 7 and 8 are the best spectra for surface visualisation (figure 22). These spectra contain a broad range of wavelengths. It was hypothesized that light intensity is positively and linearly correlated with successful texture visualisation. However, the texture visualisation quantifications were found to be poorly correlated to the spectrum intensity ( $\rho = 0.073, 0.247, -0.095, -0.135$ ). With p-values above 0.05, the zero hypothesis of no correlation between the variables could not be rejected. This result can be explained by the high variability in spectrum intensity measurements. The USB spectrometer is a sensitive instrument and is prone to measurement errors. When inspecting the values for spectrum intensity for the measurement of the polymer clay model and the porcine bronchus (Table II in appendix 7.4), the values differ a lot while the emitted spectra are supposed to be the same in both experiments. In future experiments, a plausible hypothesis for the relationship between surface visualisation and light intensity is a negative quadratic relationship. A certain level of light intensity is required to realise any surface texture visualisation at all. When increasing the light intensity, crevices of the texture phantom will get illuminated and surface texture visualisation increases. However, the visualisation starts to worsen when the amount of specular reflections increases, and the object gets overexposed by light. It would be best to assess this hypothesis by generating images of the phantom using the same illumination spectra while altering its intensity.

It was hypothesized that the histogram peak width is positively correlated with successful texture visualisation. The texture visualisation quantifications were indeed moderately to strongly correlated ( $\rho = 0.788, 0.625, -0.804, -0.836$ ) to the spectrum intensity. With p-values  $\ll 0.01$ , the zero hypothesis of no correlation needs to be rejected, meaning that the found correlation coefficients are significantly different from zero. A wide range in the RGB colour histogram is associated with successful texture visualisation. This significant relationship also supports the visual interpretation that spectrum 9, 7 and 8 contain a broad range of wavelengths.

Regarding the measurements with the clinical bronchoscope setup, an evident superior spectrum for texture visualisation was not indicated. Only little variations in surface quantifications were observed. The lack of difference in RGB contrast visualisation between these illumination modes can be explained because the polymer clay phantom is not made from living tissue and therefore does not contain multiple layers that can react differently to different wavelengths of light.



### 2.4.3 Visualisation of capillary vessels

Spectrum 7, 1 and A3 are the best spectra for capillary vessel visualisation (figure 22). It is remarkable that spectrum A3 does not contain any blue wavelengths while it was hypothesized that spectra containing blue light would perform the best capillary visualisation. [17] This discrepancy was assessed by testing if there was a significant difference between the group of spectra containing blue wavelengths, and the group of spectra not containing blue wavelengths. No significant difference in capillary vessel visualisation could be found between the groups ( $p = 0.636$ ). An explanation for this insignificant difference can be found in the porcine tracheal phantom that was used. When comparing the porcine trachea specimen to the *in vivo* conditions in humans during bronchoscopy, an unrepresentative low number of capillaries were present in the porcine trachea. It was attempted to use other parts of the porcine airway system, but there was no piece of airway available that had more visible capillaries than the trachea. This can be explained because the *ex vivo* porcine tracheal tissue is not perfused. Due to the few capillaries in the phantom, the region of interests that were used were small, making them prone to measurement artefacts.

The relationship between capillary vessel visualisation and spectrum intensity was assessed. Positive linear correlation between contrast quantification and spectrum intensity was expected. However, the RGB contrast quantifications were poorly correlated ( $\rho = 0.130, -0.050, 0.249, 0.138$ ) to the spectrum intensity. With p-values above 0.05, the zero hypothesis of no correlation between the variables could not be rejected. This observation can be explained by the unrepresentative low number of capillaries that were present in the porcine trachea. When it is desired to assess the effect of light intensity on the visualisation of capillaries, different intensities of the same spectrum can be applied to a phantom with more capillaries to assess whether the capillary contrast is linearly correlated to the light intensity.

Regarding the measurements with the clinical bronchoscope setup on the underside of the human tongue, both optical enhancement settings lead to an increase in capillary RGB contrast compared to white light bronchoscopy. However, a large difference between the two white light images was seen. This inaccuracy is assumed to be caused by inaccurate region of interest selection, caused by the Procrustes transformation based on manually indicated reference points. Redefining the regions of interest did not help in minimizing this discrepancy. It is recommended to repeat these experiments with the clinical bronchoscopy system to assess whether this inaccuracy is always present.

### 2.4.4 Visualisation of deep veins

Spectrum 4, 7 and 9 are the best spectra for deep vein visualisation (figure 22). All these spectra contain wavelengths of red light, but the top 3 is followed by spectra that do not contain red wavelengths. It was hypothesized that spectra containing red light would perform the best deep vein visualisation because red wavelengths penetrate in tissue as the deepest of all visible wavelengths. [17] This hypothesis was assessed by testing if there was a significant difference between the group of spectra containing red wavelengths, and the group of spectra not containing red wavelengths. A significant difference in deep vein vessel visualisation could be found between the groups ( $p = 0.020$ ).

The relationship between deep vein visualisation and spectrum intensity was assessed. It was expected that the deep vein visualisation would be correlated to the intensity of the applied spectrum. However, the RGB contrast quantifications were poorly correlated ( $\rho = 0.1836, 0.2768, 0.2423, -0.0542$ ) to the spectrum intensity. With p-values above 0.05, the zero hypothesis of no correlation between the variables could not be rejected. This observation can be explained by the high variability in spectrum intensity measurements.

Regarding the measurements with the clinical bronchoscope setup on the back of the human hand, only optical enhancement mode 2 lead to an increase in deep vein RGB contrast. Since this optical enhancement mode contains a band of red light, this finding is in line with the hypothesis. However, a large difference between the two white light images was seen. This inaccuracy is assumed to be caused by inaccurate region of interest selection, caused by the Procrustes transformation based on manually indicated reference points. Redefining the regions of interest did not help in minimizing this discrepancy. It is recommended to repeat these experiments with the clinical bronchoscopy systems to assess whether this effect is always present.

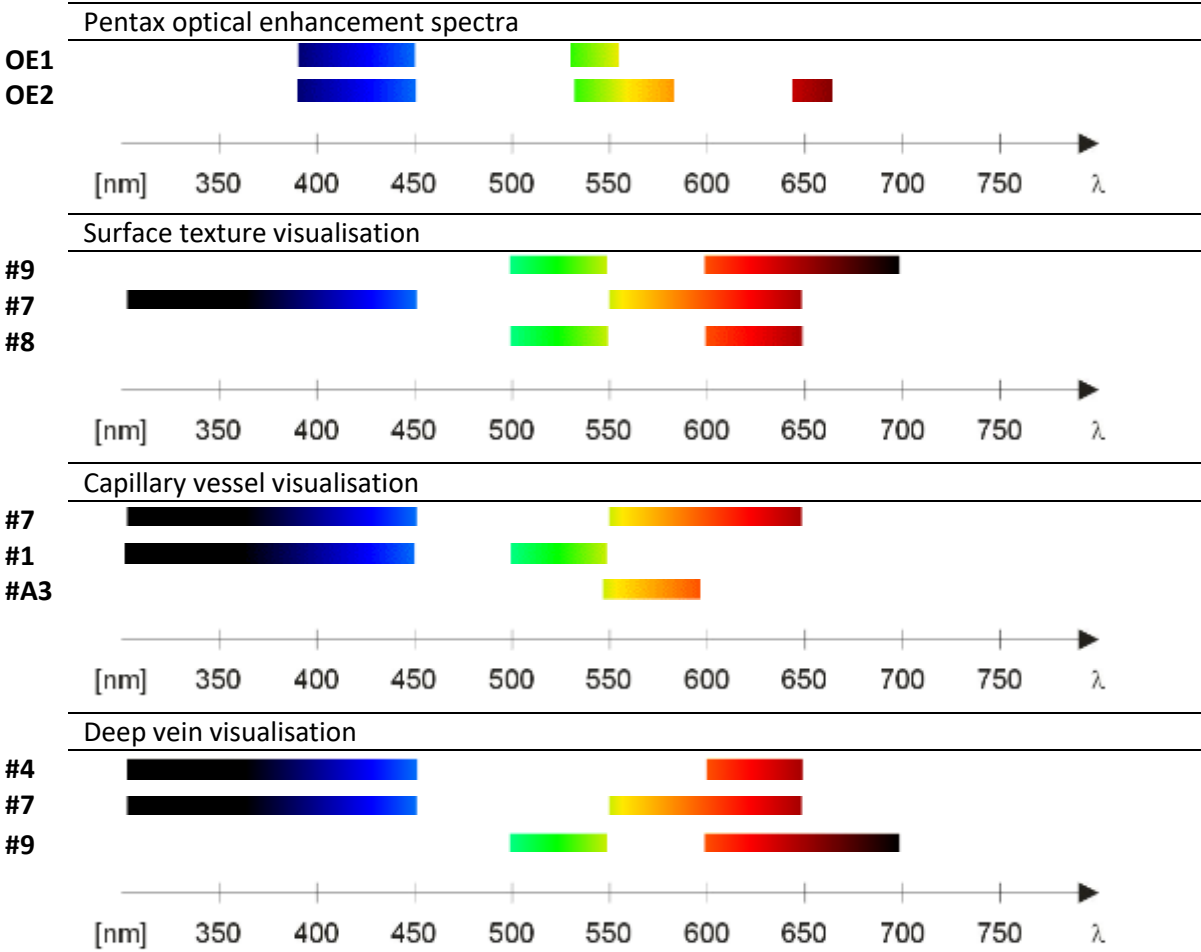


Figure 22: Overview of most successful spectra for surface texture, capillary vessels and deep veins.

#### 2.4.5 General conclusions

The setup with two incandescence lights, highpass and lowpass optical filters as shown in figure 10, has been the most effective and feasible in mimicking the optical enhancement settings and altering the spectrum of the emitted light.

Using a spectrum with a broad range of wavelengths ensures the best surface texture visualisation. As expected, the width of the peaks in the colour histogram of the image and the quantifications of texture visualisation were significantly correlated. Blue light was thought to be essential for capillary visualisation, but this could not be significantly proven. This can be explained by the unrepresentative low number of capillaries that were present in the porcine trachea phantom that was used. As expected, red light was significantly proven to be essential for deep vein visualisation. There was no significant correlation between the visualisation of texture, capillary vessels or deep vein visualisation and the total intensity of light used to illuminate the phantoms. This result can be explained by the high variability in spectrum intensity measurements. When it is desired to determine the effect of light intensity on the visualisation of surface structure, capillary vessels, and deep veins, different intensities of the same spectrum can be applied.

It should be noted that the spectra that are classified by the optical experiments as the best spectra, also appear that way to the naked eye when inspecting the phantom images. This qualitative analogy indicates that the methods used for analysis are effective in selecting favourable spectra for the visualisation of surface texture, capillaries and veins.

The optical enhancement spectra as commercially available by Pentax are suitable for the application of central airway diagnostics in bronchoscopy. Quality of central airway diagnoses was quantified in the visualisation of surface texture, capillaries and deep veins. The optical enhancement spectra by Pentax contain the essential wavelengths for capillary and vein visualisation. Further, the intensity of the light of the clinical bronchoscopy setup is adequate. Because of the large intermediate steps in the adaptable spectra that were used, it was not possible to create a spectrum that performed better than the commercially available optical enhancement spectra. Using optical highpass and lowpass filters with smaller intermediate steps can ensure a closer imitation of the commercially available spectra.

From the results of this study, there are no reasons to disapprove the Pentax optical enhancement spectra for application in bronchoscopy. The created spectra resemble the Pentax optical enhancement spectra close enough to let the *ex vivo* conclusions from this experiment serve as a justification to assess the Pentax optical enhancement spectra *in vivo* in patients.

### 3 Improvement of bronchoscopy interpretation

In this chapter, the potential clinical benefits of the application of optical enhancement in the interpretation of bronchoscopy are studied. A patient file research into bronchoscopy complications gives insight in the current pitfalls of bronchoscopy that provide possible clinical applications for optical enhancement. A case-series of bronchoscopy patients illustrates which additional information is present in optical enhancement images. This chapter aims to assess the following questions:

- What are the incidences and causes of complications in bronchoscopy in the Radboudumc hospital in Nijmegen?
- Which challenging aspects of bronchoscopic visualisation can potentially be improved by the application of optical enhancement?
- For which aspects of bronchoscopic visualisation do optical enhancement images carry additional information compared to white light bronchoscopic images?

#### 3.1 Introduction

The appearance of bronchial tissue during bronchoscopy is different when using adapted light settings. It has been explained in section 1.2.3 “Optical enhancement” that red light penetrates deeper into tissue than blue light and the depth of the vessels corresponds with the fraction of certain colours of light that reach these vessels.

White light bronchoscopy contains all visible wavelengths. The summation of this light looks white. Optical enhancement mode 1 contains blue and green wavelengths. Optical enhancement mode 2 contains blue, green and red bands of wavelengths. In the central bronchi, certain structures appear different in the different illumination methods. As can be seen in figure 23, especially the vascular bed appears different in OE mode 1 and OE mode 2 compared to white light bronchoscopy. (green arrows) Further, longitudinal bands in the bronchi are visualised different in the optical enhancement pictures compared to white light bronchoscopy. (orange arrows)

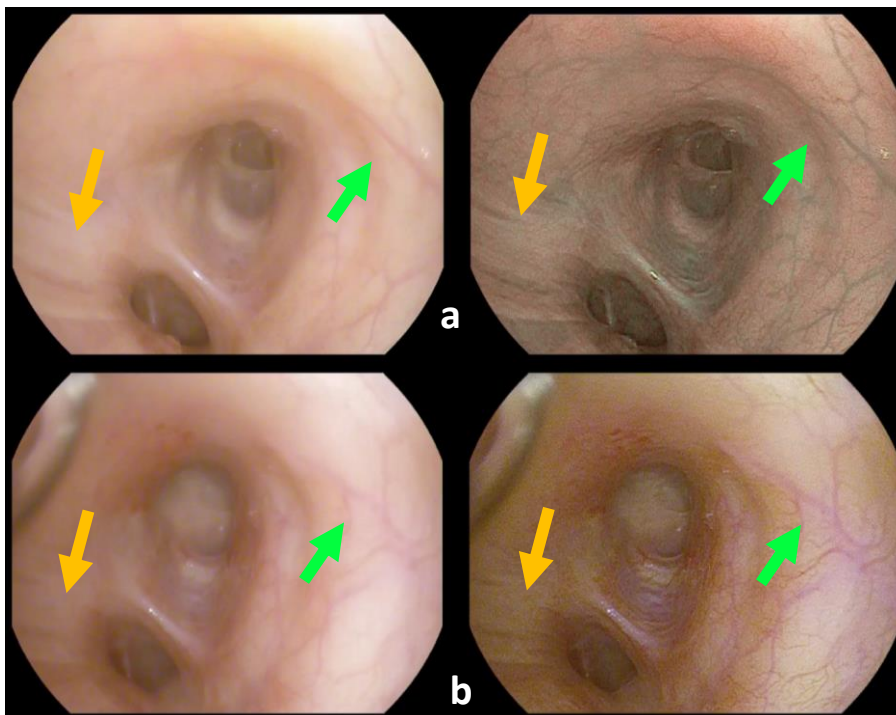


**Figure 23:** Collected endoscopic images from healthy patients. (a) White light bronchoscopy left twin image with OE mode 1 right. (b) White light bronchoscopy left twin image with OE mode 2 right. Vascular beds are indicated by the green arrows. Longitudinal bands are indicated by the orange arrows.

## 3.2 Complication registration

### 3.2.1 Methods complication registration

Patient selection was done using the medical file research program CTcue (CTcue B.V., Amsterdam, the Netherlands). Bronchoscopy procedures between January 1<sup>st</sup> 2018 and June 30<sup>th</sup> 2019 in the categories “Interventie bronchoscopie”, “Therapeutische bronchoscopie”, “Interventie long” or “Spoed interventie bronchoscopie” were included. These four search cues resulted in fifteen procedure descriptions which are all synonyms for intervention bronchoscopies. Bronchoscopy procedures without the presence of a procedure report “OK verslag” or “Scopieverslag” were excluded. This resulted in a list of bronchoscopy procedures that was downloaded from CTcue. The procedures without a hospital registration number were excluded.

The remaining bronchoscopy reports were opened in the digital patient file. When the procedure had been ordered but had not been executed, it was excluded from analysis. An additional number of 30 bronchoscopy procedures has been found in patient files that were listed only once in the CTcue list, while the patient underwent multiple bronchoscopies. These procedures were included in the analysis.

### 3.2.2 Results complication registration

#### 3.2.2.1 Patient inclusion

The patient selection resulted in the inclusion of 176 bronchoscopy reports amongst 132 unique patients, see CONSORT (consolidated standards of reporting trials) flow diagram in figure 24. The bronchoscopy reports were read by the author of this report. The occurrence and cause of reported complications were registered. Besides the clinical complications, all challenging aspects of bronchial wall visualisation that were listed in the bronchoscopy reports were registered. These challenging aspects indicate the potential added value of the application of optical enhancement in intervention bronchoscopy.

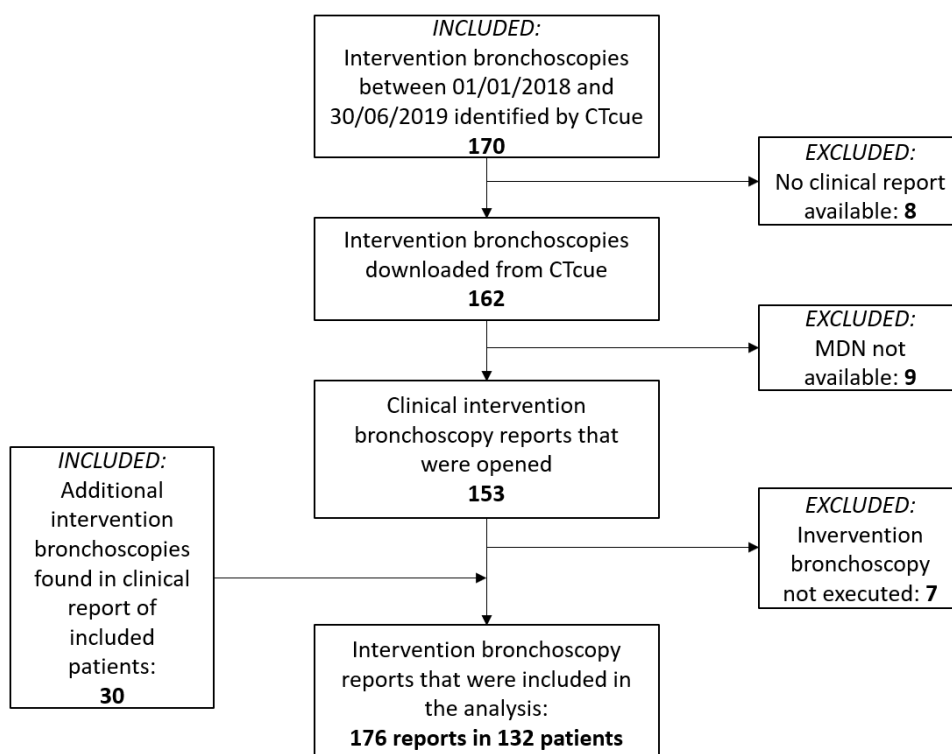


**Figure 24:** CONSORT flow diagram for the intervention bronchoscopy complication file research.

### 3.2.2.2 Numerical results complication registration

In this complication registry, 176 bronchoscopy reports amongst 132 unique were analysed. A number of 102 patients underwent a single bronchoscopy. The remaining 30 patients underwent multiple bronchoscopies in the eighteen-month timeframe. The 176 bronchoscopy procedures were categorized as 45 stent placements, 13 stent removals, 1 stent repositioning and 117 procedures without stenting.

The patient population of 132 patients consisted of 54 males and 78 females of which 3 were pregnant. The mean age of the patient population at the time of procedure was  $59.6 \pm 14.28$  years. Of the 132 patients, 20 patients had been registered in the clinical patient file as deceased on the 30<sup>th</sup> of August 2019. The deceased patients had passed away after a mean of 52 days, ranging from 0 to 269 days following their last bronchoscopy. In 13 of the 176 analyses procedures (7.4%), complications occurred. Four of these complications occurred during a stent placement procedure. The descriptive results will cover the origins of these complications.

### 3.2.2.3 Descriptive results complication registration

The registered complications were caused by various reasons as shown in table 13. Especially endobronchial bleeding and bronchial damage or perforation can be prevented by improving the visibility of structures in the bronchial wall. Besides the registered complications, all challenging aspects of bronchial wall visualisation were registered. These challenging aspects indicate the potential added value of the application of optical enhancement and are shown in table 14.

**Table 13:** Causes of complications during intervention bronchoscopy.

<i>Endobronchial bleeding</i>
Post procedural bleeding for which re-intervention was indicated
Heavy endobronchial bleeding of 400 mL for which coagulation and application of adrenalin was indicated
Heavy endobronchial bleeding of 800 mL causing substantial desaturation
Heavy endobronchial bleeding causing substantial desaturation and occlusion of bronchus
<i>Bronchial damage</i>
Damage of bronchial cartilage ring
Damage of bronchial wall needing covering with bronchial stent
<i>Desaturation</i>
Substantial desaturation after cryobiopsy causing procedure termination
Substantial desaturation caused by an occluded bronchus with a blood clot
<i>Cardiac complication</i>
Bradycardia and hypertension during cryoablation
Temporary intraprocedural electrocardiography (ECG) change revealing unknown cardiac abnormalities
<i>Technical difficulties</i>
Power supply failure
Failed stent placement despite multiple attempts of repositioning
Technical failure of stent loader
<i>Other</i>
Damage of upper jaw caused by rigid tube manipulation

**Table 14:** Challenging aspects of bronchial wall visualisation.

<i>Visualising endobronchial processes</i>
Visualising the margins of tumours and polyps before, during and after coagulation. Visualising the depth of tumour invasion in the bronchial wall. Improved visualisation of mucosal, polyp and diffuse metastatic surface texture. Visualisation of vascular abnormalities that otherwise might go unnoticed.
<i>Placement of intervention devices to prevent bleeding</i>
Strategic placement of cryobiopsies, forceps biopsies and coagulation probes to prevent bleeding. Strategic placement of diathermic needle knife incisions to prevent bleeding during dilatation of bronchial stenosis.
<i>Avoiding weak spots</i>
Avoiding contact with mucosa, polyps and tumours vulnerable for bleeding. Visualising thin areas in the bronchial wall and cartilage to prevent perforation. Assessing the vascularization and weak spots on scar tissue and anastomoses.
<i>Supporting endobronchial stenting</i>
Visualisation of stent epithelialisation and granulation to assess the stent quality. Assessing mucosal damage after stent removal.
<i>Other</i>
Improved visualisation of inflammatory, ulcerating, granulating and atrophic tissue. Assessing airway secretions and assessing the activity of nontuberculous mycobacteria infections. Assessing hematomas on vocal cords.

#### 3.2.2.4 Expert interviews

At the pulmonary department of Radboudumc in Nijmegen, two bronchoscopists have specialized into interventional bronchoscopy. These pulmonologists have been asked for potential pitfalls in bronchoscopy which might be prevented when applying optical enhancement imaging. The results of the complication registration as previously described were confirmed by the two expert bronchoscopists. As an addition, the prevention of bleeding caused by scope manipulation in contact with vulnerable tissues offers room for improvement. Visualisation of weak spots with superficial vascularisation is essential to achieve this. Lastly, a promising application of optical enhancement bronchoscopy is the evaluation of the perfusion of bronchial sleeve anastomosis.

### 3.3 Case series

A case series of bronchoscopy images of fourteen patients was analysed to determine for which aspects of bronchoscopic visualisation optical enhancement images carry additional information compared to white light bronchoscopic images.

#### 3.3.1 Methods case series

##### 3.3.1.1 Comparing optical enhancement and white light bronchoscopy images

To determine the tissue structures of which optical enhancement images carry more information, subtraction imaging was performed. Only images acquired in twin mode are suitable for analysis by this method, since the exact same bronchoscope location must be used. By subtracting the RGB pixel values of the white light bronchoscopy image from the optical enhancement spectrum, the resulting image contains information about the difference in colour between the two light settings. This image processing is visualised in figure 25. Structures that are highly different in the OE spectra compared to WLB spectra will be visualised very light (near white) or very dark (near black). Since the results of the subtraction can be positive as well as negative, structures that are exactly the same in both images appear grey. This is the case with the black corners on the outside of the pictures. This technique was used to assess the bronchoscopic images of fourteen patients included in this case series.



**Figure 25:** Image subtraction principle. Central trachea visualised in twin mode with optical enhancement mode 1 (OE1) and white light bronchoscopy (WLB). The subtracted image shows the tracheal arches and the vascular beds. Since the results of the subtraction can be positive as well as negative, pixels that are exactly the same (such as the black corners on the outside of the image) appear grey.

##### 3.3.1.2 Patients without central abnormalities

For the analysis of the visualisation of blood vessels and endobronchial arches, seven patients without central bronchial abnormalities were included in this case series. This group consisted of four male and three female patients. All seven patients underwent a navigational bronchoscopy procedure. During a navigational bronchoscopy, it is attempted to collect diagnostic material of peripheral lung lesions. The central airways of these patients did not show any abnormalities but suspected peripheral malignancies were present in all patients.

A double inspection bronchoscopy was performed using the Pentax OptiVista EPK-i7010 processor combined with the Pentax E1990i HD bronchoscope. [18][21] The images were acquired in twin-mode, meaning that the light source in the bronchoscope processor alternates between white light and the optical enhancement filter. This alteration is done with a frequency of 30 Hz. The first inspection bronchoscopy shows white light bronchoscopy and optical enhancement mode 1 side by side. The second inspection bronchoscopy shows white light bronchoscopy and optical enhancement mode 2 side by side. The videos were exported from the bronchoscope processor directly onto a USB-stick.



The images were analysed using MATLAB 2018a (MathWorks, Natick, United states of America). The visualisation of blood vessels and bronchial arches was assessed.

Subtraction imaging was performed to visually assess the differences in visualisation of endobronchial vessels and arches in optical enhancement compared to white light bronchoscopy. In the images of the seven included patients, regions of interest for blood vessels, bronchial arches and background mucosa were selected on the subtracted images to assess the colour values of these regions. When comparing the regions of interest to the corresponding background mucosa, the additional information that optical enhancement illumination provides about endobronchial vessels and arches can be quantified.

### 3.3.1.3 Patients with central abnormalities

For the analysis of the visualisation of endobronchial processes, seven patients with central bronchial abnormalities were included in this case series. This group consisted of four male and three female patients. All seven patients underwent an interventional bronchoscopy procedure. Data of these patients was acquired and collected in the same manner as the data of the patients without central abnormalities. Subtraction imaging was performed to assess the visualisation of endobronchial lesions in optical enhancement illumination compared to white light bronchoscopy.

## 3.3.2 Results case series

### 3.3.2.1 Patients without central abnormalities

Visualisation of bronchial tissue in optical enhancement mode 1

In figure 26, the subtracted images of optical enhancement mode 1 and white light bronchoscopy are depicted for three endobronchial locations. When visually inspecting these images, more information is provided about the bronchial arches and vascular beds. The increased RGB contrast for both the tracheal arches and the vascular beds are mainly stored in the red channel of the subtracted image. A mask was created from the red channel of the subtracted image by applying digital low and high intensity thresholds. The edges of the selected areas were smoothed by opening and closing with a structuring element. When superimposing the mask over the original WLB image, the structures can be clearly visualised as is seen in figure 27.

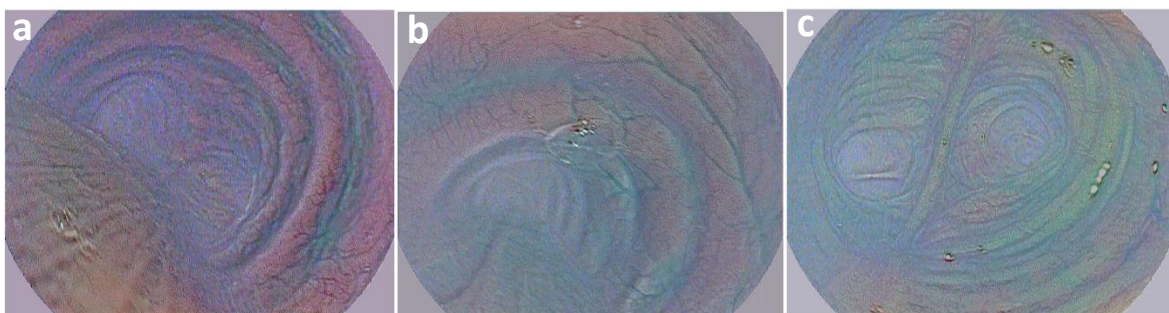


**Figure 26:** Subtraction images of OE mode 1 minus WLB. (a) Central trachea. (b) Vascular bed of the left main bronchus. (c) Bronchial structure at the deepest point that a 19 French scope can access.



**Figure 27:** Superimposed mask obtained from the red channel of the OE1 minus WLB subtraction image. The red areas indicate the superimposed mask over the original WLB image. (a) Central trachea. (b) Vascular bed of the left main bronchus. (c) Bronchial structure at the deepest point a 19 French scope can access.

#### Visualisation of bronchial tissue in optical enhancement mode 2

In figure 28, the subtracted images of optical enhancement mode 2 and white light bronchoscopy are depicted for three endobronchial locations. When visually inspecting these images, little added information is provided about the bronchial arches. Especially the vascular beds are clearly visible in the subtracted images. This is visualised in the subtracted images in figure 28. The increased RGB contrast the vascular beds is mainly stored in the green channel of the subtracted image. A mask was created from the green channel of the subtracted image. When superimposing the mask over the original WLB image, the structures can be clearly visualised as is seen in figure 29.

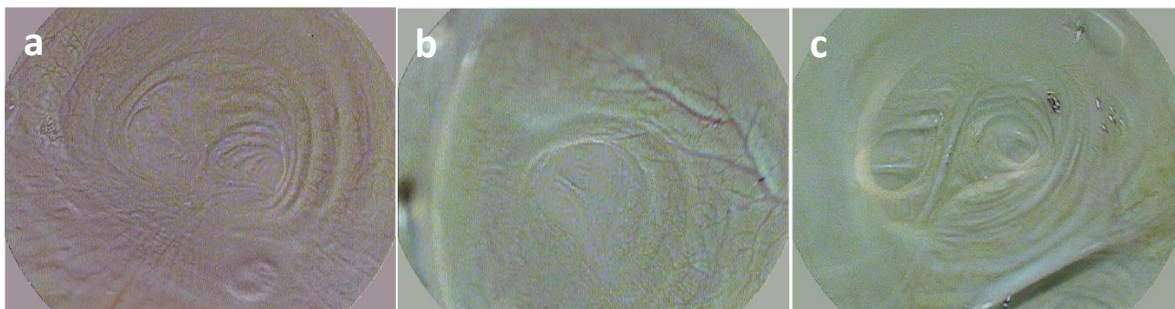


**Figure 28:** Subtraction images of OE mode 2 minus WLB. (a) Central trachea. (b) Vascular bed of the left main bronchus. (c) Bronchial structure at the deepest point a 19 French scope can access.



**Figure 29:** Superimposed mask obtained from the green channel of the OE2 minus WLB subtraction image. The green areas indicate the superimposed mask over the original WLB image. (a) Central trachea. (b) Vascular bed of the left main bronchus. (c) Bronchial structure at the deepest point a 19 French scope can access.

#### Analysis of subtraction images for visualisation of bronchial arches and vessels

Subtraction images as shown in figure 26 and 28 were generated for all seven included subjects. Structures that are highly different in the OE spectra compared to WLB spectra are visualised very light (near white) or very dark (near black). A large difference in visualisation was expected for the blood vessels, since the working mechanism of optical enhancement relies on vessel visualisation. It was a surprising observation that optical enhancement images also contained additional information about the position of bronchial arches compared to the white light bronchoscopic images. For that reason, the RGB values of the bronchial arches and surrounding tissue have been quantified as well. When comparing the RGB colour values of the four different regions of interest in the subtracted image, the additional information in optical enhancement images can be quantified.

Four regions of interest were manually selected as shown in figure 30. The colour value of the vessels was compared to an adjacent area of mucosa. The colour value of the bronchial arches was compared to an adjacent area of mucosa. For every picture, this analysis resulted in four mean RGB colour values, corresponding with the selected areas. The 3D distance between the RGB colour values of the bronchial vessels and arches and their corresponding background colours was calculated and is provided in table 15.

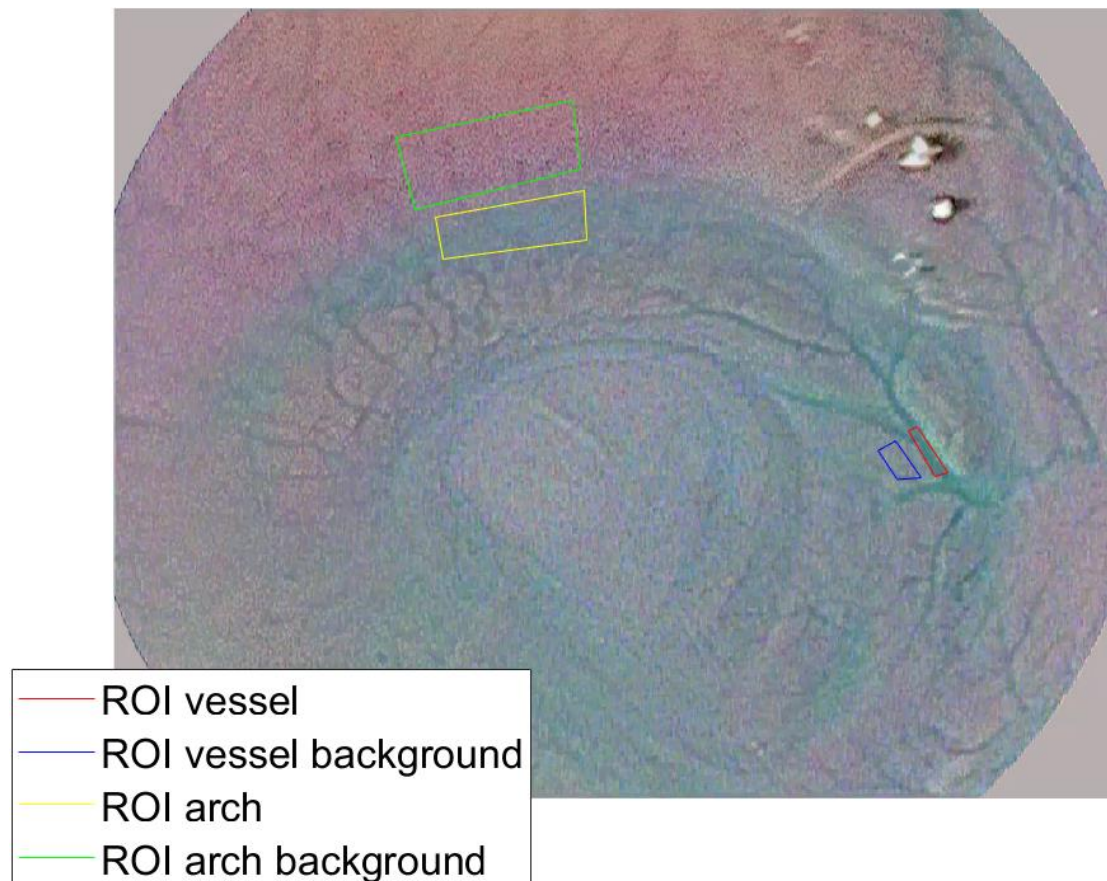


**Figure 30:** Subtraction image of OE mode 1 minus WLB. Four regions of interest for the analysis of vessel-to-background RGB contrast and bronchial arch-to-background RGB contrast are indicated in red, blue, yellow and green.

**Table 15:** 3D RGB colour distance for the quantification of vessel-to-background contrast and bronchial arch-to-background contrast.

Subject identification number ↓	RGB Contrast vessels – background [3D RGB distance]		RGB Contrast bronchial arch – background [3D RGB distance]	
	OE1	OE2	OE1	OE2
S1	39.7673	23.2881	37.5993	12.8232
S2	22.3185	4.3263	11.4886	8.9755
S4	8.4194	3.8250	24.0450	12.5835
S5	17.8572	13.3743	21.9506	14.1284
S7	8.2403	14.0328	29.0078	5.0606
S8	2.9072	7.0054	29.8432	4.2989
S9	11.6919	3.3106	9.8864	23.4256
<b>Mean</b>	<b>15.8860</b>	<b>9.8804</b>	<b>23.4030</b>	<b>11.6137</b>

As seen in table 15, most cases of optical enhancement mode 1 provide more information about bronchial vessels and bronchial arches than optical enhancement mode 2 does. This difference is bigger in bronchial arches than in bronchial vessels.

### 3.3.2.2 Patients with central abnormalities

Twin mode images of seven patients with central abnormalities were acquired and analysed. In figure 31, the collected optical enhancement images, white light bronchoscopy images and corresponding subtraction images of three different patient cases are depicted. All processes are depicted in OE1 since that visualisation provides more visual information.

The other bronchial processes of which images have been collected were cobblestone mucosa, a necrotic tumour, and a tracheal stenosis before circotracheal resection. For those applications, optical enhancement did not provide noticeable additional information about the bronchial abnormalities.

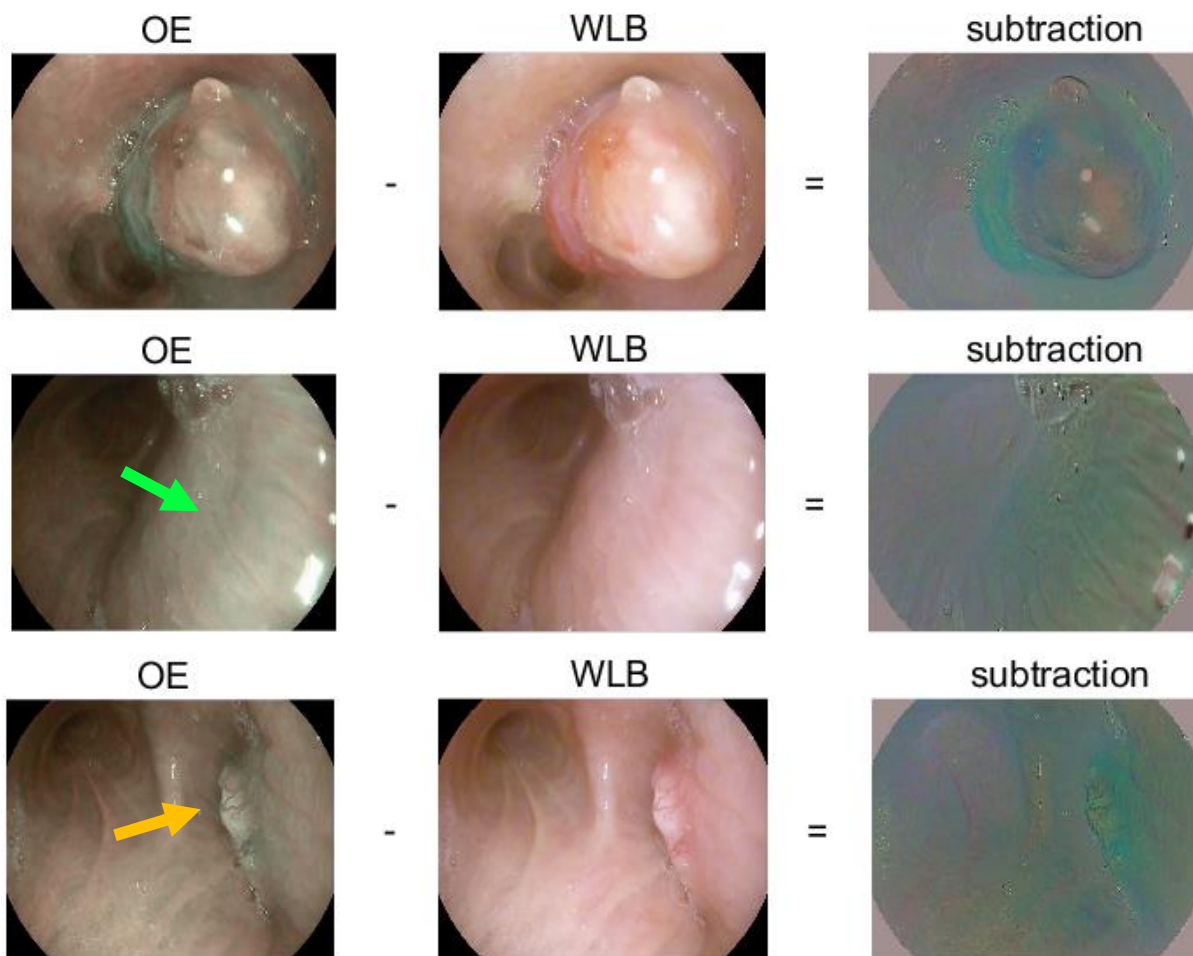


**Figure 31:** Three central bronchial abnormalities under optical enhancement mode 1 illumination, white light illumination and their corresponding subtraction images. (a) Carcinoid tumour obstructing a bronchus. (b) Tissue dysplasia with longitudinal crevices indicated with green arrow, which was proven to be adenocarcinoma by biopsy. (c) Ulcerating tumour indicated with orange arrow.

### 3.4 Discussion and conclusion

#### 3.4.1 Complication registration

Of the 176 bronchoscopy procedures that were retrospectively analysed, complications occurred in 7.4% (13) cases. The complications that could have been prevented using optical enhancement are endobronchial bleeding and bronchial damage. Optical enhancement could be used to visualise endobronchial processes, aid the placement of interventional devices, avoiding contact with bronchial weak spots and supporting endobronchial stenting.

An additional number of 30 bronchoscopy procedures was found in patient files that were listed only once in the CTcue list, while the patient underwent multiple bronchoscopies. The existence of these procedures make it seem like the medical file research program CTcue does not filter all procedures correctly. The only way to validate the CTcue search results is to manually go through the planning of the endoscopy and surgery departments. This time-consuming method is prone to mistakes as well. Therefore, the inclusion of patients in the complication registration was not validated. There are no reasons to suspect a selection bias in terms of amount and types of complications in the included bronchoscopy reports within the analysed timeframe.

### 3.4.2 Case series

#### 3.4.2.1 Patients without central abnormalities

In most cases, optical enhancement mode 1 provides more information about bronchial vessels and bronchial arches than optical enhancement mode 2 does. This difference is bigger in bronchial arches than in bronchial vessels. It should be noted that the group of patients without central abnormalities is not a population of healthy people. All patients were included during navigation bronchoscopies, meaning that they had peripheral lung lesions suspected for malignancies and possibly other pathologies. This inclusion bias makes the acquired data unsuitable to be representative for healthy airways.

It was a surprising observation that optical enhancement images contain additional information about the position of bronchial arches compared to white light bronchoscopic images. This phenomenon could be explained by the more superficial position of the vascular bed in between the rings of bronchial cartilaginous tissue. As displayed in table 15, optical enhancement mode 1 generally provides more information about bronchial vessels and bronchial arches than optical enhancement mode 2 does. This difference is more outspoken for bronchial arches than for bronchial vessels. When visually inspecting the subtraction images, optical enhancement mode 1 contains more additional information than optical enhancement mode 2. This observation supports the quantification results.

However, the quantification for RGB contrast visualisation must be seen as an indication because the analysis method is prone to selection bias. First of all, regions of interest were selected manually and therefore results can differ per iteration and per observer. The manual selection currently was the best option because the bronchoscope positions in twin mode OE1 and twin mode OE2 were not reproducible. Since the applied method is prone to selection bias, calculating significance levels would provide false insights in the visualisation properties of optical enhancement.

When repeating this experiment in the future, more reliable results can be obtained when acquiring the different modes of optical enhancement directly after each other using the same bronchoscope position. For the dataset of the seven patients without central abnormalities, it was challenging to select similar time frames for OE1 and OE2 within the bronchoscopy videos.

#### 3.4.2.2 Patients with central abnormalities

Optical enhancement mode 1 contains additional information about bronchial abnormalities, as also seen when visually interpreting figure 31. The analysis of the seven patients with central abnormalities functions as a demonstration for possible applications of optical enhancement and the appearance of these abnormalities in subtracted images. For a more objective quantification of the improved visualisation, more data should be collected. It would be wise to classify different types of endobronchial lesions and compare patients with similar lesions.

It should be noted that when bleeding occurs during a procedure, the added value of optical enhancement is nihil. Because the wavelengths of the light spectra are fine tuned for vessel RGB contrast, all bleedings appear black in optical enhancement. When scope contact bleedings occur, it is difficult to obtain comparable images. When applying optical enhancement in interventional bronchoscopy, this optical technique is of most value when obtaining images before executing the intervention, while avoiding touching the bronchial wall with the bronchoscope.

#### *3.4.2.3 Technological remarks of twin mode bronchoscopy imaging*

The white balance of a clinical bronchoscopy system is corrected for the current colour of the image. This white balance correction takes some time, appearing as a delay in optimal image quality. When inspecting the airways with optical enhancement in twin mode, the spectrum of the light source changes with a frequency of 30 Hz. This frequency seems too high for constant adaption of the white balance, making images seem over- or underexposed. This phenomenon disappears when using single mode illumination. A possible explanation for this phenomenon is the suspicion that the twin mode images are acquired very fast after each other, exactly timed around the alteration of the light source. In that case, the mutual time intervals between the two light settings is not constant. This suspicion would need to be tested by contacting the manufacturer of the bronchoscope processor. Future testing should include a comparison of optical enhancement images of the same object in dual mode and twin mode. Based on clinical observations, blending of white light bronchoscopy and optical enhancement occurs when using twin mode.

The previously mentioned white balance is determined when a certain threshold of photons have reached the CCD chip in the tip of the camera. When removing a certain colour of input light, such as is done in optical enhancement, the threshold needs to be reached by the remaining colour channels. This automatic adaption of integration time of the camera chip can cause measurement artefacts when mutually comparing different spectra. The raw image output of the bronchoscope processor unfortunately does not contain information about the white balance settings. More information from the manufacturer of the image processing software must be acquired when assessment of this phenomenon is desired. It would be desirable to eliminate the automatic white balance and execute all measurements with the same white balance settings. The gain of the image, which indicates the digital amplification of signal on the camera chip, should also be set at a predefined level without automatic adaption of the bronchoscope processor.

The twin images can suffer from movement artefacts because of the bronchoscope movement. A balance needs to be found between the movement artefacts that happen between the twin mode images and the white balance adaption of the image. When the spectrum alteration frequency would be lowered, more movement artefacts would occur, but also the white balance would have more time to adapt, resulting in higher image quality. When paying attention to maintaining the scope at a steady position inside bronchi, movement artefacts can be kept to a minimum. Because the inspection bronchoscopy videos used in the case study were made dynamically, it was difficult to get comparable screenshots without movement artefacts. For future purposes, maintaining a steady bronchoscope position is advised.

#### *3.4.2.4 Future outlook*

In this case series, comparison of optical enhancement and white light bronchoscopy images was done by subtracting the RGB values of the WLB image from the RGB values of the OE image to create the RGB values of a new image as illustrated in equations 7a-c.

**Equations 7a-c:** Calculation of new RGB values by subtracting WLB and OE images

$$R_{new} = R_{WLB} - R_{OE} \quad (7a)$$

$$G_{new} = G_{WLB} - G_{OE} \quad (7b)$$

$$B_{new} = B_{WLB} - B_{OE} \quad (7c)$$

$RGB_{new}$  = RGB values of image that shows the difference between WLB and OE per colour channel

$RGB_{WLB}$  = RGB values of white light bronchoscopy image, twin imaged with  $RGB_{OE}$

$RGB_{OE}$  = RGB values of optical enhancement bronchoscopy image, twin imaged with  $RGB_{WLB}$

But subtracting the RGB values from each other as shown in equations 7a-c is only one of the many calculations that can be done to extract additional information from optical enhancement imaging. More generally, equations 8a-c provide the calculation of a colour channel value by combining information from all colour channels. The RGB values of the new image can be computed by combining RGB values of the OE and WLB images in a way that provides the most information.

**Equations 8a-c:** Calculation of new RGB values by combining RGB values of all colour channels of both image settings into the RGB values of the new image.

$$R_{new} = a_1 \cdot R_{WLB} + a_2 \cdot R_{OE} + a_3 \cdot G_{WLB} + a_4 \cdot G_{OE} + a_5 \cdot B_{WLB} + a_6 \cdot B_{OE}$$

$$G_{new} = b_1 \cdot R_{WLB} + b_2 \cdot R_{OE} + b_3 \cdot G_{WLB} + b_4 \cdot G_{OE} + b_5 \cdot B_{WLB} + b_6 \cdot B_{OE}$$

$$B_{new} = c_1 \cdot R_{WLB} + c_2 \cdot R_{OE} + c_3 \cdot G_{WLB} + c_4 \cdot G_{OE} + c_5 \cdot B_{WLB} + c_6 \cdot B_{OE}$$

$RGB_{new}$  = RGB values of image that shows the difference between WLB and OE per colour channel

$RGB_{WLB}$  = RGB values of white light bronchoscopy image, twin imaged with  $RGB_{OE}$

$RGB_{OE}$  = RGB values of optical enhancement bronchoscopy image, twin imaged with  $RGB_{WLB}$

$a_{1-6}, b_{1-6}, c_{1-6}$  = coefficients to indicate mutual weighing of the six colour channels of  $RGB_{OE}$  and  $RGB_{WLB}$

When analysing additional information about a bronchial structure in optical enhancement images, optimal values for the eighteen coefficients in equations 8a-c should be found. By manual or automatic segmentation, a region of interest for the bronchial structure should be indicated in an OE image and in a WLB image which were acquired in twin mode. The two regions of interest should be plotted in a three-dimensional colour space in which the red, blue and green channels are the axis. Altering the values of coefficients  $a_{1-6}, b_{1-6}, c_{1-6}$  results in a scaling in this three-dimensional space. This scaling can be chosen in a way that the pixel colours in the regions of interest show the least overlap and therefor provide the greatest mutual distinction. [41]

### 3.4.3 General conclusion

Of the 176 bronchoscopy procedures that were retrospectively analysed, complications occurred in 7.4% (13) cases. The complications that could have been prevented using optical enhancement are endobronchial bleeding and bronchial damage. Optical enhancement could be used to visualise endobronchial processes, aid the placement of interventional devices, avoiding contact with endobronchial weak spots and supporting endobronchial stenting. Optical enhancement provides additional information about bronchial arches, vascular beds and bronchial abnormalities.



## 4 Automatic detection of systemic disease

In this chapter, possibilities for the automatic detection of systemic disease in bronchoscopy images are assessed. Literature research has resulted in a list of systemic diseases and their distinctive tissue properties whose detection can potentially be improved by the application of optical enhancement. A prospective database registry was set up to provide the infrastructure needed to assess the automatic detection of disease in bronchoscopy images in the future. This chapter aims to assess the following questions:

- Which diagnosis of systemic pulmonary diseases can potentially be improved by the application of optical enhancement?
- How should data acquisition for future clinical research on optical enhancement be executed?
- How can automatic detection of systemic disease in bronchoscopy images be realized in clinical practice?

### 4.1 Introduction

#### 4.1.1 Systemic pulmonary diseases and their tissue properties

In order to explore the diseases in which optical enhancement imaging can be of added value, focus was placed on pathologically altered vascular bed aspects. Further, structural changes of the bronchial mucosal surface can potentially be visualised more clearly using optical enhancement imaging. In the selection of pulmonary diseases that require further investigation into the added value of optical enhancement, it was taken into consideration which pathologies present themselves regularly in Radboudumc Nijmegen for the indication of bronchoscopy. This was done in order to allow for *in vivo* data collection possibilities.

In general, in case of pathology, there is more irritation and inflammation in the tissue. The higher activity in the irritated tissue is accompanied by more vessel growth or dilatation of the vessels. This leads to a higher vessel to mucosa surface area ratio and a mucosal colour that generally appears red.

In the following sections, background will be given on three central and/or systemic airway pathologies: lung cancer, nontuberculous mycobacteria infection and sarcoidosis. These three airway pathologies are likely to be more effectively recognisable using optical enhancement.

##### 4.1.1.1 Lung cancer

Lung cancer is a malignant growth of cells in the lungs. In the Netherlands, over 13.000 people are diagnosed with lung cancer on a yearly basis. [42] Lung cancer can be classified as a primary malignancy which originates from pulmonary tissue, or as metastases originating from a cancerous process elsewhere in the body. Lung cancer tends to be non-symptomatic until a far progressed phase of the disease. Tumours in peripheral parts of the lung mostly go undetected for longer compared to central bronchial lung cancers. It is common for lung cancer to have metastasised to lymph nodes or other body parts are common at the time the cancer is detected. [43] Because early phases of disease are commonly asymptomatic, improving recognition of early lesions is essential. Lung cancer is classified as the most lethal cancer with a five-year survival after diagnosis of only 8% for small cell lung cancers (SCLCs) and 20% for non-small cell lung cancers (NSCLCs). [42]

### Endobronchial representation of lung cancer

General airway inflammation and irritation cause the mucosa to appear red in lung cancer, because of the more erythematous bronchial mucosa. [15] As seen from within the bronchi, lung cancer can be recognized by a higher vessel-to-mucus ratio in which the blood vessels have an unorganized topography. [44] Vascular abnormalities and irregular vascular enlargement can be indicators for lung cancer. [9] Dotted vessels, as seen in figure 32a are more common for adenocarcinoma and their growth is mostly limited to the mucosa only. Abrupt vessel endings as seen in figure 32b are more common for squamous cell carcinoma. This lung cancer type mostly invades in the submucosa. Lastly, vessel abnormalities can appear as torturous or spiral vessels as seen in figure 32c. These vascular abnormalities are more common for squamous cell carcinoma. [6][11][10][15][45]

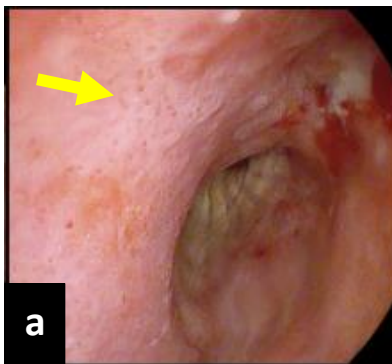


**Figure 32a:** Dotted vessels (yellow arrow) as most commonly seen in adenocarcinoma. [10]

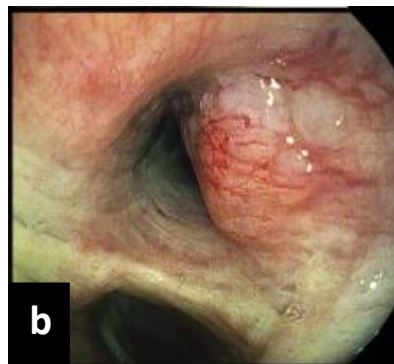


**Figure 32b:** Abrupt vessel endings most commonly seen in squamous cell carcinoma. [10]

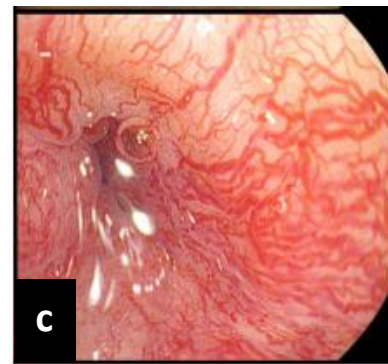


**Figure 32c:** Torturous and spiral vessels most commonly seen in squamous cell carcinoma. [10]

Besides vascular abnormalities, other endobronchial characteristics can indicate lung cancer. Swelling or thickening of the mucosa, fibrosis, the presence of granulation tissue and thickening of the carinas are risk indicators for the presence of lung cancer. Besides, nodular polypoid lesions and an irregular surface texture of the mucosa are signs for lung cancer. [15]

#### 4.1.1.2 Nontuberculous mycobacteria infection

Nontuberculous mycobacteria (NTM) are mycobacteria which do not cause tuberculosis or leprosy. Over 150 species of these mycobacteria have been discovered, most of which are found in our natural environment. [46] NTM infections cause pulmonary symptoms that resemble tuberculosis or lymphadenitis. Unlike tuberculosis or leprosy, which can be transferred by animal-to-human and human-to-human contact, NTM are acquired by environmental exposure. [47] NTM infections are most often seen in post-menopausal woman and patients with existing lung diseases such as cystic fibrosis or prior tuberculosis infection. Individuals with acquired immune deficiency syndrome (AIDS) or malignancies are more susceptible for pulmonary nontuberculous mycobacteria infections.

Treatment is a combination of pulmonary care, intermittent or continuous antibiotics or surgical treatment. The most suitable treatment depends on the bacterial species, patient tolerance and individual symptoms. Recovery of a nontuberculous mycobacteria infection remains challenging, but is possible. [48]

#### Endobronchial representation of nontuberculous mycobacteria

A higher vessel-to-mucus ratio appears in endobronchial tissue that is infected by nontuberculous mycobacteria, but this increase in vessel growth and diameter appears in an organized manner. [44] Airway inflammation caused by the infection causes the mucosa to become more erythematous and appear red. Swelling and thickening of the mucosa are also caused by the infection. [15] In patients suffering from NTM, more and thicker mucus can be expected. The appearance of airway mucus in NTM patients is more opaque compared to mucus of healthy subjects. [46]

#### 4.1.1.3 Sarcoidosis

Sarcoidosis is a not fully understood interstitial lung disease in which spontaneous inflammation occurs. The collections of inflammatory cells that arise in reaction to the inflammation are called granulomas. This process can occur in any part of the body but is most common in the lungs and lymph nodes. Other affected body parts are the eyes, skin and heart. [43] In 90% of sarcoidosis patients, the disease is present in the lungs. [49] In most patients, the granulomas spontaneously disappear over the course of two to three years. In 20-30% of cases, the disease becomes chronic. Chronic sarcoidosis can lead to fibrosis of the lung tissue which irreversibly affects the organ function. [43][49] The aetiology of sarcoidosis is still unclear. [50] The diagnosis of sarcoidosis should be made after excluding other possible causes of similar symptoms.

#### Endobronchial representation of sarcoidosis

The most recognisable cue in bronchoscopy of sarcoidosis are cobblestone lymph nodes. The lymph nodes appear as flattened and pale-coloured plaques arising from the bronchial mucosa (figure 33a). [43] Clusters of nodes can cause bronchial lumen crowding (figure 33b). Sarcoidosis presents itself with a higher vessel-to-mucus ratio in an organized topography. [44] The inflammation causes erythematous bronchial mucosa. [15] The vascular abnormalities can present themselves as mucosal hypervascularisation with vessels running perpendicular to the cartilage rings of the bronchi (figure 33c). Vascular network formation of mucosal vessels with mucosal oedema can be observed in sarcoidosis (figure 33d). [49]

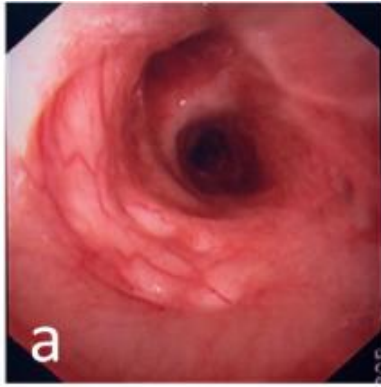


**Figure 33a:** Cobblestone lymph nodes in sarcoidosis. [49]

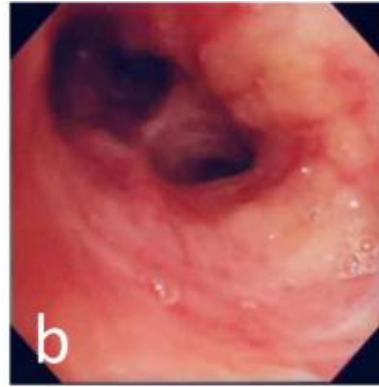


**Figure 33b:** Bronchial lumen crowding in sarcoidosis. [49]

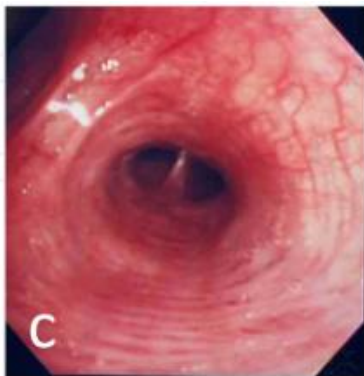


**Figure 33c:** Mucosal hypervascularisation in sarcoidosis. [49]

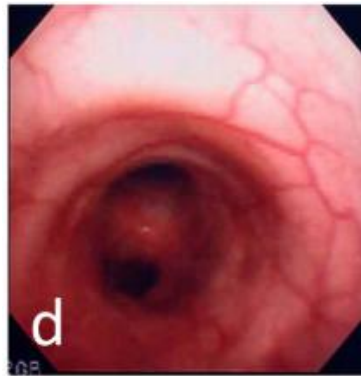


**Figure 33d:** Network formation of mucosal vessels in sarcoidosis. [49]

#### 4.1.2 Tissue properties caused by comorbidities and individual patient factors

Various comorbidities and individual patient factors can alter the visual aspect of the endobronchial wall. This causes a less rigid classification between healthy tissue, tissue affected by disease and individual anatomical differences. When trying to automatically analyse endobronchial images, these comorbidities and individual factors must be taken as variables to distinguish between endobronchial cues caused by the presence of a disease or endobronchial cues caused by comorbidities and individual patient factors. In this section, four comorbidities and individual patient factors that affect the appearance of the bronchial wall, are outlined.

One of the comorbidities that affects the endobronchial appearance is chronic obstruction pulmonary disease (COPD). COPD is a collective name for chronic bronchitis and emphysema. The airway obstruction is irreversible and is paired with an abnormal inflammatory response as a reaction to external stimuli. More mucus is produced in the lungs of COPD patients. [43][51] Furthermore, lungs that have been treated by ionizing radiation in radiotherapy tend to develop an altered endobronchial presentation. The walls appear thinner, and strength of the tissue relies more on the longitudinal connective tissue strands. The tissue is more erythematous and bleeds easily when touched by the bronchoscope. In general, radiotherapy manifests as traction bronchiectasis, volume loss and scarring. [52] Black discolouration of the bronchial wall can also occur, a process called anthracosis. Exposure to dust and wood smoke is the most postulated etiology for anthracosis. It may be seen as superficial black discolouration or scattered black spots with retracted mucosa. [53][54] Lastly, smoking or smoke inhalation injury can have a direct effect on the bronchial visualisation. The airway mucosa is denuded and can appear sloughed. Also smoke particles can appear in the central airways. [55]

#### 4.1.3 Bronchial wall in systemic disease

The possibilities of disease recognition by optical enhancement are limited to depths in tissue that can be reached by light in the visible spectrum. Blue light with a wavelength of 440 nm generally reaches depths less than 1 mm. Because of the short wavelength, photon energy is reflected, absorbed or scattered in this shortest distance of all visible light wavelengths. For red light with a wavelength of 650 nm, depths of 4 mm can be reached. [56]

In bronchial tissue affected by disease, tissue properties change. These changes occur at different depths in the tissue. Since the penetration depth of different wavelengths of light is different, the effect of the affected tissue on the reflected optical enhancement spectrum (and therefore the appearance of the resulting images) can be hypothesised. This section provides information about the depths of disease processes in bronchial pathologies which are useful when hypothesizing the effect of bronchial disease on reflected spectra.

All systemic diseases are associated with erythema, redness of the tissue caused by dilation or an increase in number of capillaries. The expansion or increase in number of capillaries occurs inside the submucosa of the bronchial wall, in between the mucus-secreting cells. The capillaries in tracheal and central bronchial tissue are situated 80 – 130  $\mu\text{m}$  away from the epithelial surface. [57] When measuring the distance from capillary walls to the epithelial surface in numerous histological slides, a mean distance of 146  $\mu\text{m}$  was found. [58] Capillaries have a diameter of 5 to 10  $\mu\text{m}$ . Deeper vessels which are embedded in between the muscle tissue of the trachea are situated at a depth of 300 – 360  $\mu\text{m}$  from the epithelial tissue. [59] This number was confirmed by measuring the capillary to mucosal distance in histological slides. The absorption of blue light within the superficial capillaries and the absorption of green light within the deeper blood vessels is visualised in figure 34.

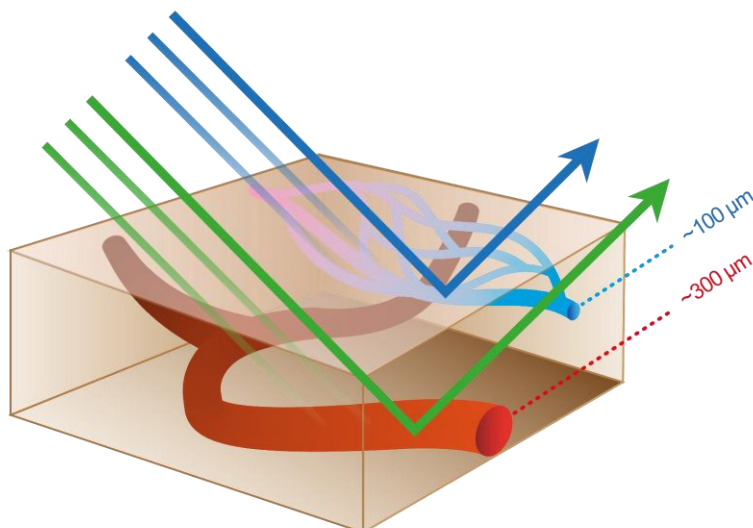


**Figure 34:** Schematic representation of absorption of blue light in superficial capillaries and absorption of green light in deeper blood vessels. [17]

Lymph nodes are embedded deep in the bronchial wall, unable to be reached by light from the visible spectrum. However, when suffering from lymph node cobble stones in sarcoidosis, the lymph nodes thicken and rise the surface of epithelium. Lymph nodes have a whiter colour than surrounding mucosa, causing thickened lymph nodes to be detectable by the visible light spectrum. [49]

The layer of mucus on top of the epithelium is 2 to 10  $\mu\text{m}$  in healthy tracheal tissue and has a transparent and viscous appearance. [60][61] More opaque white mucus indicates thickening of mucus which causes slow passage of mucus through the respiratory tract. Coloured lung mucus can indicate bleeding, infections and fungal infections. [61]

#### 4.1.4 Need for automatic interpretation

As indicated in the paragraphs above, bronchial tissue can appear in numerous variations in colour, mucosal aspect, surface texture and vascular patterns. These visual cues can be an indication for pathology or can be assigned to individual patient differences. The different options for diagnosis arising from these nonspecific bronchial aspects make it challenging for a fully accurate visual interpretation of bronchoscopy images. Besides the intrinsic ambiguous interpretation of bronchoscopy images because of the numerous tissue variabilities, the quality of the image acquisition and interpretation is dependent on the bronchoscopist. [62][63]

These inevitable inaccuracies in bronchoscopy procedure interpretation might be solved by automatic interpretation of bronchoscopy images. Automatic detection and interpretation is being introduced in multiple fields of medicine and will become of inestimable value in the near future of diagnostic interpretation. [64] Ideally, automatic detection would operate real-time. The acquired images are compared to a database and are classified as normal or abnormal. The bronchoscopist receives immediate feedback to decide on the collection of material.

#### 4.1.5 Optical enhancement as input for automatic detection

Automatic detection of medical images can potentially distinguish normal from abnormal tissue when taking features visible and invisible to the naked eye into account. Optical enhancement illumination of tissue is providing an optical preselection of certain tissue features that would not be detected using regular white light bronchoscopy. This feature preselection provides different information than conventional white light bronchoscopy, making optical enhancement image acquisition an interesting source for automatic detection algorithms.

A Technical Medicine intern at the department of Pulmonology in Radboudumc hospital, the Netherlands, focused on the automatic classification of vascular patterns in bronchoscopy images in 2015. [65] She concluded that automatic detection and classification was not yet possible with the current database size and the convolutional neural network that was used. Virtual chromoendoscopy, the i-scan settings by Pentax Medical, were used in the analysed images. It was tried to classify the regions of the images in which vessels were present by applying various segmentation methods. However, successful vessel structure segmentation was not achieved. The failed feature extraction has been explained by the little RGB contrast between vessels and tissue obtained using the i-scan settings. Collecting datasets using the optical enhancement settings can possibly solve this problem.

The accuracy of an automatic detection algorithm is correlated with the amount of annotated data that is used to build the algorithm. However, there is not a single correct answer to the minimally required size of a dataset. Depending on the complexity of the problem and the complexity of the learning algorithm, the appropriate sample size can be determined. [66] One of the rules of thumb in artificial intelligence is to have at least ten times more data points as the number of dimensions. [67] However, more efficient deep learning can be achieved using transfer learning, needing less data points. Because the definition of the problem being solved with artificial intelligence is unknown and the complexity of the chosen neural network is unknown, the recommendation is to collect as many datasets as possible. Lots of datasets can be created by taking multiple image frames from the same procedure and presenting them to the algorithm as individual cases. However, one should be alert that this causes irrational proportions of patient characteristics within the study populations.

## 4.2 Prospective database registry for bronchoscopy

In order to develop automatic detection algorithms, a lot of annotated bronchoscopy videos are necessary for the training and validation of neural networks. To do so, the start of a prospective database registry without a fixed end goal was requested to the Medical Ethical committee of Arnhem Nijmegen. The approval was officially granted on the 1<sup>st</sup> of August 2019 under file number 2019-5583.

The research protocol of this prospective database registry can be found in appendix 7.5. The most important considerations are the undetermined duration of the study with a re-evaluation of the persistence of the database every five years. Parameters that will be stored are categorized in bronchoscopic images and their settings, data from the clinical report and patient demographics. The patient information letter, which was written in Dutch, can be found in appendix 7.6. When giving consent to participate in the bronchoscopy database, patients approve that coded medical data is saved, stored and used for research without a fixed end goal. It is optional to consent to being approached for further research in the future, as well as the option to request patient data from a central Dutch registration system.

## 4.3 Applications of bronchoscopy database registry

In automatic image analysis, two main methods can be distinguished. On one hand, we have model-based methods. Here, features are defined either manually by hypothesizing that a set of features carries information about the disease, or by mathematically and physically modelling the relationship between image data and the effects of the disease on the anatomy. On the other hand, we have data driven models, in which features are found automatically using artificial neural networks. These networks are fed with images and the underlying diseased or healthy state of the subjects. For the application of the bronchoscopy database, focus is placed on this artificial intelligence image analysis. [68]

Before artificial intelligence can be applied, an annotated database of bronchoscopy images must be created. Since visual interpretation by bronchoscopists is the current standard of clinical practice, these observations will be taken as the golden standard. For every video, a timeframe of interest must be selected, and a clinical conclusion needs to be coupled to these images. These image processing steps might be worth automating but will most likely still require manual input.

The next step, after the time frames of interest have been selected, is to perform segmentation to exclude regions that are not of interest. In 2015, a Technical Medicine intern evaluated different segmentation methods and concluded that Canny, Hessian and Laws algorithms show potential for vascular pattern segmentation. The dark endobronchial regions of the lumen were successfully detected. [69] Besides the dark lumen, regions of the bronchial tissue covered in bubbles can be filtered out. An end product of this intermediate step can be an algorithm that detects the lumen and bubbles in every frame and filters these out of the image.

When the bronchoscopic data has been annotated with the clinical outcome and uninteresting time frames and image parts have been filtered out, detection algorithms can be designed. The first possible application of the automatic detection algorithm is the detection of areas with a high risk for bleeding during bronchoscopy. Examples of this are bronchial tube anastomoses or bronchial lumen constrictions. The vessels in these detected areas can be projected on top of the white light bronchoscopic images.

The second application of the automatic detection algorithm is to distinguish between healthy and affected tissue. By offering the algorithm annotated parts of videos in which the disease is present, and parts of videos which are unaffected, distinction can be learned. From literature research, numerous pathological tissue properties are recognisable using optical enhancement. Especially surface texture, protruding lymph nodes and vascular bed aspects have potential for automatic recognition.

#### 4.4 General conclusion

Lung cancer, nontuberculous mycobacteria infection and sarcoidosis are the systemic pulmonary diseases whose diagnosis can potentially be improved by application of optical enhancement. These three airway pathologies are likely to be more effectively recognisable using optical enhancement. For future clinical research on optical enhancement, a clinical database of bronchoscopy images was set up. This database is the basis for future research regarding bronchoscopic imaging. Automatic detection of systemic disease in bronchoscopy can be realized by analysing the bronchoscopic images in the database and distinguishing healthy from affected tissue.



## 5 General discussion and conclusion

The aim of this research was to assess the value of optical enhancement in endobronchial diagnostics and interventions. The empirical cycle of this research differs from the standard because the optical enhancement technology had already been implemented in the clinical bronchoscopes and processors without an elaborate assessment of the suitability of these spectra for bronchial application. The optical enhancement spectra have initially been designed for endoscopic application during gastroscopy and colonoscopy.

To assess the feasibility of the optical enhancement spectra for application in bronchoscopy, a validation of the spectra was done in the second chapter of this report. An optical setup using lowpass and highpass filters was built to resemble the optical enhancement spectra and alternate the optical settings. Resulting images were analysed using texture and contrast analysis. It can be concluded that a broad range of wavelengths results in the best surface texture visualisation. As expected, blue light seems to be essential for capillary visualisation, but this could not be significantly proven. Red light is proven to significantly enhance deep vein visualisation. Besides these three quantitative variables, it would have been interesting to incorporate the thickness of the mucus layer in the analysis because it plays an essential role in the presentation of lung diseases. However, it was beyond the scope of this graduation research to develop a method to produce mucus layers of reproducible thickness for the *ex vivo* assessment of the mucus measurement.

The optical setup has shown that the commercially available optical enhancement spectra contain the essential wavelengths for tissue surface, capillary and vein visualisation. Further, the intensity of the light of the clinical bronchoscopy setup was adequate. This makes the commercially available optical enhancement spectra suitable for clinical application. Because of the large intermediate steps in the adaptable spectra caused by the limited availability of optical filters, it was not possible to create a spectrum that performed better than the Pentax optical enhancement spectra. The resemblance of the created spectra is close to the optical enhancement spectra and therefore this *ex vivo* conclusion serves as a justification to assess the Pentax optical enhancement spectra *in vivo*.

In the third chapter, direct improvement of bronchoscopy interpretation by the application of optical enhancement was investigated. A complication registration during interventional bronchoscopy was done. This resulted in a list with bronchoscopy aspects that offer room for improvement. Fourteen patient cases were included to assess the value of optical enhancement in patients with and without central lung abnormalities. Subtraction imaging has showed that optical enhancement images contain more information regarding bronchial arches and vessel structures as compared to conventional white light bronchoscopy images.

To assess if automatic detection of systemic disease using optical enhancement is feasible in the future, a literature research was performed in chapter four. The tissue properties of bronchi affected by lung cancer, nontuberculous mycobacteria and sarcoidosis were investigated. A research proposal for a prospective database registry for bronchoscopy images with the registration code 2019-5583 was submitted and approved. Every patient eligible for bronchoscopy will be asked to participate in the prospective registry during their pre-procedural consultation. Because of the large timeframe which is required to collect the needed amount of data, the results of this chapter remain at the preparations of the necessities to start building automatic detection algorithms. All work has been done to let physicians in the Radboudumc collect bronchoscopy images in a database which future researchers can work with.

The first application of the automatic detection algorithm is the detection of areas with a high risk for bleeding during bronchoscopy. Examples of these areas are bronchial tube anastomoses or bronchial lumen constrictions. The vessels in these detected areas can be projected on top of the white light bronchoscopic images. The second application of the automatic detection algorithm is to distinguish between healthy and affected tissue by quantifying parameters both visible as invisible to the naked eye. Especially surface texture, protruding lymph nodes and vascular bed aspects have potential for automatic recognition.

An image analysis method that is worth looking into is motion magnification. This method detects motion and enlarges the amplitude of the movements. [70][71][72] Motion magnification can be used to exaggerate vessel pulsation in endobronchial videos. This method might be suitable for the detection of deep vessels that cannot be reached by the wavelengths of visible light.

Optical enhancement is an innovation that has potential for endobronchial application in routine practice. Because of the improved vessel visualisation, endobronchial bleeding can be prevented. The first step in future research in optical enhancement is to fill a database of endobronchial images to be the basis for automatic detection algorithms.

## 6 References

- [1] P. F. Clementsen, L. J. Nayahangan, and L. Konge, *Bronchoscopy - A Practical Handbook*. Copenhagen: Simulation Centre Rigshospitalet, 2016.
- [2] Mayo Clinic, "Bronchoscopy," 2019. [Online]. Available: <https://www.drugs.com/mcp/bronchoscopy>. [Accessed: 15-Aug-2019].
- [3] T. S. Panchabhai and A. C. Mehta, "Historical perspectives of bronchoscopy: Connecting the dots," *Ann. Am. Thorac. Soc.*, vol. 12, no. 5, pp. 631–641, 2015.
- [4] T. Miyazawa, "History of the Flexible Bronchoscope," in *Interventional Bronchoscopy*, C. T. Bolliger and P. N. Mathur, Eds. Cape Town, 2000, pp. 16–21.
- [5] H. D. Becker and R. Marsh, "History of the Rigid Bronchoscope," in *Interventional Bronchoscopy*, C. T. Bolliger and P. N. Mathur, Eds. Cape Town, 2000, pp. 2–15.
- [6] B. Zaric, B. Perin, and V. Stojisic, "Relation between vascular patterns visualized by narrow band imaging ( NBI ) videobronchoscopy and histological type of lung cancer," *Med. Oncol.*, vol. 30, no. 1, p. 374, 2013.
- [7] S. Kodashima and M. Fujishiro, "Novel image-enhanced endoscopy with i-scan technology," *World J. Gastroenterol.*, vol. 16, no. 9, pp. 1043–1049, 2010.
- [8] PENTAX medical, "Gaining a complete picture of the GI tract through new image enhancement technology," 2017. [Online]. Available: [https://www.i-scanimaging.com/fileadmin/user\\_upload/PENTAX\\_White\\_Paper.pdf](https://www.i-scanimaging.com/fileadmin/user_upload/PENTAX_White_Paper.pdf).
- [9] PENTAX medical, "i-scan Atlas for Gastroenterology," 2016. [Online]. Available: [https://www.i-scanimaging.com/fileadmin/user\\_upload/i-scan\\_Atlas\\_GI\\_05.2016.pdf](https://www.i-scanimaging.com/fileadmin/user_upload/i-scan_Atlas_GI_05.2016.pdf).
- [10] E. H. F. M. Van Der Heijden *et al.*, "Image enhancement technology in bronchoscopy : a prospective multicentre study in lung cancer," *BMJ Open Respiratory Res.*, vol. 5, no. 1, pp. 1–10, 2018.
- [11] E. H. F. M. van der Heijden, W. Hoefsloot, H. W. H. van Hees, and O. C. J. Schuurbiers, "High definition bronchoscopy: A randomized exploratory study of diagnostic value compared to standard white light bronchoscopy and autofluorescence bronchoscopy," *Respir. Res.*, vol. 16, no. 1, pp. 1–7, 2015.
- [12] M. Filip, S. Iordache, A. Săftoiu, and T. Ciurea, "Autofluorescence imaging and magnification endoscopy," *World J. Gastroenterol.*, vol. 17, no. 1, pp. 9–14, 2011.
- [13] K. Gono, "Narrow band imaging: Technology basis and research and development history," *Clin. Endosc.*, vol. 48, no. 6, pp. 476–480, 2015.
- [14] H. Neumann, M. Fujishiro, C. M. Wilcox, and K. Mönkemüller, "Present and future perspectives of virtual chromoendoscopy with i-scan and optical enhancement technology," *Dig. Endosc.*, vol. 26, pp. 43–51, 2014.
- [15] F. J. F. Herth, R. Eberhardt, and D. Anantham, "Narrow-Band Imaging Bronchoscopy Increases the Specificity of Bronchoscopic Early Lung Cancer Detection," *JTO Acquis.*, vol. 4, no. 9, pp. 1060–1065, 2009.
- [16] S. Kodashima *et al.*, "Evaluation of a new image-enhanced endoscopic technology using band-limited light for detection of esophageal squamous cell carcinoma," *Dig. Endosc.*, vol. 26, no. 2, pp. 164–171, 2014.
- [17] OLYMPUS, "NBI in een oogopslag," 2019. [Online]. Available: [http://www.nbi-portal.eu/nl/uro/nbi\\_2/](http://www.nbi-portal.eu/nl/uro/nbi_2/). [Accessed: 20-Aug-2019].
- [18] PENTAX medical, "Pentax OPTIVISTA EPK-i7010 High-Definition Video Processor," 2019. [Online]. Available: <https://www.pentaxmedical.com/pentax/nl/107/17/OPTIVISTA-EPK-i7010-High-Definition-Video-Processor>.
- [19] I. H. Iftikhar and A. I. Musani, "Narrow-band imaging bronchoscopy in the detection of premalignant airway lesions : a meta-analysis of diagnostic test accuracy," *Ther. Adv. Respir. Dis.*, vol. 9, no. 5, pp. 207–216, 2015.
- [20] PENTAX medical, "HD+ Bronchoscope EB-1990i," 2019. [Online]. Available: [https://www.pentaxmedical.com/pentax/download/fstore/uploadFiles/Pdfs/Product\\_Datasheets/EMEA\\_PULM\\_BR\\_Product\\_Flyer\\_EB-1990i\\_02.2012.pdf](https://www.pentaxmedical.com/pentax/download/fstore/uploadFiles/Pdfs/Product_Datasheets/EMEA_PULM_BR_Product_Flyer_EB-1990i_02.2012.pdf). [Accessed: 20-Aug-2019].
- [21] PENTAX medical, "EB-19090i Video Bronchoscope," 2019. [Online]. Available: <https://www.pentaxmedical.com/pentax/en/95/1/EB-1990i-Ultrasound-Video-Bronchoscope>. [Accessed: 19-Aug-2019].
- [22] PENTAX medical, "EG29-i10 Video Gastroscope i10 Standard HD+," 2019. [Online]. Available: <https://www.pentaxmedical.com/pentax/en/99/3/EG29-i10-Video-Gastroscope-i10-Standard-HD>. [Accessed: 19-Aug-2019].
- [23] Wikipedia, "RGB color space," 2019. [Online]. Available: [https://en.wikipedia.org/wiki/RGB\\_color\\_space](https://en.wikipedia.org/wiki/RGB_color_space). [Accessed: 20-Aug-2019].
- [24] Wikipedia, "List of color spaces and their uses," 2019. [Online]. Available: [https://en.wikipedia.org/wiki/List\\_of\\_color\\_spaces\\_and\\_their\\_uses](https://en.wikipedia.org/wiki/List_of_color_spaces_and_their_uses). [Accessed: 20-Aug-2019].
- [25] Wikipedia, "Color Histogram," 2019. [Online]. Available: [https://en.wikipedia.org/wiki/Color\\_histogram](https://en.wikipedia.org/wiki/Color_histogram). [Accessed: 20-Aug-2019].

- [26] A. Gijsenij, T. Gevers, and M. P. Lucassen, "Perceptual analysis of distance measures for color constancy algorithms," *J. Opt. Soc. Am.*, vol. 26, no. 10, pp. 2243–2256, 2009.
- [27] M. Sarifuddin and R. Missaoui, "A New Perceptually Uniform Color Space with Associated Color Similarity Measure for Content-Based Image and Video Retrieval," in *28th Annual ACM SIGIR Conference*, 2005.
- [28] R. C. Gonzales and R. E. Woods, *Digital Image Processing*, 3rd ed. New Jersey: Pearson Education (US), 2008.
- [29] Medical Image Analysis, "Texture in Medical Images," 2017. [Online]. Available: [https://www.youtube.com/watch?v=Y\\_zQ9B4rWMY](https://www.youtube.com/watch?v=Y_zQ9B4rWMY).
- [30] MathWorks, "Gray-level co-occurrence matrix," 2019. [Online]. Available: <https://nl.mathworks.com/help/images/ref/graycomatrix.html>. [Accessed: 24-Jul-2019].
- [31] J. S. Bae, S. H. Lee, K. S. Choi, and J. O. Kim, "Robust skin-roughness estimation based on co-occurrence matrix," *J. Vis. Commun. Image Represent.*, vol. 46, pp. 13–22, 2017.
- [32] MathWorks, "Properties of gray-level co-occurrence matrix," 2019. [Online]. Available: <https://nl.mathworks.com/help/images/ref/graycoprops.html>. [Accessed: 22-Jul-2019].
- [33] B. W. Pogue and M. S. Patterson, "Review of tissue simulating phantoms for optical spectroscopy, imaging and dosimetry," *J. Biomed. Opt.*, vol. 11, no. 4, p. 041102, 2006.
- [34] E. P. Judge, J. M. L. Hughes, J. J. Egan, M. Maguire, E. L. Molloy, and S. O'Dea, "Anatomy and bronchoscopy of the porcine lung: A model for translational respiratory medicine," *Am. J. Respir. Cell Mol. Biol.*, vol. 51, no. 3, pp. 334–343, 2014.
- [35] K. Gono *et al.*, "Endoscopic Observation of Tissue by Narrowband Illumination," *Opt. Rev.*, vol. 10, no. 4, pp. 211–215, 2003.
- [36] K. Gono, T. Obi, M. Yamaguchi, N. Ohyama, and Y. Sano, "Appearance of enhanced tissue features in narrow-band endoscopic imaging," *J. Biomed. Opt.*, vol. 9, no. 3, pp. 568–577, 2004.
- [37] Ocean Optics, "Overture user's guide," 2011. [Online]. Available: <https://oceanoptics.com/wp-content/uploads/Overture.pdf>. [Accessed: 19-Aug-2019].
- [38] F. van der Heijden, "Lecture sheets Technical Medicine, University of Twente: Registration and Alignment," 2017.
- [39] J. C. van Houwelingen, T. Stijnen, and R. van Strik, *Inleiding tot de Medische Statistiek*, 3rd ed. Bohn Stafleu van Loghum, 2016.
- [40] H. Akoglu, "User's guide to correlation coefficient," *Turkish J. Emerg. Med.*, vol. 18, no. August, pp. 91–93, 2018.
- [41] F. van der Heijden, *Image Based Measurement Systems*, 1st ed. Chichester: John Wiley & Sons Ltd., 1994.
- [42] Integraal Kankercentrum Nederland, "Cijfers over Kanker," 2019. [Online]. Available: <https://www.cijfersoverkanker.nl/>. [Accessed: 26-Feb-2019].
- [43] Long Alliantie Nederland, *Longziekten feiten en cijfers 2013*. Amersfoort: Long Alliantie Nederland, 2013.
- [44] K. Shibuya *et al.*, "Subepithelial vascular patterns in bronchial dysplasias using a high magnification bronchovideoscope," *Thorax*, vol. 57, pp. 902–907, 2002.
- [45] J. E. East *et al.*, "Advanced endoscopic imaging: European Society of Gastrointestinal Endoscopy (ESGE) Technology Review," *Endoscopy*, vol. 48, pp. 1029–1045, 2016.
- [46] American Thoracic Society, "Diagnosis and Treatment of Disease Caused by Nontuberculous Mycobacteria," *Am J Respir Crit Care Med*, vol. 156, pp. S1–S25, 1997.
- [47] J. M. Bryant *et al.*, "Whole-genome sequencing to identify transmission of Mycobacterium abscessus between patients with cystic fibrosis: A retrospective cohort study," *Lancet*, vol. 381, no. 9877, pp. 1551–1560, 2013.
- [48] I. Porvaznik, I. Solovic, and J. Mokřý, "Non-Tuberculous Mycobacteria: Classification, Diagnostics and Therapy," in *Respiratory Prevention and Treatment*, vol. 44, no. 4, M. Pokorski, Ed. 2017, pp. 19–26.
- [49] K. Watanabe, "Physiological Manifestation in Pulmonary Sarcoidosis," *Intech Open*, vol. 2, p. 64, 2015.
- [50] R. P. Baughman, D. A. Culver, M. A. Judson, and S. Carolina, "A Concise Review of Pulmonary Sarcoidosis," *Am J Respir Crit Care Med*, vol. 183, no. 11, pp. 573–581, 2011.
- [51] B. F. Dickey, J. V. Fahy, M. Kesimer, C. M. Evans, and D. Thornton, "Measuring Airway Mucin 2 in Patients with Severe Chronic Obstructive Pulmonary Disease with Bacterial Colonization," *AnnalsATS*, vol. 13, no. 11, 2016.
- [52] Y. W. Choi *et al.*, "Effects of Radiation Therapy on the Lung: Radiologic Appear- ances and Differential Diagnosis 1 CME FEATURE LEARNING OBJECTIVES FOR TEST 2," *Radio Graph.*, pp. 985–997, 2004.
- [53] M. Mirsadraee, "Anthracosis of the lungs: etiology, clinical manifestations and diagnosis: a review.," *Tanaffos*, vol. 13, no. 4, pp. 1–13, 2014.
- [54] S. Spalgais, D. Gothi, A. Jaiswal, and K. Gupta, "Nonoccupational anthracofibrosis/anthracosilicosis from Ladakh in Jammu and Kashmir, India: A case series," *J. Occup. Environ. Med.*, vol. 19, no. 3, pp. 159–166, 2015.
- [55] R. H. Demling, "Smoke inhalation lung injury: an update.," *Eplasty*, vol. 8, p. e27, 2008.
- [56] L. Fodor, "Light Tissue Interactions," in *Aesthetic Applications of Intense Pulsed Light*, 2011, pp. 11–21.

- [57] Faculty of Biological Sciences University of Leeds, "Respiratory histology | Trachea, bronchioles and bronchi," 2019. [Online]. Available: <https://www.histology.leeds.ac.uk/respiratory/conducting.php>. [Accessed: 13-Jul-2019].
- [58] WebScope5, "Histology Respiratory System," 2019. [Online]. Available: [http://141.214.65.171/Histology/RespiratorySystem/126\\_HISTO\\_40X.svs/view.apml?X=-0.445522294958721&Y=0.462915644111184&zoom=20](http://141.214.65.171/Histology/RespiratorySystem/126_HISTO_40X.svs/view.apml?X=-0.445522294958721&Y=0.462915644111184&zoom=20). [Accessed: 13-Jul-2019].
- [59] M. H. and V. M. L. Resources, "Respiratory System," 2019. [Online]. Available: <http://histology.medicine.umich.edu/resources/respiratory-system>. [Accessed: 13-Jul-2019].
- [60] B. K. Rubin, "Physiology of airway mucus clearance," *Respir. Care*, vol. 47, no. 7, pp. 761–8, 2002.
- [61] J. V Fahy and B. F. Dickey, "Airway Mucus Function and Dysfunction," vol. 363, no. 23, pp. 2233–2247, 2014.
- [62] H. Minami, Y. Ando, F. Nomura, S. Sakai, and K. Shimokata, "Interbronchoscopist variability in the diagnosis of lung cancer by flexible bronchoscopy," *Chest*, vol. 105, no. 6, pp. 1658–1662, 1994.
- [63] M. A. Jantz and W. C. McGaghie, "It's Time for a STAT Assessment of Bronchoscopy Skills," *Am. J. Respir. Crit. Care Med.*, vol. 186, no. 8, pp. 701–703, 2012.
- [64] M. H. Hesamian, W. Jia, X. He, and P. Kennedy, "Deep Learning Techniques for Medical Image Segmentation: Achievements and Challenges," *J. Digit. Imaging*, vol. 3, pp. 582–596, 2019.
- [65] C. Tenbergen, "Technical Medicine internship report: Automatic endobronchial vascular pattern classification," Longziekten, Radboudumc, Nijmegen, 2015.
- [66] J. Brownlee, "How much training data is required for Machine Learning?," 2017. [Online]. Available: <https://machinelearningmastery.com/much-training-data-required-machine-learning/>. [Accessed: 15-Aug-2019].
- [67] Y. Abu-Mostafa, "Online Lecture - The VC Dimension," 2012. [Online]. Available: <https://www.youtube.com/watch?v=Dc0sr0kdbVI>.
- [68] E. J. Topol, "Human and Artificial intelligence," *Nat. Med.*, vol. 25, no. January, 2019.
- [69] T. J. P. Jansen, "Technical Medicine internship report: Endobronchial Vascular Pattern Analysis," Longziekten, Radboudumc, Nijmegen, 2015.
- [70] N. Wadhwa, M. Rubinstein, F. Durand, and W. T. Freeman, "Phase-based video motion processing," *ACM Trans. Graph.*, vol. 32, no. 4, 2013.
- [71] Y. Zhang, S. L. Pinteá, and J. C. Van Gemert, "Video acceleration magnification," *Proc. - 30th IEEE Conf. Comput. Vis. Pattern Recognition, CVPR 2017*, vol. 2017-Janua, pp. 502–510, 2017.
- [72] C. Liu, A. Torralba, W. T. Freeman, F. Durand, and E. H. Adelson, "Motion magnification," *ACM Trans. Graph.*, vol. 24, no. 3, pp. 519–526, 2005.
- [73] C. Mauer, "Measurement of the spectral response of digital cameras with a set of interference filters," University of Applied Sciences Cologne, 2009.
- [74] MonoSpektra, "Noninvasive Tissue Monitoring Using UV-Vis and NIR Spectroscopy," 2019. [Online]. Available: <https://www.monospektra.com/noninvasive-tissue-monitoring-using-uv-vis-and-nir-spectroscopy/>. [Accessed: 01-Dec-2019].
- [75] S. Jacques and S. Prahl, "Optical Absorption of Hemoglobin," 2018. [Online]. Available: <https://omlc.org/spectra/hemoglobin/>. [Accessed: 01-Dec-2019].
- [76] F. Meng and A. I. Alayash, "Determination of extinction coefficients of human hemoglobin in various redox states," *Anal. Biochem.*, vol. 521, pp. 11–19, 2017.
- [77] V. N. Du Le, Q. Wang, T. Gould, J. C. Ramella-Roman, and T. Joshua Pfefer, "Vascular contrast in narrow-band and white light imaging," *Appl. Opt.*, vol. 53, no. 18, p. 4061, 2014.

## 7 Appendices

### 7.1 Camera response model

The response model for a digital camera is expressed in equation 9.

**Equation 9:** Calculation of camera response signal

$$r_k = t_e \int_{\lambda_{min}}^{\lambda_{max}} S_e(\lambda) R_n(\lambda) S_k(\lambda) d\lambda \quad [73] \quad (9)$$

$r_k$  = camera response signal in colour channel  $k$ . The surface below this graph is a measure for the energy of the signal in the specific colour channel.

$k$  = index for the three colour channels red ( $k = 1$ ), green ( $k = 2$ ), and blue ( $k = 3$ ).

$t_e$  = exposure time in seconds.

$\lambda$  = wavelength of light in nanometre, of which the limits  $\lambda_{min}$  and  $\lambda_{max}$  enclose the sensitive spectral area of the image. These limits are often chosen in agreement with the limits of the human visual range.

$S_e(\lambda)$  = light emittance spectrum with which the object is illuminated as a function of the wavelength  $\lambda$ . This emittance spectrum is altered in optical enhancement imaging by applying optical filters.

$R_n(\lambda)$  = reflection spectrum reflected by the illuminated object as a function of the wavelength  $\lambda$ . This reflection spectrum is specific for the tissue or material  $n$ .

$S_k(\lambda)$  = sensitivity spectrum for colour channel  $k$  as a function of the wavelength  $\lambda$ . The sensitivity spectrum for each of the colour channels is unique for every camera type. For a comparable camera that has been used in this experiment, the sensitivity spectrum as given in figure 35 is true.

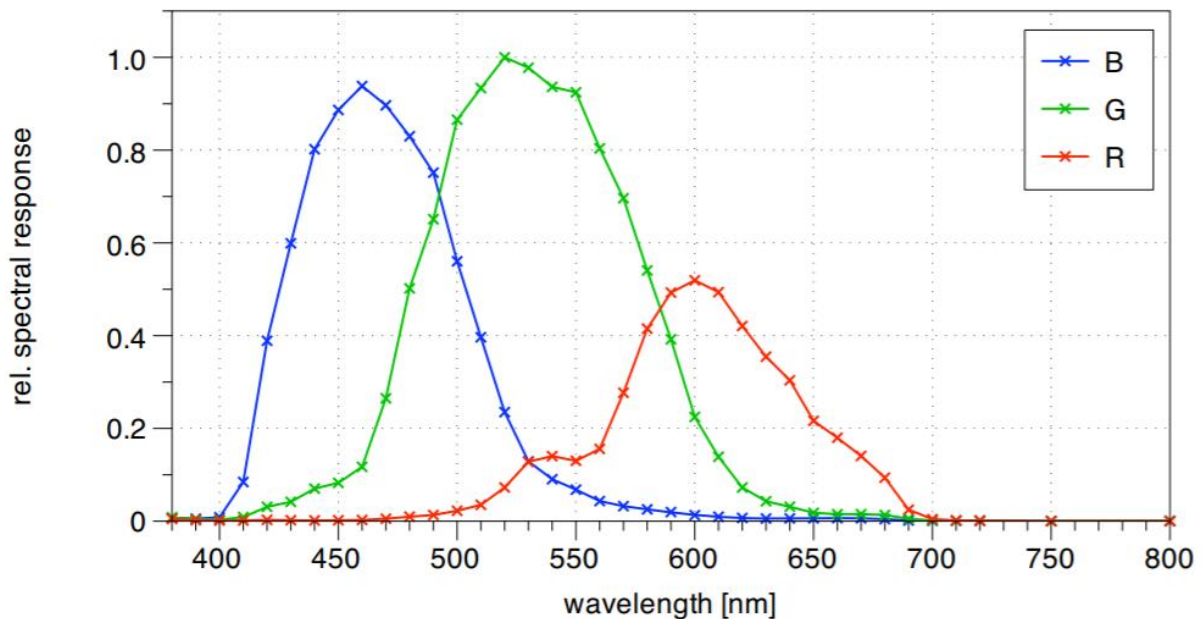


**Figure 35:** Camera sensitivity spectrum as a function of the wavelength for the colour channels of red, green, and blue light. [73]

## 7.2 Interaction of tissue and light of various wavelengths

When light encounters a tissue, reflection, absorption or transmission can occur. The principle of optical enhancement relies on the differences in light interaction between blood vessels and surrounding tissue. When simplifying tissue as a superficial layer and a deep layer in either of which blood vessels can be present, four different tissue types can be distinguished. In table I, the interaction of tissue and light is given for three different colours of light. The percentages are estimations of relative reflection, absorption and transmission based on the molar attenuation coefficient of haemoglobin for different wavelengths of light. [74][75][76][77]

**Table I:** Interaction of tissue and light for superficial versus deep layers and blood vessels versus surrounding tissue. Percentages are estimations and serve to illustrate the effect of illumination by different wavelengths on different tissues.

Light colour (wavelength)	Incoming light in superficial layer	Superficial layer (~1 mm)		Incoming light in deep layer	Deep layer (~3 mm)	
		Blood vessel	Surrounding tissue		Blood vessel	Surrounding tissue
<b>Red</b> 620-750 nm	100%	4% Ref 6% Abs 90% Trans	6% Ref 4% Abs 90% Trans	90%	10% Ref 80% Abs	90% Ref 0% Abs
<b>Green</b> 495-570 nm	100%	15% Ref 35% Abs 50% Trans	35% Ref 15% Abs 50% Trans	50%	15% Ref 35% Abs	50% Ref 0% Abs
<b>Blue</b> 450-495 nm	100%	10% Ref 90% Abs 0% Trans	90% Ref 10% Abs 0% Trans	0%	-	-
Ref = reflection Abs = absorption Trans = transmission						

Red light has a slightly different interaction with blood vessels as compared to surrounding tissue in the superficial layer, meaning that the red channel of the signal contains a slight difference in signal between blood vessels and tissue in the superficial layer. Most of the red light is transmitted to the deeper layer, where the difference in reflection and absorption of light between blood vessels and surrounding tissue is more outspoken.

The blue light shows a large difference in interaction with blood vessels as compared to surrounding tissue in the superficial layer. A larger portion of the blue light is absorbed when blood vessels are present. The blue light is either reflected or absorbed in the superficial layer and is not transmitted to the deeper layer.

The interaction of the green light shows a pattern that lies in between the red and blue light tissue interactions. There is a difference in interaction with blood vessels as compared to surrounding tissue in the superficial layer, meaning that the green channel of the signal contains a difference in signal between superficial blood vessels and tissue. A substantial portion of the light is transmitted to the deeper layer, where a difference in reflection and absorption of light between blood vessels and surrounding tissue is observed.

### 7.3 Names and descriptions of MATLAB scripts

Analysis of the results have been executed in MATLAB 2018a (MathWorks, Natick, United states of America). These scripts and example data sets are available on the digital research server of the Pulmonary department of the Radboudumc in Nijmegen, the Netherlands.

SPECTRUM INTENSITY		
Input data	Script name	Description
Spectrometer measurements	<i>visualiseSpectraPhantom.m</i>	Calculating spectrum intensity from spectrometer data for the phantom measurements
	<i>visualiseSpectraBronchus.m</i>	Calculating spectrum intensity from spectrometer data for the porcine bronchus measurements
SURFACE STRUCTURE VISUALISATION		
Input data	Script name	Description
Pictures of surface visualisation phantom	<i>clickFiducialsPhantom.m</i>	Manually indicate five fiducial points for Procrustes alignment
	<i>generateQuantificationsPhantom.m</i>	Select ROI, perform Procrustes alignment, create co-occurrence matrix, create histograms, determine RGB values
	<i>analyseQuantificationsPhantom.m</i>	Determine the top 5 best performing spectra.
	<i>correlateTexturePhantom.m</i>	Calculate the correlation between co-occurrence matrix descriptors and spectrum intensity. Calculate the correlation between co-occurrence matrix descriptors and histogram peak width.
Pictures of surface visualisation phantom with clinical system	<i>analysePentaxImagesPhantom.m</i>	Select ROI, create co-occurrence matrix, calculate the co-occurrence matrix descriptors



*CAPILLARY VISUALISATION*

<b>Input data</b>	<b>Script name</b>	<b>Description</b>
Pictures of superficial capillaries phantom	<i>clickFiducialsBronchus.m</i>	Manually indicate four fiducial points for Procrustes alignment
	<i>generateQuantificationsBronchus.m</i>	Select ROI, perform Procrustes alignment, create co-occurrence matrix, create histograms, determine RGB values
	<i>analyseQuantificationsBronchus.m</i>	Determine the top 5 best performing spectra. Correlate the performance with spectrum intensity and t-test of spectrum groups.
Pictures of underside of human tongue with clinical system	<i>clickFiducialsTongue.m</i>	Manually indicate five fiducial points for Procrustes alignment
	<i>analysePentaxImagesTongue.m</i>	Select two ROI, calculate colour difference

*DEEP VEIN VISUALISATION*

<b>Input data</b>	<b>Script name</b>	<b>Description</b>
Pictures of deep vein vessel phantom	<i>clickFiducialsHand.m</i>	Manually indicate three fiducial points for Procrustes alignment
	<i>generateQuantificationsHand.m</i>	Select ROI, perform Procrustes alignment, create co-occurrence matrix, create histograms, determine RGB values
	<i>analyseQuantificationsHand.m</i>	Determine the top 5 best performing spectra. Correlate the performance with spectrum intensity and t-test of spectrum groups.
Pictures of deep vein vessel phantom with clinical system	<i>clickFiducialsHand.m</i>	Manually indicate five fiducial points for Procrustes alignment
	<i>analysePentaxImagesHand.m</i>	Select two ROI, calculate colour difference

*PATIENT CASE SERIES*

<b>Input data</b>	<b>Script name</b>	<b>Description</b>
Video stills of patients undergoing bronchoscopy	<i>subtractWLBOEnoLesions</i>	Analyse twin mode images of patients without central bronchial lesions. Create subtraction images.
	<i>AnalyseArchesVessels.m</i>	Select bronchial arch, vessel and background ROI. Quantify the RGB contrast.
	<i>subtractWLBOELesions.m</i>	Analyse twin mode images of patients with central bronchial lesions. Create subtraction images.

#### 7.4 Tables results technique validation of optical enhancement for bronchoscopy

**Table II:** Spectrum light intensity for the 28 tested spectra. Intensity was measured twice, during the polymer clay surface texture phantom measurements, and during the porcine bronchus phantom measurements.

<b>Spectrum name</b>	<b>Light intensity polymer clay phantom measurements</b> [number of photons]	<b>Light intensity porcine bronchus phantom measurements</b> [number of photons]
1	256278756	124184777
2	410219065	790799580
3	292916184	544339725
4	304870862	645105980
5	417570049	978129097
6	235453300	584043728
7	470489314	1029339812
8	1195021650	2465242813
9	1446598162	3261668708
10	1041568738	2092164464
11	3336523624	3489842283
12	4033034563	4364634144
13	2960405180	3442926927
14	2309145379	2606279907
15	3075130550	3358281706
16	2122085102	2324794365
17	32438195952	77040324795
A1	340135391	422032743
A2	944503343	1066049063
A3	1159222969	1327701947
A4	1185153703	1342490515
A5	984565215	1023416073
B1	109950695	130406765
B2	65013985	70787933
B3	71367918	75872109
M1	89748518	168626609
M2	96376008	109353631
M3	141274751	163068824

**Table III:** Mean co-occurrence matrix (CM) contrast, correlation, energy and homogeneity of the eight co-occurrence matrices as quantifications for surface texture for all 28 spectra. The top 5 spectra with the most favourable values for surface visualisation are indicated in green.

\* data for spectrum 17 was not saved effectively and could therefore not be included in the analysis

Spectrum name	CM contrast	Correlation	Energy	Homo-geneity
1	0.0173	0.6619	0.9776	0.9961
2	(5) 0.0896	(5) 0.7781	(5) 0.9418	(4) 0.9888
3	(4) 0.0998	(1) 0.7901	(4) 0.9405	(5) 0.9894
4	0.0284	0.7162	0.9635	0.9941
5	0.0233	0.7544	0.9635	0.9941
6	0.0154	0.6447	0.9755	0.9962
7	(3) 0.1277	(3) 0.7846	(2) 0.9400	(3) 0.9882
8	(2) 0.1427	0.7693	(1) 0.9383	(1) 0.9877
9	(1) 0.1456	(2) 0.7870	(3) 0.9403	(2) 0.9878
10	0.0277	0.7273	0.9717	0.9951
11	0.0300	0.6641	0.9702	0.9939
12	0.0292	0.6649	0.9683	0.9939
13	0.0831	0.7413	0.9428	0.9897
14	0.0091	0.6209	0.9944	0.9988
15	0.0094	0.6568	0.9925	0.9985
16	0.0149	0.6924	0.9807	0.9965
A1	0.0084	0.5261	0.9889	0.9976
A2	0.0098	0.6780	0.9932	0.9985
A3	0.0178	0.5820	0.9854	0.9970
A4	0.0106	0.6263	0.9883	0.9977
A5	0.0141	(4) 0.7785	0.9555	0.9965
B1	0.0077	0.4739	0.9864	0.9972
B2	0.0010	0.5877	0.9996	0.9999
B3	0.0102	0.1999	0.9945	0.9983
M1	0.0132	0.3216	0.9903	0.9978
M2	0.0026	0.5147	0.9972	0.9994
M3	0.0078	0.7406	0.9732	0.9970

**Table IV:** R+G+B colour histogram peak width for all 28 spectra

Spectrum name	R+G+B colour histogram peak width
1	258
2	274
3	242
4	290
5	262
6	190
7	321
8	422
9	417
10	204
11	163
12	175
13	264
14	106
15	103
16	290
A1	167
A2	146
A3	213
A4	83
A5	141
B1	144
B2	19
B3	25
M1	154
M2	22
M3	161

**Table V:** Resulting 3D distance in the RGB colour space and the individual colour channels as quantifications for capillary visualisation for all 28 spectra. The top 5 spectra with the most favourable values for capillary visualisation are indicated in green.

Spectrum name	3D distance RGB	Colour difference red channel	Colour difference green channel	Colour difference blue channel
1	(2) 31.7550	0.0024	16.4988	27.1324
2	(5) 30.0961	1.3610	16.3092	25.2574
3	23.3370	5.8616	9.4477	20.5182
4	26.2201	20.6812	0.0004	16.1178
5	27.1602	21.4215	0.0027	16.6972
6	17.0180	6.1737	0.0084	15.8587
7	(1) 33.1114	17.0434	14.6955	24.2884
8	19.2628	12.1402	8.6192	12.2221
9	20.8615	12.9631	8.4018	14.0203
10	17.3968	0	10.5067	13.8656
11	20.1514	5.2745	8.7114	17.3888
12	22.1045	7.8835	10.9860	17.4862
13	29.3380	23.8981	5.3237	16.1635
14	21.9930	3.0075	21.7864	0
15	22.3059	0.1817	22.3051	0
16	27.3323	20.5274	18.0466	0
17	24.8008	4.4935	16.4066	18.0475
A1	8.9180	0.0664	3.9538	7.9934
A2	14.9062	0	7.4229	12.9265
A3	(3) 30.5616	23.5194	19.5154	0
A4	14.1759	0	12.7002	6.2977
A5	(4) 30.3669	30.2907	0.1264	2.1464
B1	15.4854	0.3973	0.0001	15.4803
B2	1.0665	0.1376	0.9201	0.5214
B3	2.0848	1.9408	0.4104	0.6413
M1	14.2300	0.5344	0.0056	14.2200
M2	1.6437	1.1282	1.1336	0.3792
M3	16.1979	1.6376	0.0020	16.1149

**Table VI:** Resulting 3D distance in the RGB colour space and the individual colour channels as quantifications for deep vein visualisation for all 28 spectra. The top 5 spectra with the most favourable values for deep vein visualisation are indicated in green.

Spectrum number	3D distance RGB	Colour difference red channel	Colour difference green channel	Colour difference blue channel
1	15.8860	0.0001	8.4794	13.4337
2	(5) 23.4195	5.4690	16.8020	15.3706
3	(4) 23.5632	7.2517	13.9688	17.5360
4	(1) 26.6567	20.1334	0.0295	17.4706
5	22.0346	15.8447	0.0093	15.3124
6	17.6520	6.9327	0.2591	16.2316
7	(2) 25.0291	16.8840	13.3117	12.8134
8	20.6876	17.2200	9.8421	5.8805
9	(3) 24.7438	19.4822	12.6714	8.4931
10	15.1305	7.7674	8.9597	9.3981
11	18.3738	12.8722	13.1081	0.2847
12	17.4604	12.6685	12.0153	0.0851
13	19.8729	16.0425	11.6838	1.0275
14	16.8302	11.1883	12.5728	0.0003
15	17.2657	10.8160	13.4580	0.0000
16	12.4308	9.3994	8.1348	0.0026
17	21.0271	15.7063	10.7690	8.9151
A1	2.2665	0.1362	0.9825	2.0379
A2	8.0374	0	5.8902	5.4685
A3	16.9235	15.2510	7.3357	0.0007
A4	8.3222	0.0289	8.1906	1.4740
A5	12.7928	12.7090	0.0033	1.4618
B1	13.1628	0.7552	0.0117	13.1411
B2	0.8353	0.2200	0.6991	0.4008
B3	2.6022	2.5637	0.3298	0.3003
M1	16.7465	0.8839	0.4684	16.7166
M2	3.2991	3.0399	1.2731	0.1483
M3	14.2092	3.4627	0.1366	13.7801

## 7.5 Research protocol prospective database registry

CMO 2019-5583 – BEELDBANK BRONCHOSCOPIE onderzoeksprotocol versie 2, July 18th 2019

### RESEARCH PROTOCOL

#### BeeldBank Bronchoscopie

Evaluating the diagnostic value of different light settings and image processing in bronchoscopy data obtained in patients with any indication for bronchoscopy

Radboud University Medical Center  
Nijmegen, The Netherlands  
July 18<sup>th</sup> 2019  
Version 2

Erik (HFM) van der Heijden, MD, PhD

CMO 2019-5583 – BEELDBANK BRONCHOSCOPIE onderzoeksprotocol versie 2, July 18th 2019

PROTOCOL TITLE 'Evaluating the diagnostic value of different light settings and image processing in bronchoscopy data obtained in patients with any indication for bronchoscopy'

Protocol ID	CMO 2019-5583: BeeldBank Bronchoscopie
Short title	BeeldBank Bronchoscopie (BBB)
Version	2
Date	July 18 <sup>th</sup> 2019
Coordinating investigator/project leader	<i>Erik (HFM) van der Heijden, MD, PhD</i> <i>Associate Professor Interventional Pulmonology</i>  <i>Radboud University Medical Center Nijmegen</i> <i>Department of Pulmonary Diseases</i> <i>Internal postal code 614</i> <a href="mailto:erikvanderheijden@radboudumc.nl">erikvanderheijden@radboudumc.nl</a> <i>Postbus 9101, 6500HB Nijmegen, The Netherlands</i> <i>T 024-3610325, F 024-3610324</i>
Principal investigator(s)	<i>Erik (HFM) van der Heijden, MD, PhD</i> <i>Associate Professor Interventional Pulmonology</i>
Sponsor (in Dutch: verrichter/opdrachtgever)	<i>Radboudumc Nijmegen,</i> <i>Department of Pulmonary Diseases</i> <i>Internal postal code 614</i> <i>Postbus 9101, 6500HB Nijmegen, The Netherlands</i> <i>T 024-3610325, F 024-3610324</i>
Independent expert(s)	<i>Dr. Monique Reijers, MD, PhD, Chest Physician</i> <i>Radboudumc Nijmegen,</i> <i>Department of Pulmonary Diseases,</i> <i>Internal postal code 614</i> <i>Postbus 9101, 6500HB Nijmegen, The Netherlands</i> <i>T 024-3619220 F 024-361032</i>
Co-investigators:	NA

PROTOCOL SIGNATURE SHEET

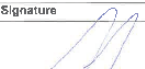

Name	Signature	Date
Head of Department: Prof. Dr. M. van den Heuvel		18-07-2019
Coordinating Investigator/Project leader/Principal Investigator: Dr. Erik (HEM) van der Heijden		18-07-2019

TABLE OF CONTENTS

1. INTRODUCTION AND RATIONALE .....	8
2. OBJECTIVES .....	10
3. STUDY DESIGN .....	10
4. STUDY POPULATION .....	10
4.1 Population (base) .....	10
4.2 Inclusion criteria .....	10
4.3 Exclusion criteria .....	10
4.4 Sample size calculation .....	10
5. TREATMENT OF SUBJECTS .....	11
5.1 Investigational product/treatment .....	11
5.2 Use of co-intervention (if applicable) .....	11
5.3 Escape medication (if applicable) .....	11
6. INVESTIGATIONAL PRODUCT .....	11
6.1 Name and description of investigational product(s) .....	11
6.2 Summary of findings from non-clinical studies .....	11
6.3 Summary of findings from clinical studies .....	11
6.4 Summary of known and potential risks and benefits .....	12
6.5 Description and justification of route of administration and dosage .....	12
6.6 Dosages, dosage modifications and method of administration .....	12
6.7 Preparation and labelling of Investigational Medicinal Product .....	12
6.8 Drug accountability .....	12
7. NON-INVESTIGATIONAL PRODUCT .....	12
7.1 Name and description of non-investigational product(s) .....	12
7.2 Summary of findings from non-clinical studies .....	12
7.3 Summary of findings from clinical studies .....	12
7.4 Summary of known and potential risks and benefits .....	12
7.5 Description and justification of route of administration and dosage .....	12
7.6 Dosages, dosage modifications and method of administration .....	12
7.7 Preparation and labelling of Non Investigational Medicinal Product .....	12
7.8 Drug accountability .....	12
8. METHODS .....	12
8.1 Database registry parameters .....	12
8.2 Randomisation, blinding and treatment allocation .....	14
8.3 Study procedures .....	14
8.4 Withdrawal of individual subjects .....	14
8.4.1 Specific criteria for withdrawal (if applicable) .....	14
8.5 Replacement of individual subjects after withdrawal .....	14
8.6 Follow-up of subjects withdrawn from treatment .....	14
8.7 Premature termination of the study .....	14
9. SAFETY REPORTING .....	14
9.1 Temporary halt for reasons of subject safety .....	14
9.2 AEs, SAEs and SUSARs .....	14

9.2.1	Adverse events (AEs)	14
9.2.2	Serious adverse events (SAEs)	14
9.2.3	Suspected unexpected serious adverse reactions (SUSARs)	14
9.3	Annual safety report	14
9.4	Follow-up of adverse events	14
9.5	[Data Safety Monitoring Board (DSMB) / Safety Committee]	14
10.	STATISTICAL ANALYSIS	14
10.1	Primary study parameter(s)	15
10.2	Secondary study parameter(s)	15
10.3	Exploratory study parameter(s)	15
10.4	Other study parameters	15
10.5	Interim analysis (if applicable)	15
11.	ETHICAL CONSIDERATIONS	15
11.1	Regulation statement	15
11.2	Recruitment and consent	15
11.3	Objection by minors or incapacitated subjects (if applicable)	15
11.4	Benefits and risks assessment, group relatedness	15
11.5	Compensation for injury	16
11.6	Incentives (if applicable)	16
12.	ADMINISTRATIVE ASPECTS, MONITORING AND PUBLICATION	16
12.1	Handling and storage of data and documents	16
12.2	Monitoring and Quality Assurance	16
12.3	Amendments	17
12.4	Annual progress report	17
12.5	Temporary halt and (prematurely) end of study report	17
12.6	Public disclosure and publication policy	17
13.	STRUCTURED RISK ANALYSIS	17
13.1	Potential issues of concern	17
13.2	Synthesis	17
14.	REFERENCES	18

LIST OF ABBREVIATIONS AND RELEVANT DEFINITIONS

AE	Adverse Event
AR	Adverse Reaction
BBB	BeeldBank Bronchoscopie
CA	Competent Authority
CRF	Case Report Form
DSMB	Data Safety Monitoring Board
EU	European Union
GCP	Good Clinical Practice
GDPR	General Data Protection Regulation; in Dutch: Algemene Verordening Gegevensbescherming (AVG)
IB	Investigator's Brochure
IC	Informed Consent
IMP	Investigational Medicinal Product
IMPD	Investigational Medicinal Product Dossier
METC	Medical research ethics committee (MREC); in Dutch: medisch-ethische toetsingscommissie (METC)
NBI	Narrow Band Imaging
OE	Optical Enhancement
(S)AE	(Serious) Adverse Event
Sponsor	The sponsor is the party that commissions the organisation or performance of the research, for example a pharmaceutical company, academic hospital, scientific organisation or investigator. A party that provides funding for a study but does not commission it is not regarded as the sponsor, but referred to as a subsidising party.
SUSAR	Suspected Unexpected Serious Adverse Reaction
UAVG	Dutch Act on Implementation of the General Data Protection Regulation; in Dutch: Uitvoeringswet AVG
WLB	White Light Bronchoscopy
WMO	Medical Research Involving Human Subjects Act; in Dutch: Wet Medisch-wetenschappelijk Onderzoek met Mensen



#### SUMMARY

**Rationale:** Bronchoscopy allows for visual inspection of the bronchial walls, collecting material for cytological and histological analysis as well as the execution of pulmonary interventions such as tumour debulking, bronchial stenting, abscess drainage or foreign body removal. Narrow band imaging (NBI) uses optical filters that define the spectral characteristics of the emitted light. The application of NBI in gastro-intestinal endoscopy is useful for the classification of polyp lesions and gastric abnormalities. [1][2][3] NBI has also been used in the diagnosis of oesophageal squamous cell carcinoma. [4] Most papers about NBI in bronchoscopy focus on (pre)malignant airway lesions. [2][5][6][7][8] While the possibilities of NBI are promising, especially because of the increased vessel-to-background contrast, the added value of applying narrow band imaging during bronchoscopy has not been assessed in a broad patient population. Besides, modern image processing allows for a more in-depth analysis of the bronchial tissue.

This research aims to build a database of bronchoscopy photos and videos to allow for analysis in order to assess the diagnostic value of narrow band imaging. This database registry also aims to be used for the development of new image processing algorithms.

**Objective:** This research aims to build a database of bronchoscopy photos and videos to investigate if, and for which pathologies, the application of narrow band imaging during bronchoscopy is useful. Besides, modern image processing allows for a broader analysis of the features in bronchial tissue, both visible and invisible to the naked eye. The photos and videos in this database registry are also meant to be used for the development of image processing algorithms to discover more diagnostic information in the bronchoscopy images. These findings may lead to improvement of bronchoscopy protocols, development of new image analysis methods and improvement of the diagnostics that can be performed during the procedure.

**Study design:** Prospective case registry.

**Study population:** All patients referred and eligible for a bronchoscopy procedure can participate in the study.

**Intervention (if applicable):** NA

**Main study parameters/endpoints:** Prospective database registry of bronchoscopy images and videos combined with the illumination and image processing settings. Secondary study parameters allow for a link between the bronchoscopy images and medical status of the patient.

**Nature and extent of the burden and risks associated with participation, benefit and group relatedness:** None.

Version number: 2, date 18-07-2019

7 of 18

#### 1. INTRODUCTION AND RATIONALE

##### Bronchoscopy

Bronchoscopy is a pulmonary intervention in which a flexible endoscope is inserted in the central airways. Bronchoscopy allows for visual inspection of the bronchial walls, collecting material for cytological and histological analysis and the execution of pulmonary interventions such as tumour debulking, bronchial stenting, abscess drainage or foreign body removal. Diffuse or localized lung infiltrates, recurrent or unresolved pneumonia, bronchiectasis, haemoptysis, persistent cough and symptoms of endobronchial obstructions are indications for bronchoscopy. [9]

##### Narrow Band Imaging

Recognising visual cues during the procedure is the main method to locate central lung pathologies. White light bronchoscopy (WLB) is the most broadly used method to illuminate the bronchial tissue. However, the PENTAX (Pentax Medical, Japan) processors also support an image-enhanced bronchoscopic technology that emits selective wavelengths of light to illuminate the tissue. This technique is called Narrow Band Imaging (NBI). NBI is also referred to as optical enhancement (OE) by Pentax Medical. The NBI technology uses optical filters that define the spectral characteristics of the emitted light. [1] NBI uses multiple bandwidths of light to enhance certain tissue features. A typical example is emittance of light between 390 and 445 nm (blue light) which is absorbed by superficial capillaries combined with emittance of light between 530 and 550 nm (green light) that is absorbed by blood vessels below the mucosal capillaries. [7] Illuminating the tissue with these specific parts of the light spectrum cause more contrast between the blood vessels and the mucosal background. [10]

##### Clinical evidence on Narrow Band Imaging

In gastrointestinal endoscopy, narrow band imaging optically enhances certain tissue properties, which can be used for the classification of polyp lesions and gastric abnormalities. [1][2][3] NBI has also been used in the diagnosis of oesophageal squamous cell carcinoma. [4] Most papers about NBI in bronchoscopy focus on (pre)malignant airway lesions. [2][5][6][7][8] For bronchial tissue, a relationship between vessel diameter, capillary pattern and malignancy grade has been proven. [6] Shibuya et al. have shown high correlation between increased vessel growth and complex networks of tortuous capillaries on one side and bronchial dysplasia on the other. [11] In 2003, Shibuya et al. published a study that included heavy smokers with a high risk of lung cancer. Significant correlation was found between the frequencies of dotted vessels visualised by NBI and the tissues pathologically confirmed as angiogenic squamous dysplasia. [5] Herth et al. evaluated the value of narrow band imaging compared to autofluorescence imaging and white light bronchoscopy. The relative sensitivity of NBI compared to WLB was statistically significant at 3.0. Further, combining autofluorescence imaging and narrow band imaging did not increase the diagnostic yield significantly. [7]

Version number: 2, date 18-07-2019

8 of 18

#### Narrow Band Imaging in bronchoscopy

As indicated in the paragraph above, the application of narrow band imaging in bronchoscopy has merely been described for the indication of cell dysplasia and lung cancer. The possibilities of the application of NBI in bronchoscopy are promising, especially because vessel and surface mucosa changes play a role in almost all central lung diseases. However, the added value of NBI during bronchoscopy has not been assessed in a broad patient population.

Zaric et al. mention in 2013 that the major advantage NBI compared to other imaging techniques is the quantitative assessment of the airway vascularity after lung transplantation. [12] A study in COPD patients showed that NBI is capable of quantifying endobronchial erythema, being a valuable tool for evaluating mucosal microvasculature and surface changes. [13]

It is unknown if and for which lung diseases narrow band imaging can add diagnostic yield during bronchoscopy. The added value of applying narrow band imaging during bronchoscopy has not been assessed in a big patient population. This research proposal aims to build a database of bronchoscopy photos and videos to allow for analysis in order to answer for which kind of pathology narrow band imaging is useful.

#### Image analysis algorithms

But besides assessing the added value of narrow band imaging, we would like to use the bronchoscopy database for other research purposes as well. We would like to find distinctive spectral characteristics of airway pathologies that can be visualised using WLB or NBI. This analysis can be done by analysing the image contrast and features in a quantitative manner, but can also be done by using artificial intelligence. The use of deep-learning algorithms to support clinicians is going to have a big impact on medicine in the future. [14] Building a consistent database of bronchoscopy photos and videos, obtained in both the WLB and NBI settings, will form the basis to develop deep-learning algorithms to improve bronchoscopy interpretation in the future.

#### Practical endnote

The NBI settings can be activated during the procedure by a button press on the bronchoscope. The button press causes optical filters in the bronchoscope processor to shift, ensuring that the bronchoscope emits selected bandwidths of light. Currently, the image settings from WLB are switched to narrow band imaging settings when the interpretation of mucosal abnormalities in the central airway are unclear and need further examination. For this research, bronchoscopists will need to change the settings and save the photos and videos. Everything about the clinical procedure stays the same. The duration of the bronchoscopy procedure is not influenced by this research.

## 2. OBJECTIVES

This research aims to build a database of bronchoscopy photos and videos to investigate if, and for which pathologies, using narrow band imaging during bronchoscopy is useful. Besides, modern image processing allows for a broader analysis of the features in bronchial tissue, both visible and invisible to the naked eye. The photos and videos in this database registry are also meant to be used for the development of image processing algorithms to discover more diagnostic information in the bronchoscopy images. These findings may lead to improvement of bronchoscopy protocols, development of new image analysis methods and improvement of the diagnostics that can be performed during the procedure.

## 3. STUDY DESIGN

Prospective database registry. The duration of the study is undetermined. The registry will continue as long as technological improvements and clinical applications of the light settings and image processing are being developed. The need for this bronchoscopy database registry will be re-evaluated every five years.

## 4. STUDY POPULATION

### 4.1 Population (base)

Every patient referred for a bronchoscopy procedure is eligible. Patient selection for participation in the registry follows the conventional selection of patients elected for bronchoscopy.

### 4.2 Inclusion criteria

In order to be eligible to participate in this study, a subject must meet all of the following criteria:

- Age 18 years or older
- Have an indication for bronchoscopy

### 4.3 Exclusion criteria

A potential subject who meets any of the following criteria will be excluded from participation in this study:

- Less than 18 years old
- Any contra-indication for a bronchoscopy procedure
- Inability to consent

### 4.4 Sample size calculation

Not applicable. The duration and sample size of this study is undetermined. The registry will continue as long as technological improvements of the light settings and image processing are being developed for clinical use. The need for this bronchoscopy database registry will be re-evaluated every five years.

5. TREATMENT OF SUBJECTS

5.1 Investigational product/treatment

NA

5.2 Use of co-intervention (if applicable)

NA

5.3 Escape medication (if applicable)

NA

6. INVESTIGATIONAL PRODUCT

NA

6.1 Name and description of investigational product(s)

NA

6.2 Summary of findings from non-clinical studies

Gono et al. have investigated the most suitable narrow band imaging wavelengths for vessel visualisation by inspecting the image contrast of the vessel bed under the human tongue. They found that the contrast of the capillary pattern versus the mucosal background is highest when using narrow-band illumination of 415±30nm. Combining this band with bands at 445±30 nm and 500±30 nm gave the optimal results for clinical interpretation. [15] These narrow bands correspond to the Narrow Band Imaging spectra provided by Pentax Medical. [4] An optical test conducted by our department using a porcine trachea specimen and a living human hand could not prove that there are any better combinations of wavelengths available than the ones provided by Pentax.

6.3 Summary of findings from clinical studies

The use of narrow band imaging during endoscopy has initially been focussed on gastrointestinal application. In gastrointestinal endoscopy, narrow band imaging optically enhances certain tissue properties, which can be used for the classification of polyp lesions and gastric abnormalities. [1][2][3] NBI has also been used in the diagnosis of oesophageal squamous cell carcinoma. [4]

For the application of NBI during bronchoscopy, signs of airway pathology could hypothetically be enhanced using narrow band imaging. Especially capillary bed aspects (capillary loops, dotted vessels, complex vascular networks of tortuous vessels, abrupt ending vessels) are signs of pathology. [7] Further colour, tissue surface pattern and thickness of the mucus layer are potential characteristics that can be enhanced using NBI. [2][7]

For bronchial tissue, a relationship between vessel diameter, capillary pattern and malignancy grade has been proven. [8] Shibuya et al. have shown high correlation between increased vessel growth and complex networks of tortuous capillaries and bronchial dysplasia. [11] In 2003, Shibuya et al. published a study that included heavy smokers with a high risk of lung cancer. Significant correlation was found between the frequencies of dotted vessels visualised by NBI and the tissues pathologically confirmed as angiogenic squamous

Version number: 2, date 18-07-2019

11 of 18

dysplasia. [5] Herth et al. evaluated the value of narrow band imaging compared to autofluorescence imaging and white light bronchoscopy. The relative sensitivity of NBI compared to WLB was statistically significant at 3.0. Further, combining autofluorescence imaging and narrow band imaging did not increase the diagnostic yield significantly. [7]

6.4 Summary of known and potential risks and benefits

Participation in this database registry does not add any risks or benefits for the participants.

6.5 Description and justification of route of administration and dosage

NA

6.6 Dosages, dosage modifications and method of administration

NA

6.7 Preparation and labelling of Investigational Medicinal Product

NA

6.8 Drug accountability

NA

7. NON-INVESTIGATIONAL PRODUCT

NA

7.1 Name and description of non-investigational product(s)

NA

7.2 Summary of findings from non-clinical studies

NA

7.3 Summary of findings from clinical studies

NA

7.4 Summary of known and potential risks and benefits

NA

7.5 Description and justification of route of administration and dosage

NA

7.6 Dosages, dosage modifications and method of administration

NA

7.7 Preparation and labelling of Non Investigational Medicinal Product

NA

7.8 Drug accountability

NA

8. METHODS

8.1 Database registry parameters

The main study parameters are the bronchoscopy images and videos obtained by white light bronchoscopy and narrow band imaging bronchoscopy. Secondary study parameters allow for a link between the medical condition and follow-up of the patient and the primary data.

Version number: 2, date 18-07-2019

12 of 18

Table 1 - Summary of database registry bronchoscopy parameters		
Registry parameters listed according to importance		
Parameter type	Variable type	Reporting method
<b>Main parameters</b>		
Bronchoscopic images	Images	Intra-procedural images
Bronchoscopic videos	Videos	Intra-procedural images
Tissue illumination settings	Nominal	The bronchoscopic images and videos display the current tissue illumination settings within the stored image frames
Post-acquisition processing	Nominal	The bronchoscopic images and videos display the current post-acquisition processing within the stored image frames
<b>Secondary parameters</b>		
Indication for bronchoscopy	Nominal	Clinical report
Outcomes of pre-procedural imaging and diagnostics	Nominal	Clinical report
Results and images of pre-procedural imaging	2D medical images or 3D medical volumes	Clinical report
Intra-procedural findings	Nominal	Bronchoscopy procedure report
Outcome of collected cytological and histological material during the procedure	Nominal	Pathological report
Outcome of collected specimens for culture	Nominal	Microbiology report and lab results
Outcome of future procedures and consultations	Nominal	Clinical report
<b>Patient demographics and characteristics</b>		
Age	Interval	Number
Gender	Ordinal	[F/M]
Body length	Interval	Body length in cm
Body weight	Interval	Body weight in kg
Smoking / exposure to toxic substances	Nominal	Smoking habits, alcohol use, drugs use, asbestos exposure, exposure to other toxic substances
Prior diseases / treatment	nominal	Disease etiology from clinical report
Comorbidity	nominal	Disease etiology from clinical report

Version number: 2, date 18-07-2019

13 of 18

## 8.2 Randomisation, blinding and treatment allocation

NA

## 8.3 Study procedures

Database registry of bronchoscopy procedures. No additional questionnaires need to be answered. No psychological / psychiatric investigations need to be performed.

## 8.4 Withdrawal of individual subjects

Subjects can leave the registry at any time for any reason if they wish to do so without any consequences.

### 8.4.1 Specific criteria for withdrawal (if applicable)

NA

## 8.5 Replacement of individual subjects after withdrawal

NA

## 8.6 Follow-up of subjects withdrawn from treatment

NA

## 8.7 Premature termination of the study

NA

## 9. SAFETY REPORTING

### 9.1 Temporary halt for reasons of subject safety

NA

### 9.2 AEs, SAEs and SUSARs

#### 9.2.1 Adverse events (AEs)

Normal clinical complication registry will be applied.

#### 9.2.2 Serious adverse events (SAEs)

NA

#### 9.2.3 Suspected unexpected serious adverse reactions (SUSARs)

NA

### 9.3 Annual safety report

NA

### 9.4 Follow-up of adverse events

NA

### 9.5 [Data Safety Monitoring Board (DSMB) / Safety Committee]

NA

## 10. STATISTICAL ANALYSIS

NA

Version number: 2, date 18-07-2019

14 of 18

**10.1 Primary study parameter(s)**

The primary parameters of this ongoing data registry will be used to assess the diagnostic value of advanced light settings and image processing in bronchoscopy images.

**10.2 Secondary study parameter(s)**

Secondary study parameters are included to link the primary parameters (endobronchial images) to the medical status and follow-up of the patient. In order to do so, multiple parameters will be recorded (see chapter 8.1 table 1; database registry parameters). In case of partially missing data in these variables, missing data fields will be left empty and excluded from analysis.

**10.3 Exploratory study parameter(s)**

NA

**10.4 Other study parameters**

NA

**10.5 Interim analysis (if applicable)**

NA

**11. ETHICAL CONSIDERATIONS**

**11.1 Regulation statement**

This database registry will be conducted according to the principles of the Declaration of Helsinki (as adopted by the 64<sup>th</sup> WMA General assembly, 19<sup>th</sup> October 2013) and in accordance with the Medical Research Involving Human Subjects Act (WMO).

**11.2 Recruitment and consent**

As described in chapter 4.1 (population (base)), patient selection for participation in the registry follows the conventional selection of patients elected for bronchoscopy. Eligible patients will be informed during their consultation at the pulmonary outpatient clinic when the indication and informed consent of the bronchoscopy procedure itself will be discussed. After having answered any possible questions of the patient, the patient information folder and information and consent form will be handed out by the treating physician. In the standard of care, patients will have at least two days to make a decision before the procedure is performed.

If needed, patients can also refer to the independent expert. Upon the day of the bronchoscopy procedure, the treating physician will answer any remaining questions regarding the study, and will collect the informed consent form if given by the patient.

**11.3 Objection by minors or incapacitated subjects (if applicable)**

Minors and/or incapacitated subjects will not be included in this study.

**11.4 Benefits and risks assessment, group relatedness**

NA

Version number: 2, date 18-07-2019

15 of 18

**11.5 Compensation for injury**

NA

**11.6 Incentives (if applicable)**

NA

**12. ADMINISTRATIVE ASPECTS, MONITORING AND PUBLICATION**

**12.1 Handling and storage of data and documents**

The investigator will maintain adequate records of signed patients informed consent forms and the linking key of hospital identification number to study identification number. Images and videos of bronchoscopy procedures (main parameters) are initially collected following the normal clinical standard, using the clinical server. From there, the videos and images will retrospectively be coded and extracted from the clinical server. This is done by a hospital identification number query retrieval in the clinical server and immediate coding of the data. A CRF (case report form) containing the secondary study parameters and patient demographics and characteristics will retrospectively be filled out by the investigator by accessing the electronic patient file based on the hospital identification number. This is needed to correlate the primary study parameters to the secondary study parameters as well as patient demographics and characteristics. The CRF will not contain the hospital identification number, only the study identification number. The obtained coded data will be stored on a protected server according to Good Clinical Practice (GCP) and the latest regional guidelines for digital patient data storage in the Radboudumc. A back up of the data will be automatically made. Coded documents and data are kept in a secured area with limited access. All records will be signed and dated by the investigators. All records are to be retained for a period of minimally 15 years following the date the entire clinical investigation is completed, terminated or discontinued.

Data are handled confidentially and anonymously. A patient identification code (Patient ID) will be used to link the study data to the patient. The code is not based on the patient initials and birthdate. The coordinator of the study safeguards the key to the code which is collected on the patient identification log and remains in the investigator study binder. The patient registry ID consists of 7 digits: 3 alphanumeric digits referring to the bronchoscopy data registry (i.e. BBB, followed by 4 numerical digits presenting the patient enrolment number from 0001 to max. 9999). There will be no way to determine the patient's identity from the the CRFs, except by accessing the patient identification log which is stored only at the department of Pulmonology at the Radboudumc; this will protect the patient's identity during data analysis. No patient names will appear on any reports, publications or other disclosures of clinical study outcomes.

**12.2 Monitoring and Quality Assurance**

NA

Version number: 2, date 18-07-2019

16 of 18

### 12.3 Amendments

Amendments are changes made to the research after a favourable opinion by the accredited METC has been given. All amendments will be notified to the METC that gave a favourable opinion. All substantial amendments will be notified to the METC and to the competent authority (CA). Non-substantial amendments will not be notified to the accredited METC and the competent authority, but will be recorded and filed by the sponsor.

### 12.4 Annual progress report

The sponsor/investigator will submit a summary of the database registry to the accredited METC every five years. This will be when the clinical need for continuation of the database registry is re-evaluated and at the end of the registry, when the results have been finalized. Information will be provided on the date of inclusion of the first subject, numbers of subjects included and numbers of subjects that have completed the trial, serious adverse events/serious adverse reactions, other problems, and amendments.

### 12.5 Temporary halt and (prematurely) end of study report

The investigator/sponsor will notify the accredited METC of the end of the study within a period of 8 weeks. The end of the study is defined as the last patient's last diagnostic procedure. The sponsor will notify the METC immediately of a temporary halt of the study, including the reason of such an action. In case the study is ended prematurely, the sponsor will notify the accredited METC within 15 days, including the reasons for the premature termination. Within one year after the end of the study, the investigator/sponsor will submit a final study report with the results of the study, including any publications/abstracts of the study, to the accredited METC.

### 12.6 Public disclosure and publication policy

This study will be registered at [www.clinicaltrials.gov](http://www.clinicaltrials.gov). There are no restrictions in publication policy.

## 13. STRUCTURED RISK ANALYSIS

### 13.1 Potential issues of concern

NA

### 13.2 Synthesis

Not applicable, the registry records the conventional work-up.

## 14. REFERENCES

- [1] H. Neumann, M. Fujishiro, C. M. Wilcox, and K. Mönkemüller, "Present and future perspectives of virtual chromoendoscopy with i-scan and optical enhancement technology," *Dig. Endosc.*, vol. 26, pp. 43–51, 2014.
- [2] I. H. Iftikhar and A. I. Musani, "Narrow-band imaging bronchoscopy in the detection of premalignant airway lesions: a meta-analysis of diagnostic test accuracy," *Ther. Adv. Respir. Dis.*, vol. 9, no. 5, pp. 207–216, 2015.
- [3] PENTAX medical, "i-scan Atlas for Gastroenterology," 2016.
- [4] S. Kodashima *et al.*, "Evaluation of a new image-enhanced endoscopic technology using band-limited light for detection of esophageal squamous cell carcinoma," *Dig. Endosc.*, vol. 26, no. 2, pp. 164–171, 2014.
- [5] K. Shibuya *et al.*, "High magnification bronchovideoscopy combined with narrow band imaging could detect capillary loops of angiogenic squamous dysplasia in heavy smokers at high risk for lung cancer," *Thorax*, vol. 58, pp. 989–995, 2003.
- [6] K. Shibuya, T. Nakajima, T. Fujiwara, M. Chiyo, and H. Hoshino, "Lung Cancer Narrow band imaging with high-resolution bronchovideoscopy: A new approach for visualizing angiogenesis in squamous cell carcinoma of the lung," *Lung Cancer*, vol. 69, no. 2, pp. 194–202, 2010.
- [7] F. J. F. Herth, R. Eberhardt, and D. Anantham, "Narrow-Band Imaging Bronchoscopy Increases the Specificity of Bronchoscopic Early Lung Cancer Detection," *JTO Acquis.*, vol. 4, no. 9, pp. 1060–1065, 2009.
- [8] B. Zaric, B. Perin, and V. Stojisic, "Relation between vascular patterns visualized by narrow band imaging (NBI) videobronchoscopy and histological type of lung cancer," *Med. Oncol.*, vol. 30, no. 1, p. 374, 2013.
- [9] P. F. Clementsen, L. J. Nayahangan, and L. Konge, *Bronchoscopy - A Practical Handbook*. Copenhagen: Simulation Centre Rigshospitalet, 2016.
- [10] T. Yoshida, H. Inoue, S. Usui, H. Satodate, M. Fukami, and S. E. Kudo, "Narrow-band imaging system with magnifying endoscopy for superficial esophageal lesions," *Gastrointest. Endosc.*, vol. 59, no. 2, pp. 288–295, 2004.
- [11] K. Shibuya *et al.*, "Subepithelial vascular patterns in bronchial dysplasias using a high magnification bronchovideoscope," *Thorax*, vol. 57, pp. 902–907, 2002.
- [12] T. Zaric, B. Stojisic, V. Sarcev, "Advanced bronchoscopic techniques in diagnosis and staging of lung cancer," *J Thorac. Dis.*, vol. 5, no. 54, p. 359–70, 2013.
- [13] E. M. Fathy, H. Shafiek, and T. S. Morsi, "Image-enhanced bronchoscopic evaluation of bronchial mucosal microvasculature in COPD," *Int. J. COPD*, vol. 11, pp. 2447–2455, 2016.
- [14] E. J. Topol, "human and artificial intelligence," *Nat. Med.*, vol. 25, no. January, 2019.
- [15] K. Gono, T. Ohi, M. Yamaguchi, N. Ohyama, and Y. Sano, "Appearance of enhanced tissue features in narrow-band endoscopic imaging," *J. Biomed. Opt.*, vol. 9, no. 3, pp. 568–577, 2004.

## 7.6 Patient information letter prospective database registry (Dutch)

CMO 2019-5583 – BEELDBANK BRONCHOSCOPIE proefpersooninformatie versie 2, 18 juli 2019

### Proefpersooninformatie en toestemmingsformulier Beeldbank Bronchoscopie voor medisch-wetenschappelijk onderzoek

*Officiële titel onderzoek: Het evalueren van de diagnostische waarde van verschillende lichtinstellingen en beeldbewerkingstechnieken op bronchoscopiebeelden verkregen bij patiënten met een indicatie voor bronchoscopie.*

#### Inleiding

Geachte mevrouw/mijnheer,

Uw behandelend arts heeft met u besproken dat er een reden is om een bronchoscopie uit te voeren. Dat houdt in dat we met een bronchoscopus – een soepele 'slang' met een doorsnede van ongeveer een halve centimeter – de binnenzijde van uw luchtwegen gaan bekijken. Aan het uiteinde van deze slang zit een videocamera waarmee de luchtwegen geïnspecteerd kunnen worden. Meer informatie over bronchoscopie is opgenomen in bijlage 2 van deze informatiebrief.

Wij vragen u vriendelijk om mee te doen aan een medisch-wetenschappelijk onderzoek door het beschikbaar stellen van uw medische gegevens. Meedoen is vrijwillig. Om mee te doen is uw schriftelijke toestemming nodig. Voordat u beslist of u wilt meedoen aan dit onderzoek, krijgt u uitleg over het onderzoek. Lees deze informatiebrief rustig door en vraag uw behandelend arts om uitleg als u vragen heeft. U kunt er ook over praten met uw partner, vrienden of familie. Ook is er een onafhankelijke arts die eventuele vragen over het onderzoek kan beantwoorden wanneer u deze liever niet aan uw behandelend arts stelt. In bijlage 1 van deze brief vindt u de contractgegevens van deze onafhankelijke arts.

#### Wat is het doel van de BeeldBank Bronchoscopie?

De BeeldBank Bronchoscopie maakt het voor ons mogelijk om te onderzoeken of nieuwe lichtinstellingen en beeldbewerkingen meer informatie over het longweefsel uit de bronchoscopiebeelden kunnen halen. Deze informatie kan zorgen voor het verbeteren van onze diagnostiek. Eerder wetenschappelijk onderzoek heeft laten zien dat het met de nieuwe lichtinstellingen en beeldbewerkingen mogelijk is om meer informatie uit de bronchoscopiebeelden te halen. Het opslaan van afbeeldingen en video's die met de bronchoscopus worden gemaakt helpt ons de lichtinstellingen en beeldbewerkingen verder te onderzoeken en ontwikkelen. Dit is een continu proces van kwaliteitsverbetering waarvoor we de bij u verzamelde beelden nodig hebben.

#### Wat houdt deelname aan de BeeldBank Bronchoscopie in?

Als u meedoet, verandert dat niets aan de bronchoscopieprocedure. Als u deelneemt aan dit onderzoek hoeft u niets anders te doen dan voor een normaal bronchoscopie onderzoek. Bij deelname geeft u:

##### 1. Toestemming om uw medische gegevens te verzamelen, op te slaan en te gebruiken

Om dit onderzoek mogelijk te maken willen wij de afbeeldingen en video's, gemaakt door de bronchoscopus, opslaan in een database. De beelden willen we graag koppelen aan gegevens over uw huidige en toekomstige gezondheid. Daarvoor hebben wij gegevens uit uw medisch dossier nodig. Indien er bijvoorbeeld tijdens de bronchoscopie lichaamsmateriaal is afgenomen willen wij graag weten wat de uitkomst hiervan is. Uw gegevens worden geodeerd waardoor ze niet naar u persoonlijk te herleiden zijn. Op die manier zorgen we ervoor dat uw privacy gewaarborgd blijft.

pagina 1 van 9

CMO 2019-5583 – BEELDBANK BRONCHOSCOPIE proefpersooninformatie versie 2, 18 juli 2019

##### 2. Toestemming om u ook in de toekomst te mogen benaderen

Er kan in de toekomst aanleiding zijn tot het uitvoeren van extra of aanvullend wetenschappelijk onderzoek waarvoor meer gegevens nodig zijn dan wij van u hebben. Daarom vragen wij of we u ook in de toekomst mogen benaderen voor het verzamelen van extra gegevens of lichaamsmateriaal. Als u hiervoor toestemming geeft, kunt u in de toekomst altijd nog weigeren om extra gegevens te verstrekken en/of lichaamsmateriaal af te laten nemen wanneer wij u daarvoor benaderen.

##### 3. Toestemming om bestaande Nederlandse registratiesystemen te raadplegen

Om meer inzicht te krijgen in het ontstaan en verloop van longziekten, kan het zijn dat wij in de toekomst aanvullende gegevens nodig hebben. Indien deze niet aanwezig zijn in uw medisch dossier, kunnen de gegevens verkregen worden door ze op te vragen bij bestaande Nederlandse medische registratiesystemen en registratiesystemen op het gebied van de volksgezondheid. Het doel van het raadplegen van de registratiesystemen is om de bronchoscopiebeelden te kunnen koppelen aan gegevens over uw gezondheid. Indien nodig zullen we op gezette tijden deze systemen raadplegen, in sommige gevallen tot 10 jaar na de bronchoscopie. Daarnaast kan het soms nodig blijken voor het wetenschappelijke onderzoek om u of uw huisarts te benaderen voor aanvullende informatie.

#### Wat zijn mogelijke voor- en nadelen van deelname aan dit onderzoek?

U heeft zelf geen voordeel of nadeel door deelname aan dit onderzoek. Wel kan dit wetenschappelijk onderzoek nuttige gegevens opleveren voor mensen die in de toekomst een bronchoscopie zullen ondergaan.

#### Toezicht op de uitvoering

Het wetenschappelijke onderzoek met uw gegevens wordt zorgvuldig uitgevoerd. De geldende regels worden in acht genomen en het onderzoek wordt getoetst door de medisch-ethische toetsingscommissie van het Radboudumc.

#### Hoe is uw privacy gewaarborgd?

Voor dit onderzoek worden uw persoonsgegevens verzameld, gebruikt en bewaard. Al uw gegevens vallen onder het medisch beroepsgeheim. Uw persoonlijke gegevens (zoals uw naam, adres, geboortedatum en andere persoonlijke gegevens die naar u als persoon kunnen worden herleid) blijven bewaard in het ziekenhuis waar u onder behandeling bent. De bronchoscopiebeelden en medische gegevens die verband houden met het onderzoek worden opgeslagen onder een codenummer om uw privacy te beschermen. Uw naam en andere gegevens die u direct kunnen identificeren worden daarbij weggelaten. Alleen met de sleutel van de code zijn gegevens tot u te herleiden. De sleutel van de code blijft veilig opgeborgen in de onderzoeksinstelling in het Radboudumc. De gegevens die naar de opdrachtgever worden gestuurd bevatten alleen de code, maar niet uw naam of andere gegevens waarmee u kunt worden geïdentificeerd. Alle wettelijke regels worden hierbij in acht genomen. Vanzelfsprekend zullen al uw gegevens vertrouwelijk worden behandeld. Wij zijn verplicht uw onderzoeksgegevens 15 jaar na voltooiing, beëindiging of stopzetting van dit onderzoek te bewaren op de onderzoekslocatie in het Radboudumc.

Behalve de arts die als hoofdonderzoeker bij dit onderzoek betrokken is (dit kan, maar hoeft niet uw behandelend arts te zijn) en zijn vaste medewerkers zullen uitsluitend daartoe wettelijk bevoegde personen/vertegenwoordigers van toezichhoudende instanties onder strikte geheimhouding uw gegevens kunnen inzien. Uw medische gegevens die kunnen worden gebruikt voor wetenschappelijk onderzoek worden bewaard onder een unieke code.

pagina 2 van 9

zodat verwisseling van gegevens wordt voorkomen, maar ook zodat degene die met de database wetenschappelijk onderzoek uitvoert of waarmee wordt samengewerkt geen beschikking krijgt over uw persoonsgegevens.

De resultaten van het wetenschappelijk onderzoek zullen worden gepubliceerd, bijvoorbeeld in rapporten en wetenschappelijke tijdschriften. Uw persoonlijke gegevens zijn daarin nooit terug te vinden.

#### **Intrekken toestemming gebruik gegevens**

Uw deelname aan dit onderzoek is voor onbepaalde tijd. Terugtrekking uit het onderzoek is op ieder moment mogelijk, zonder verdere gevolgen. U kunt uw toestemming voor deelname aan dit onderzoek intrekken door het invullen van het *Formulier voor intrekken eerder verleende toestemming*. Deze vindt u in bijlage 3 van deze informatiebrief. Het ingevulde formulier kunt u toesturen aan dr. HFM van der Heijden, afdeling longziekten ip 614, Radboudumc, Postbus 9101, 6500 HB Nijmegen. U krijgt een bevestiging van de ontvangst van uw intrekking. Na de intrekking van uw toestemming wordt met uw gegevens geen nieuw wetenschappelijk onderzoek meer gedaan. De onderzoeksgegevens die zijn verzameld tot het moment dat u uw toestemming intrekt worden nog wel gebruikt in het onderzoek.

#### **Meer informatie over uw rechten bij verwerking van gegevens**

Voor algemene informatie over uw rechten bij verwerking van uw persoonsgegevens kunt u de website van de Autoriteit Persoonsgegevens raadplegen. Bij vragen over uw rechten kunt u contact opnemen met de verantwoordelijke voor de verwerking van uw persoonsgegevens: Functionaris Gegevensbescherming (Data Protection Officer) Radboudumc, Route 624, Postbus 9101, 6500 HB Nijmegen; email: gegevensbescherming@radboudumc.nl

#### **Kosten, eigendom en samenwerking met bedrijven**

Uw deelname aan dit project brengt voor u geen extra kosten met zich mee. U wordt niet betaald voor het meedoen aan dit onderzoek. De BeeldBank Bronchoscopie is een niet-commercieel wetenschappelijk initiatief. De opdrachtgever is het Radboudumc. Echter, voor sommige wetenschappelijke onderzoeken is het van belang om samen te werken met commerciële bedrijven. De resultaten uit een dergelijke samenwerking kunnen eigendom worden van het bedrijf. Ook kunnen de resultaten door het bedrijf worden gebruikt voor verdere commerciële ontwikkelingen, zoals octrooien. Alle onderzoeksresultaten komen de gezondheidszorg ten goede. U zult geen eigendomsrechten verkrijgen op de resultaten en u zult geen aanspraak kunnen maken op eventueel toekomstig financieel voordeel. Uiteraard zijn uw rechten en uw privacy, die zijn beschreven in deze informatiebrief, ook bij commerciële samenwerking gewaarborgd.

#### **Wat gebeurt er als u niet wenst deel te nemen aan dit onderzoek?**

U beslist zelf of u meedoet aan het onderzoek. Deelname is vrijwillig. Als u besluit niet mee te doen aan het onderzoek, hoeft u niets te doen. U hoeft niets te ondertekenen. U hoeft ook niet te zeggen waarom u niet wilt meedoen. Wanneer u niet meedoet aan het onderzoek, krijgt u gewoon de behandeling die u anders ook zou krijgen.

pagina 3 van 9

Als u wel meedoet aan dit onderzoek, kunt u zich altijd bedenken en toch stoppen, ook tijdens het onderzoek. U hoeft niet te zeggen waarom u stopt. De gegevens die tot dat moment zijn verzameld, worden gebruikt voor het onderzoek. Als u wilt, kan verzamelde informatie worden vernietigd.

Als er nieuwe informatie over het onderzoek is die belangrijk voor u is, laat de onderzoeker dit aan u weten. U wordt dan gevraagd of u blijft meedoen.

#### **Heeft u vragen?**

Bij vragen kunt u contact opnemen met de hoofdonderzoeker. Voor onafhankelijk advies over meedoen aan dit onderzoek kunt u terecht bij de onafhankelijke arts. Zij weet veel over het onderzoek, maar heeft niets te maken met het onderzoek. De contactinformatie staat in bijlage 1 van deze proefpersoneninformatie.

Indien u klachten heeft over het onderzoek, kunt u dit bespreken met de onderzoeker of uw behandelend arts. Wilt u dit liever niet, dan kunt u zich wenden tot de klachtencommissie van het Radboudumc. De contactinformatie staat in bijlage 1 van deze proefpersoneninformatie.

#### **Ondertekening toestemmingsformulier**

Wanneer u voldoende bedenktijd heeft gehad, wordt u gevraagd te beslissen over deelname aan dit onderzoek. Indien u toestemming geeft, zullen wij u vragen deze op de bijbehorende toestemmingsverklaring schriftelijk te bevestigen. Door uw schriftelijke toestemming geeft u aan dat u de informatie heeft begrepen en instemt met deelname aan het onderzoek.

Zowel uzelf als de onderzoeker ontvangen een ondertekende versie van deze toestemmingsverklaring.

Hartelijk bedankt voor uw aandacht.

pagina 4 van 9



**Toestemmingsformulier deelname BeeldBank Bronchoscopie**  
Kopie voor persoonlijke administratie patiënt

*Het evalueren van de diagnostische waarde van verschillende lichtinstellingen en beeldbewerkingstechnieken op bronchoscopiebeelden verkregen bij patiënten met een indicatie voor bronchoscopie.*

Ik ben naar tevredenheid geïnformeerd over de doelstellingen van de BeeldBank Bronchoscopie en over het beschikbaar stellen van mijn medische gegevens. Ik heb de informatiebrief ontvangen en gelezen (versie 1, 28 juni 2019) en er is mij voldoende gelegenheid gegeven hierover vragen te stellen. Ik heb voldoende bedenktijd gehad en goed kunnen nadenken over mijn deelname. Ik weet dat meedoen vrijwillig is. Ook weet ik dat ik op ieder moment kan beslissen om toch niet mee te doen of te stoppen met het onderzoek. Daarvoor hoef ik geen reden te geven.

- Ik wil meedoen aan dit onderzoek.
1. Ik geef toestemming om mijn gecodeerde medische gegevens te verzamelen, op te slaan en te gebruiken op de manier zoals is beschreven en voor de doelen die in deze informatiebrief worden genoemd.
2. Ik geef toestemming om in de toekomst te mogen worden benaderd voor het verstrekken van extra gegevens, indien dit voor een onderzoek noodzakelijk is. Zo nodig mogen in de toekomst mijn actuele adresgegevens opgevraagd worden bij de burgerlijke stand.
3. Ik geef toestemming voor het opvragen van mijn gegevens bij bestaande Nederlandse medische registratiesystemen en registratiesystemen op het gebied van de volksgezondheid indien hiervoor aanleiding is, onder voorwaarden dat mijn privacy gewaarborgd blijft.

**Ondertekening en dagtekening**

Achternaam en voorletters proefpersoon: .....

Geboortedatum: ...../...../.....

Handtekening:..... Datum: ...../...../.....

Ik verklaar dat ik deze proefpersoon volledig heb geïnformeerd over het genoemde onderzoek. Als er tijdens het onderzoek informatie bekend wordt die de toestemming van de proefpersoon zou kunnen beïnvloeden, dan breng ik hem/haar daarvan tijdig op de hoogte.

Naam onderzoeker: .....

Handtekening:..... Datum: ...../...../.....

*De proefpersoon krijgt een volledige informatiebrief mee, samen met een ondertekende versie van het toestemmingsformulier.*

pagina 5 van 9

**Bijlage 1 – Contactinformatie**

Tijdens kantooruren kunt u contact opnemen met de volgende personen:

**Hoofdonderzoeker:** dr. H.F.M. van der Heijden  
via het secretariaat op telefoonnummer **024-3610325**

**Casemanager Longziekten:** Ineke Bles-Sluis  
via telefoonnummer **06-11514854**

Buiten kantooruren kunt u in spoedeisende gevallen contact opnemen met de verpleegafdeling Longziekten via telefoonnummer **024-3614590**.

**Onafhankelijk arts:** dr. M. Reijers via telefoonnummer **024-3610325**. U kunt haar benaderen voor inlichtingen en advies betreffende deze studie. Zij is niet bij de uitvoering van de bronchoscopie of het onderzoek betrokken.

**Klachtencommissie:** Alle medewerkers van het Radboudumc zetten zich in om u goede, professionele zorg te geven. Toch kunt u ergens ontevreden over zijn. U kunt hiervoor ons benaderen via:

Radboudumc Afdeling Klachtenbemiddeling  
Huispost 628  
Antwoordnummer 540  
6500 VC Nijmegen  
(024) 361 31 91  
Bereikbaar van maandag t/m vrijdag van 9.00-17.00 uur

**Adres ziekenhuis:**  
Radboudumc  
Geert Grooteplein Zuid 10 (route 725)  
Postbus 9101  
6500 HB Nijmegen

pagina 6 van 9

**Bijlage 2 – Algemene informatie over bronchoscopie**

Uw arts heeft met u besproken dat bij u een bronchoscopie zal worden uitgevoerd. Dit wordt gedaan met behulp van een dunne flexibele slang (bronchoscoop) via de mond, om op die manier de luchtwegen in te gaan. Tijdens een bronchoscopie kan de arts het longweefsel inspecteren, lichaamsmateriaal verzamelen voor nader onderzoek of een ingreep aan de luchtwegen verrichten. Dit onderzoek wordt gedaan terwijl u in slaap bent gebracht.

Om de binnenkant van de long te bekijken is het uiteinde van de bronchoscoop uitgerust met een fel lampje en een videocamera. De videobeelden worden tijdens de procedure door de arts bekeken en beoordeeld.

**Hoe een bronchoscopie wordt uitgevoerd**

De belangrijkste voorbereiding voor een bronchoscopie is dat u nuchter bent wanneer wij het onderzoek uitvoeren (minimaal 6 uur van tevoren niet eten en drinken). Uw arts zal beoordelen of u uw medicatie, zoals bijvoorbeeld bloedverdunners, tijdelijk moet stoppen of omzetten naar een ander soort medicijn.

U wordt aangesloten op apparatuur om uw hartfrequentie, bloeddruk en ademhaling te controleren. Daarna wordt u in slaap gebracht. Terwijl u slaapt worden bij u de keel en de bovenste luchtwegen verdoofd en wordt vervolgens de bronchoscoop ingebracht tot in de luchtpijp. Daarna voeren we een onderzoek uit waarbij we eerst de luchtwegen en het weefsel rondom de luchtwegen inspecteren. Afhankelijk van de indicatie kunnen we daarnaast nog lichaamsmateriaal verzamelen of een ingreep aan de luchtwegen uitvoeren.

Na het onderzoek gaat u naar de uitslaapkamer ter observatie. Zodra u goed wakker bent en alle controlemetingen normaal zijn, kunt u naar huis. U mag nog niet zelf autorijden en moet vervoer naar huis geregeld hebben. Bent u alleenstaand? Dan moet er gedurende de eerste nacht iemand bij u thuisblijven.

**Welke bijwerkingen kunt u verwachten van een bronchoscopie?**

Mogelijke bijwerkingen van bronchoscopie zijn bloedingen, een klaplong, koorts, en in zeldzame gevallen een infectie. Als u een klaplong zou krijgen, dan kan het nodig zijn om een slangetje in uw long achter te laten. We doen dit om de lucht af te zuigen en de long weer goed te laten functioneren. U moet in dit geval opgenomen worden in het ziekenhuis.

Het komt heel vaak voor dat iemand na het afnemen van biopsieën wat bloed ophoest. Dit is niet verontrustend. Een enkele keer kan er 's avonds wat verhoogde temperatuur optreden. Ook dat is niet verontrustend. U kan dan worden behandeld met een koortswerend medicijn zoals bijvoorbeeld paracetamol. U wordt tijdens dit onderzoek in slaap gebracht door middel van een beademingsmasker in de keelholte of een beademingsbuis in de luchtwegen. In zeldzame gevallen kan het masker of de buis lijden tot milde keelpijn en heesheid. Mogelijke bijwerkingen in de eerste nacht(en) zijn: onregelmatige ademhaling gedurende uw slaap en spierspasmen.

**Bijlage 3 – Formulier voor intrekken eerder verleende toestemming**

Ik geef hiermee te kennen dat ik mijn deelname aan het onderzoek BeeldBank Bronchoscopie intrek, voor zover het betreft:

Nieuw wetenschappelijk onderzoek met over mij verzamelde gegevens.

Na ontvangst en verwerking van het ingevulde en ondertekende formulier voor intrekken wordt geen nieuw wetenschappelijk onderzoek meer gedaan met uw gegevens. De verzamelde gegevens blijven wel bewaard, zolang als dit nodig is voor de onderzoeken waarvoor uw gegevens inmiddels worden of zijn gebruikt.

**Naam:** .....

**Geboortedatum:** .....

**Datum:** .....

**Handtekening:** .....

U bent niet verplicht een reden van intrekken eerder verleende toestemming te geven, maar wij stellen het wel op prijs. Met uw informatie kunnen wij in de toekomst onze onderzoeksactiviteiten verbeteren.

**Reden van intrekken toestemming:**

.....  
.....  
.....  
.....

Toestemmingsformulier deelname BeeldBank Bronchoscopie  
Kopie voor administratie onderzoekers BeeldBank Bronchoscopie Radboudumc

Het evalueren van de diagnostische waarde van verschillende lichtinstellingen en beeldbewerkingstechnieken op bronchoscopiebeelden verkregen bij patiënten met een indicatie voor bronchoscopie.

Ik ben naar tevredenheid geïnformeerd over de doelstellingen van de BeeldBank Bronchoscopie en over het beschikbaar stellen van mijn medische gegevens. Ik heb de informatiebrief ontvangen en gelezen (versie 1, 28 juni 2019) en er is mij voldoende gelegenheid gegeven hierover vragen te stellen. Ik heb voldoende bedenktijd gehad en goed kunnen nadenken over mijn deelname. Ik weet dat meedoen vrijwillig is. Ook weet ik dat ik op ieder moment kan beslissen om toch niet mee te doen of te stoppen met het onderzoek. Daarvoor hoef ik geen reden te geven.

- Ik wil meedoen aan dit onderzoek.
- 1. Ik geef toestemming om mijn gecodeerde medische gegevens te verzamelen, op te slaan en te gebruiken op de manier zoals is beschreven en voor de doelen die in deze informatiebrief worden genoemd.
- 2. Ik geef toestemming om in de toekomst te mogen worden benaderd voor het verstrekken van extra gegevens, indien dit voor een onderzoek noodzakelijk is. Zo nodig mogen in de toekomst mijn actuele adresgegevens opgevraagd worden bij de burgerlijke stand.
- 3. Ik geef toestemming voor het opvragen van mijn gegevens bij bestaande Nederlandse medische registratiesystemen en registratiesystemen op het gebied van de volksgezondheid indien hiervoor aanleiding is, onder voorwaarden dat mijn privacy gewaarborgd blijft.

**Ondertekening en dagtekening**

Achternaam en voorletters proefpersoon: .....

Geboortedatum: ...../...../.....

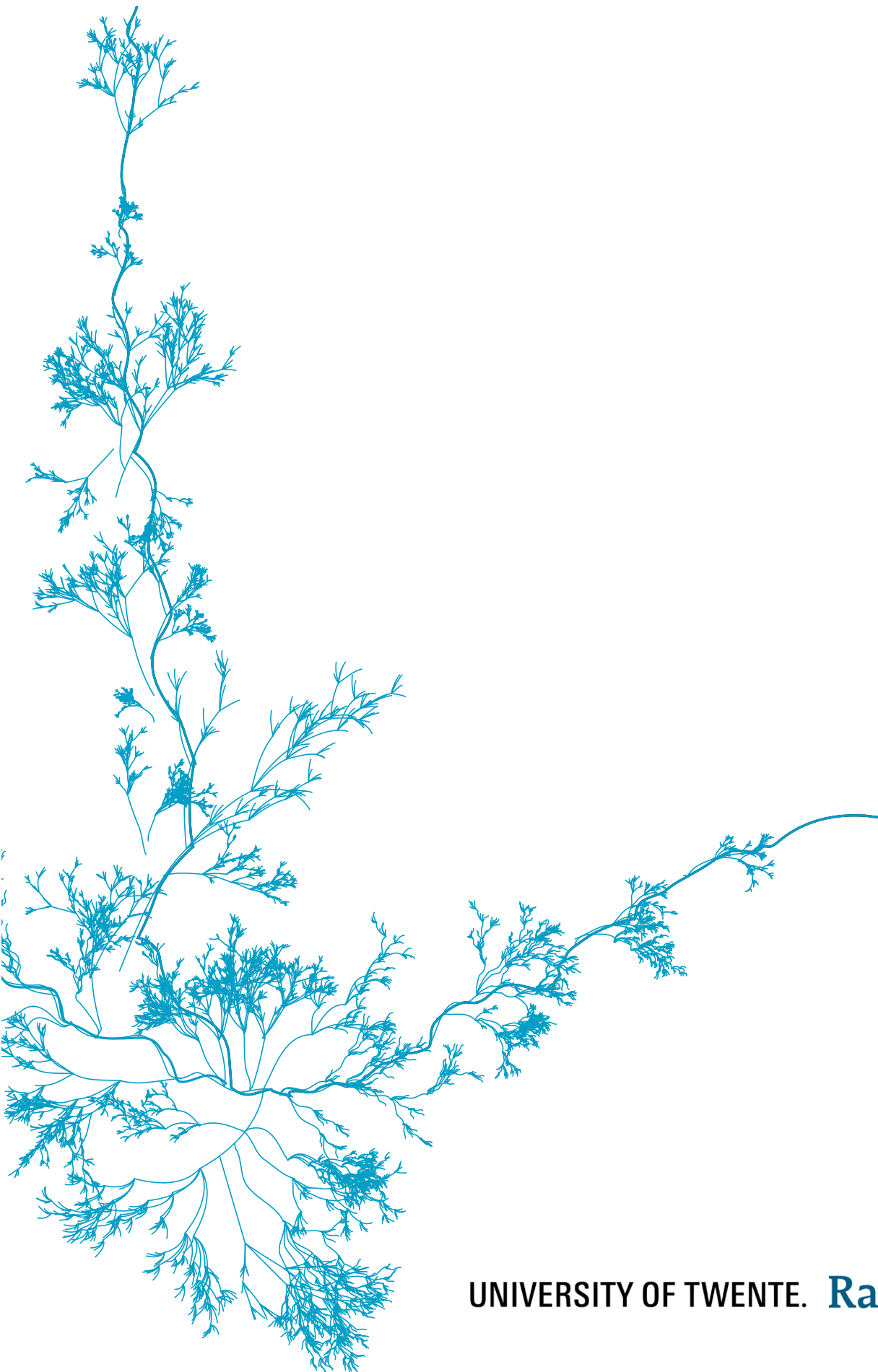
Handtekening:..... Datum: ...../...../.....

Ik verklaar dat ik deze proefpersoon volledig heb geïnformeerd over het genoemde onderzoek. Als er tijdens het onderzoek informatie bekend wordt die de toestemming van de proefpersoon zou kunnen beïnvloeden, dan breng ik hem/haar daarvan tijdig op de hoogte.

Naam onderzoeker: .....

Handtekening:..... Datum: ...../...../.....

*De proefpersoon krijgt een volledige informatiebrief mee, samen met een ondertekende versie van het toestemmingsformulier.*



UNIVERSITY OF TWENTE. **Radboudumc**